Investigating Respiration and Gas Exchange in the Aquatic Bug Aphelocheirus aestivalis (Hemiptera: Aphelocheiridae), and Surface Dwelling and Subterranean Diving Beetles (Coleoptera: Dytiscidae)

Karl Koch Jones

Presented for the degree of Doctor of Philosophy

School of Biological Sciences, Department of Ecology and Evolutionary Biology

University of Adelaide, South Australia, Australia

February 2019

CONTENTS

Publications included in this thesis

Jones, K.K., Hetz, S.K., Seymour, R.S., 2018. The effects of temperature, activity and convection on the plastron PO_2 of the aquatic bug *Aphelocheirus aestivalis* (Hemiptera; Aphelocheiridae). Journal of Insect Physiology 106, 155-162.

Jones, K.K., Cooper, S.J.B., Seymour, R.S., 2019. Cutaneous respiration by diving beetles from underground aquifers of Western Australia (Coleoptera: Dytiscidae). Journal of Experimental Biology 222, jeb196659

Abstract

Insects evolved in a terrestrial environment as indicated by their gas filled respiratory system, the tracheal system. Those insects that have become aquatic secondarily contend with the challenge of interfacing their tracheal system with the water, where O_2 diffuses 250,000 times slower than through air. These aquatic insects use a range of mechanisms to overcome this challenge, including gas exchange through the body surface (cutaneous respiration), siphons/snorkels that provide a direct link with the atmosphere, and air bubbles on the surfaces of the insects that store O_2 (air stores) or passively gain O_2 from the water (gas gills). Studies within this thesis investigate respiration, gas exchange, and dive behaviour in the aquatic bug *Aphelocheirus aestivalis* (Hemiptera) which uses an incompressible gas gill (plastron), and diving beetles (Dytiscidae: Coleoptera) that use air stores, gas gills, and varying forms of cutaneous respiration while underwater. Chapter two investigates under what temperature and convective conditions the metabolic demands of *Aphelocheirus* may become O_2-limited, and it compares these to the ecological niche in which the species can survive. Chapter three tests the hypothesis that subterranean diving beetles use cutaneous respiration to help them to survive in subterranean environments where few or no air-water interfaces occur. It also tests if cutaneous respiration in these beetles limits them to small size. Chapter four investigates respiration, gas exchange and dive behaviour in a surface-dwelling diving beetle *Platynectes decempunctatus*. This study develops an understanding of how gas exchange relates to dive behaviour and quantifies aspects of the dive including the decline in O_2 pressure within the respiratory gas store and the amount of O_2 gained from the water. Chapter five investigates respiration, gas exchange and dive behaviour in diving beetles more broadly, undertaking allometric analyses with several surface-dwelling diving beetles across a >300-fold mass range. This study shows the relationships between beetle size, O_2-consumption rate, respiratory gas volume held during a dive and dive behaviour. The data from this and previous studies are then incorporated into a mathematical model to assess four modes of gas exchange with the water in dytiscids, including cutaneous respiration, setal tracheal gills, respiratory pores and gas gills. There is a common theme throughout the research chapters of undertaking a range of experiments and then developing a mathematical model based on Fick's general diffusion equation. This approach enables a deeper understanding of the underlying mechanisms and allows model manipulations to determine the limits of the respiratory modes and their ecological and evolutionary consequences.

Author declaration

I certify that this work contains no material which has been accepted for the award of any other degree or diploma in my name in any university or other tertiary institution and, to the best of my knowledge and belief, contains no material previously published or written by another person, except where due reference has been made in the text. In addition, I certify that no part of this work will, in the future, be used in a submission in my name for any other degree or diploma in any university or other tertiary institution without the prior approval of the University of Adelaide and where applicable, any partner institution responsible for the joint award of this degree.

The author acknowledges that copyright of published works (as listed below*) contained within this thesis resides with the copyright holder(s) of those works.

I give permission for the digital version of my thesis to be made available on the web, via the University's digital research repository, the Library Search and also through web search engines, unless permission has been granted by the University to restrict access for a period of time.

I acknowledge the support I have received for my research through the provision of an Australian Government Research Training Program Scholarship.

* Jones, K.K., Hetz, S.K., Seymour, R.S., 2018. The effects of temperature, activity and convection on the plastron PO_2 of the aquatic bug *Aphelocheirus aestivalis* (Hemiptera; Aphelocheiridae). Journal of Insect Physiology 106, 155-162.

Jones, K.K., Cooper, S.J.B., Seymour, R.S., 2019. Cutaneous respiration by diving beetles from underground aquifers of Western Australia (Coleoptera: Dytiscidae). Journal of Experimental Biology 222, jeb196659

Karl Jones

February 2019

Acknowledgements

I would like to thank Roger Seymour for imparting a vast trove of physiological knowledge to me and guiding my scientific journey from undergraduate, through honours and my PhD. Roger has provided valuable direction and knowledge for me to become an effective scientist, developing my critical thinking, ability to design and undertake experiments, and writing manuscripts, the latter being a particular challenge. What I have learnt from Roger impacts my life everyday down to the minutiae of pondering the water vapour boundary layers surrounding wet clothes on the line. To Steve Cooper, your support and belief in me during the difficult times was instrumental in getting me to this point now. Both Roger and Steve have changed the trajectory of my life for the better and I am immensely grateful for that and for the opportunities this journey will provide. I am also extremely grateful to my wife Ali Walsh, and my parents Diana Koch and Ralph Jones for their incredible support during my PhD journey. We had innumerable conversations that helped clarify my ideas, provided useful feedback and different points of view. Thank you Jenna Crowe-Riddell, you have been an amazing friend, someone I could confide in and understands the here and now of undertaking a PhD. Thank you to my lab/office mates, Ned Snelling in the early days, and Tom Nelson and Vivi Hu for their support, constructive criticism and help along the way. Others I would like to thank are Lyn Waterhouse (Adelaide Microscopy), Chris Watts (SA Museum), Lisa O'Donovan (Adelaide Microscopy), the Axford Family (Sturt Meadows Station), Brendan and Carmel Reynolds (Willow Springs Station), Terry Walsh and Jo Morton, and Kym and Iris Gladigau.

Chapter One: Introduction

Animal physiology is about understanding how animals function, why they function the way they do, and how they respond to their environment to acquire resources and survive (Schmidt-Nielsen, 1997). Within the discipline of animal physiology, we may ask and investigate questions like how does an animal breathe, how do its muscles turn chemical energy into mechanical energy, and how does an animal survive in the extremes of its environment. In line with the premise of animal physiology, the research in this thesis sets out to improve our understanding of how different modes of respiration in aquatic insects function and how the ability of these modes to supply O_2 changes in response to physiological and environmental variables under a range of physical constraints. This introductory chapter summarises the development of the understanding of aquatic insect respiration, highlights the modes of aquatic respiration relevant to *Aphelocheirus aestivalis* (Aphelocheiridae; Hemiptera) and diving beetles (Dytiscidae; Coleoptera), the focal species of this research, and outlines the specific aims of the studies within this thesis.

The tracheal system and aquatic respiration

The insect respiratory system consists of a network of branching semi-rigid tubes that run from openings on the outside of the insects' body through to the tissues and cells (Wigglesworth, 1953). The tracheal system allows delivery of O_2 and removal of CO_2 through diffusion and forced convection, and supplies the tissues with the highest known mass-specific metabolic rates, such as those found in flying insects (Snelling et al., 2017). The gas-filled tracheal system is evidence that insects evolved in a terrestrial environment (Pritchard et al., 1993), where O_2 diffuses 250,000 times faster in air than water (Dejours, 1981). However, many insects have become aquatic secondarily, which presents a challenge for their respiratory system. Some insects respire directly with the atmosphere through tubes called siphons or snorkels, while others use bubbles on the outsides of their bodies, or respire directly through the cuticle (Seymour and Matthews, 2013).

The function of bubbles on aquatic insects

Early investigations revolved around determining if the bubbles on the surfaces of aquatic insects had a respiratory or buoyancy role (Ege, 1915). Experiments and measurements demonstrated that the bubbles do have respiratory function and in some cases can act as a physical gill allowing the passive extraction of O_2 from the water. In reality, many bubbles have mixed purposes providing both O_2 as well as buoyancy function (Matthews and Seymour, 2006). These bubbles are divided into two categories. Air stores, which are simple bubbles from which O_2 is

consumed during a dive, and gas gills where O_2 diffuses into the bubble from the water due to a partial pressure gradient (Ege, 1915; Rahn and Paganelli, 1968; Thorpe and Crisp, 1947a). There are two types of gas gill: compressible and incompressible or plastrons. Compressible gas gills require periodic replenishment at the surface due to O_2-consumption and N_2 and CO_2 loss to the water. However, the plastron is prevented from collapse by structures on the insects' body, and can therefore be maintained indefinitely (Marx and Messner, 2012; Thorpe and Crisp, 1947a). The distinction between the different types of respiratory bubbles is not always clear, and a bubble may more or less function as an air store as well as a gas gill (Jones et al., 2015).

Modelling O_2 diffusion into gas gills

Understanding of how gas gills functioned developed further with mathematical models based on Fick's general diffusion equation (Chaui-Berlinck and Bicudo, 1994; Chaui-Berlinck et al., 2001; Rahn and Paganelli, 1968);

$$\dot{M}_{O_2} = K_{O_2} \times A/X \times \Delta P_{O_2}$$

where $\dot{M}_{O_2}$ is the O_2-consumption rate of the animal, K_{O_2} is the Krogh's diffusion coefficient, the product of O_2 diffusivity and capacitance in water, A is the surface area for gas exchange, X is the boundary layer thickness, a fluid layer above the respiratory surface that is deficient in O_2 and offers resistance to diffusion, and ΔP_{O_2} is the O_2 partial pressure difference between the bulk surrounding water and inside the gas gill.

With the development of these models, a question arose on whether compressible gas gills should have fixed or declining surface area as bubble volume declines during a dive (Chaui-Berlinck and Bicudo, 1994; Chaui-Berlinck et al., 2001; Rahn and Paganelli, 1968). Surface area change, or lack thereof, affects how much O_2 can be gained from the water before the bubble becomes exhausted. Advancements in technology, in particular fibre-optic O_2-sensing optodes, allowed direct measurements of P_{O_2} within the gas gill of the aquatic bug *Agraptocorixa eurynome* (Matthews and Seymour, 2010). With the addition of gas gill surface area and buoyant force measurements, a fixed surface area model was found to be most representative model for the behaviour of a compressible gas gill during a dive. Optodes also helped confirm the role of haemoglobin stores in *Anisops* backswimmers, as both an O_2 store and a buoyancy aid extending a period of near-neutral buoyancy during the dive (Matthews and Seymour, 2006; Matthews and Seymour, 2008). Boundary layer thickness values used in the models remained undetermined experimentally until a study on the plastron breathing aquatic bug *Aphelocheirus aestivalis* (Seymour et al., 2015). Optode measurements showed boundary layer thicknesses

were greater than the values used in the models, and showed that boundary layer thickness decreased with an increase in water convection (Chaui-Berlinck and Bicudo, 1994; Rahn and Paganelli, 1968; Seymour et al., 2015).

The plastron breathing aquatic bug Aphelocheirus aestivalis

A. aestivalis is one of the largest known plastron breathing insects (40 mg), where the gas-water interface is maintained by tiny hairs at a density of ~4,000,000 per mm^2 across its dorsoventrally flattened body (Hinton, 1976; Seymour et al., 2015). Previous experimental work measured the PO_2 within the plastron for short periods by placing a bubble, with an optode inside, onto the plastron (Seymour et al., 2015). The plastron PO_2 was measured under different convective conditions at 20°C and declined with less convection due to lower O_2 conductance through the boundary layer. A recent study used *Aphelocheirus* to test whether thermal tolerance may be set by a mismatch between O_2-consumption and O_2 supply through the respiratory system with rising temperature (Verberk and Bilton, 2015). The results suggested that thermal tolerance is set by O_2-limitation, with critical temperatures, where the insect cannot escape adverse conditions, being between ~31 – 36°C depending on water PO_2. However, there are several factors, indicated by Fick's diffusion equation, including boundary layer thickness, water PO_2, and O_2 demand, which regulate gas exchange through the plastron. These factors interact and result in O_2-limitation under a range of conditions.

Cutaneous respiration and subterranean diving beetles

Several aquatic insects do not use bubbles interfaced with the water to exchange O_2, but diffusion occurs through the body surface. In many insects, often larval stages, diffusion occurs though the unelaborated body surface (Rasmussen, 1996; Thorpe and Crisp, 1947b; Yee and Kehl, 2015). However, in some cases, diffusion is assisted by exvaginations that greatly increase the surface area available for gas exchange, like the tracheal gills of mayfly and damselfly larvae (Bäumer et al., 2000; Eriksen, 1986). These plate-like structures have tracheoles running through them which bring gas within the tracheal system into close proximity with the water.

Species that use cutaneous respiration are restricted to small size because of the relative difference between surface area and metabolic rate as the insects become larger, as with plastron breathers (Seymour and Matthews, 2013). However, cutaneously respiring insects also contend with the additional resistance of the cuticle. The smaller surface area relative to mass of metabolising tissue, and thickening of the cuticle as the insects become larger, reduces the

conductance of respiratory gases to and from the insect's body, restricting them to an even smaller size than plastron breathers.

Previous studies have suggested that subterranean aquatic beetles may use cutaneous respiration. The reasons for this include; small or non-existent gas stores, a lack of compressible gas gills or plastrons, rich tracheation of the elytra, the ability to remain under water for long periods and the likelihood of having a low metabolic rate as in other subterranean animals (Ordish, 1976; Smrž, 1981; Ueno, 1957). Additionally, in their subterranean environment, the beetles may not have access to an air-water interface to replenish their air stores.

Western Australia has the most diverse assemblage of subterranean dytiscids in the world with approximately 100 species from ~50 isolated calcrete aquifers (Balke et al., 2004; Watts and Humphreys, 2009). The calcrete aquifers are thought to have formed during the Oligocene as Australia become more arid (Morgan, 1993). Surface water drainages that fed inland lakes began to dry up, leaving only underground waters which flow through paleodrainages to salt lakes (Humphreys et al., 2009). The groundwater flow and near-surface evaporation resulted in the deposition of porous calcrete layers 10-30 m thick, forming the aquifers (Humphreys et al., 2009; Morgan, 1993), which have no or few air-water interfaces. Surface-dwelling aquatic fauna adapted to subterranean life as the surface water disappeared, and populations became isolated within individual aquifers. Each aquifer now contains unique assemblages of subterranean aquatic fauna, including the dytiscids where there may be up to three species of different size classes, although none are larger than 5 mm long (Balke et al., 2004; Watts and Humphreys, 2009). Most of the dytiscids in the aquifers have evolved from surface-dwelling ancestors and are thought to have colonised the aquifers between ~10 and 3 Ma (Cooper et al., 2007; Guzik et al., 2011; Leijs et al., 2012). However, there is evidence that some species have evolved within isolated aquifers from subterranean ancestors (Leijs et al., 2012). As these dytiscids live in environments with limited or no air access, are small sized, and apparently lack the setal tracheal gills that are found in some surface dwelling species (Kehl, 2014), they are good candidates to test for cutaneous respiration and whether this form of respiration restricts them to small size.

Gas exchange in surface dwelling diving beetles

The general dive cycle of surface dwelling dytiscids begins with the beetles at the surface replenishing their sub-elytral air store (Calosi et al., 2007). Once the air store is filled they dive and continue consuming O_2. Sometimes a small bubble is pushed from the tip of the abdomen that acts as a compressible gas gill, but when the O_2 level becomes too low or gas volume too

small the beetle returns to the surface. The dive cycle can be divided into quantifiable components including dive duration, surfacing duration and surfacing frequency, which are collectively called dive characteristics. These variables are related to O_2 exchange and influence the beetles' energy and time investment in activities like foraging, mating and predator avoidance (Aiken, 1985; Calosi et al., 2007; Calosi et al., 2012; Miller and Bergsten, 2016).

Despite the prevalence of dytiscids, which are found in most freshwater habitats worldwide (Miller and Bergsten, 2016), few studies have investigated the link between gas exchange and dive characteristics. A previous study noted that increased temperature increased surfacing frequency in dytiscids as well as other aquatic insects, related to higher O_2-consumption rates (Ege, 1915). The dytiscid *Ilybius montanus*, when exposed to increased temperature, increased its surfacing frequency, decreased dive duration, and surfacing duration remained constant. These results are similar to the combined responses of two genera and 25 species of dytiscids, although there is variation in the response to temperature between genera and species (Calosi et al., 2012). However, none of the studies have measured O_2-consumption rate and gas exchange in dytiscids and related this to dive characteristics under various environmental conditions, which is partly due to the difficulty in measuring gas exchange in insects that utilise both aquatic and atmospheric O_2 (Calosi et al., 2007).

In addition to dytiscids using air stores and gas gills, other forms of respiration have been identified in submergence-tolerant surface dytiscids. Some species have small spoon-shaped setae at high densities on the cuticle surface through which tracheoles run (Kehl and Dettner, 2009). These setae reduce the diffusion distance through the cuticle to <1 μm, presumably increasing O_2 diffusion from the water. In others, pore structures that may function like plastrons with small bubble interfaces, or have tracheated structures in them, have been suggested to have respiratory function (Madsen, 2012). Species that use these forms of respiration are small, and are often found in cool, fast-flowing waters (Kehl and Dettner, 2009; Madsen, 2012; Miller and Bergsten, 2016; Verberk et al., 2018). The correlation between small size, living in cool fast-flowing habitats and submergence tolerance suggests the relationship between metabolic rate, surface area for gas exchange and cuticle thickness may limit the use of these modes of respiration to beetles of small size, like in plastron breathing insects (Seymour and Matthews, 2013) and those using cutaneous respiration.

Research chapter objectives

The unifying theme of the research chapters within this thesis is to better understand the functionality of different modes of respiration in aquatic insects and how the ability of those modes to supply O_2 changes in response to physiological and environmental variables under a range of physical constraints. Specifically, the aim of chapter two in this thesis, which is two-fold, is to (1) understand what temperature, water PO_2, and convective conditions, the plastron breathing bug *A. aestivalis* can exist in without O_2-limitation, and (2) to determine how the O_2 demand requirements of *A. aestivalis* change with temperature and activity. This study enables an understanding of whether *Aphelocheirus* may be O_2-limited in the conditions under which they are found in the field, as well as allowing comparisons between the results and conclusions of previous studies. Chapter three aims to test if Australian subterranean dytiscids do use cutaneous respiration, and if so, does cutaneous respiration limit these beetles to small size. The objective of chapter four is to undertake a detailed study into respiration, gas exchange and dive behaviour in the medium sized dytiscid *Platynectes decempunctatus* (7.4 mm long, 28 mg). This is to develop a more comprehensive understanding of gas exchange and dive behaviour, and how they are linked, in surface dwelling dytiscids that use air stores and compressible gas gills. The final research chapter, chapter five, aims to understand how O_2-consumption rate, gas exchange and dive characteristics change with body size, and assess how body size affects the ability of dytiscids to gain O_2 from the water using different types of aquatic gas exchange. The latter includes cutaneous respiration (Jones et al., 2018a), setal tracheal gills (Kehl and Dettner, 2009), plastron-like respiratory pores (Madsen, 2012) and gas gills (Calosi et al., 2007).

Chapter Two: The effects of temperature, activity and convection on the plastron PO_2 of the aquatic bug *Aphelocheirus aestivalis*

Statement of Authorship

Title of Paper	The effects of temperature, activity and convection on the plastron PO_2 of the aquatic bug *Aphelocheirus aestivalis* (Hemiptera; Aphelocheiridae)
Publication Status	☑ Published ☐ Accepted for Publication ☐ Submitted for Publication ☐ Unpublished and Unsubmitted work written in manuscript style
Publication Details	Jones, K.K., Hetz, S.K., Seymour, R.S., 2018. The effects of temperature, activity and convection on the plastron PO_2 of the aquatic bug *Aphelocheirus aestivalis* (Hemiptera; Aphelocheiridae). Journal of Insect Physiology 106, 155-162.

Principal Author

Name of Principal Author (Candidate)	Karl K. Jones		
Contribution to the Paper	Undertook experiments, field work, statistical and data analysis, and wrote the initial manuscript draft, and reviewed and edited subsequent drafts.		
Overall percentage (%)	65%		
Certification:	This paper reports on original research I conducted during the period of my Higher Degree by Research candidature and is not subject to any obligations or contractual agreements with a third party that would constrain its inclusion in this thesis. I am the primary author of this paper.		
Signature		Date	21/1/19

Co-Author Contributions

By signing the Statement of Authorship, each author certifies that:

i. the candidate's stated contribution to the publication is accurate (as detailed above);

ii. permission is granted for the candidate in include the publication in the thesis; and

iii. the sum of all co-author contributions is equal to 100% less the candidate's stated contribution.

Name of Co-Author	Stefan K. Hetz		
Contribution to the Paper 15%	Collected and maintained study species, undertook fieldwork and contributed to the development of experiments, and reviewed and edited manuscript drafts.		
Signature		Date	29/01/2019

Name of Co-Author	Roger S. Seymour		
Contribution to the Paper 20%	Undertook experiments and field work, and reviewed and edited manuscript drafts.		
Signature		Date	29/01/2019

1. Abstract

The aquatic bug *Aphelocheirus aestivalis* (Fabricius 1794) utilises a plastron, a thin bubble layer on the surface of its body to extract O_2 from the water. Millions of tiny hairs keep the bubble from collapsing, enabling the bug to remain submerged indefinitely. The development of fibre optic O_2-probes has allowed measurements of O_2 pressure (PO_2) surrounding the plastron, and within the plastron, although only for short periods. Here we developed methods to continuously measure plastron PO_2, and investigate how it is affected by temperature (15, 20, 25°C), activity, and water circulation. We also made measurements of water PO_2, temperature and velocity in the field and swimming velocity at the treatment temperatures. Results show that plastron PO_2 is inversely related to temperature, associated with differences in metabolic demand, and that small bouts of activity or changes in water convection result in rapid changes in plastron PO_2. A model was developed to calculate the conditions under which *Aphelocheirus* would exist without becoming O_2-limited in relation to water temperature, PO_2 and boundary layer thickness. This model suggests that *Aphelocheirus* at one of two field sites may have a reduced metabolic scope even in well convected water in association with low O_2 and moderate temperature, and that in well convected, air-saturated water, bugs may have a reduced metabolic scope where water temperatures are between 20 and 25°C. If exposed to 5 kPa PO_2, *Aphelocheirus* cannot sustain resting metabolic rate even in well-convected water and would die at temperatures above approximately 25°C.

2. Introduction

Insects have evolved in a terrestrial environment as reflected by their gas filled tracheal systems (Pritchard et al., 1993). Despite this, several insect groups have made their way into aquatic environments often for part of, or occasionally, all of their life cycles (Wallace and Anderson, 1996). Many aquatic insects utilise a bubble on the surface of their bodies in contact with the tracheal system to facilitate their excursions underwater (Ege, 1915). These bubbles can function both for respiratory and buoyancy purposes (Ege, 1915; Matthews and Seymour, 2006). The bubbles are regarded as either *air stores* or *gas gills*, although there is a continuum between them (Jones et al., 2015; Rahn and Paganelli, 1968; Seymour and Matthews, 2013; Vlasblom, 1970). Air stores are air bubbles collected from the water's surface from which O_2 can be consumed during a dive underwater, although they require replenishment at the surface once the O_2 becomes depleted (e.g. Dytiscidae) (Kehl, 2014). Gas gills are bubbles that allow O_2 to be passively extracted from the water during the dive, of which there are two types, compressible (e.g.Corixidae, Notonectidae) and incompressible or plastrons (e.g. Elmidae, Aphelochiridae) (Hinton, 1969; Marx and Messner, 2012; Rahn and Paganelli, 1968). Compressible gas gills enable O_2 uptake from the water because respiration creates a difference in O_2 partial pressure (P_{O_2}) across the bubble surface (Ege, 1915; Rahn and Paganelli, 1968). The P_{O_2} within the bubble declines below the surrounding water and O_2 diffuses down its P_{O_2} gradient into the bubble. Due to Dalton's law of partial pressures, P_{N_2} within the bubble then increases above the surrounding water, and N_2 diffuses out of the bubble but at a slower rate than O_2 in, thus allowing more O_2 gain than N_2 loss in a given period. However, due to the loss of N_2 and CO_2 to the water and consumption of O_2, compressible gas gills have a limited lifetime and require replenishment at the surface. In contrast, plastrons can be maintained indefinitely. Plastrons are a thin gas layer over part of the body where the gas-water interface is held constant by a tightly packed hair or scale layer (Flynn and Bush, 2008; Marx and Messner, 2012; Thorpe and Crisp, 1947a). As O_2 is consumed from the plastron the volume of gas remains constant due to the force of the hairs against the air-water interface, causing a decrease in both P_{O_2} and total pressure. This results in continued uptake of O_2 from the water, but because volume is constant, there is no net loss of N_2 to the water and the bubble can be maintained *ad infinitum* (Seymour and Matthews, 2013).

Plastron respiration can be investigated within the framework of Fick's general diffusion equation (Rahn and Paganelli, 1968);

$$\dot{M}_{O_2} = K_{O_2} \times A/X \times \Delta P_{O_2} \quad (1),$$

where $\dot{M}O_2$ (pmol s^{-1}) is the rate of O_2 diffusion from the water into the plastron, KO_2 (pmol s^{-1} kPa^{-1} cm^{-1}) is the Krogh's diffusion coefficient for O_2 in water, A (cm^2) is the surface area of the plastron, X (cm) is the effective thickness of the boundary layer of water above the plastron surface, and ΔPO_2 (kPa) is the difference between the PO_2 in the plastron and the bulk surrounding water.

The river bug *Aphelocheirus aestivalis* has a well-developed plastron formed by a hair pile on the surface of its body. The hairs, which are densely packed at approximately 4,000,000 per mm^{-2}, are ~3 µm tall with the top portion bent at 90° (Hinton, 1976). This hair pile can resist wetting at pressures up to 2 – 3 atm (Hinton, 1976; Thorpe, 1950). Due to the thinness of the plastron and its small gas volume, only 0.14 µl (Seymour et al., 2015), much of the previous work relating to gas exchange of *Aphelocheirus*'s plastron has been theoretical (Flynn and Bush, 2008; Rahn and Paganelli, 1968). However, recent developments in fibre-optic O_2 sensors (optodes) have allowed measurements of PO_2 within and around the plastron for short periods in response to different water convection conditions and ambient PO_2 (Seymour et al., 2015). The boundary layer thickness was approximately 500 µm in still water and 100 µm in flowing water, both values much greater than those previously used in gas gill models (8 –30 µm) (Chaui-Berlinck and Bicudo, 1994; Chaui-Berlinck et al., 2001; Rahn and Paganelli, 1968). *Aphelocheirus* often occur in fast flowing streams where forced convection of water reduces the boundary layer thickness, thereby increasing conductance of O_2 into the plastron (Polhemus and Polhemus, 1988; Seymour et al., 2015; Thorpe, 1950). Nevertheless, the severe restrictions imposed by boundary layer resistance, apparently reduce the metabolic rates of *Aphelocheirus*, and indeed many insects utilising plastrons, in comparison to insects that respire in air (Seymour and Matthews, 2013).

Our previous study on *Aphelocheirus aestivalis* was performed at only one temperature (20 °C) (Seymour et al., 2015). Because temperature affects metabolic rate, it should change the factors of Fick's diffusion equation that could lead to O_2 diffusion limitation. In particular, rising temperature has been associated with an increasing mismatch between O_2 demand and O_2 supply in aquatic animals, which results ultimately in aerobic failure leading to death (Pörtner, 2010). This paradigm has been applied to *Aphelocheirus aestivalis*, as an example of an obligate aquatically-respiring insect, and the critical thermal maximum decreased under hypoxia (5 kPa) and increased slightly under hyperoxia (60 kPa) (Verberk and Bilton, 2015). Measurements of plastron PO_2 in relation to temperature, convection and activity can aid understanding of the limitations of plastron respiration.

Our previous study permitted measurements of plastron P_{O_2} for only short periods, because the optode made connection with plastron gas *via* a small bubble which would shrink and disconnect from the plastron after a few minutes (Seymour et al., 2015). The present study allows continuous measurements of plastron P_{O_2} associated with activity and water circulation. We also measure swimming velocity, relating these data to field measurements of water P_{O_2}, temperature and flow velocities to offer an understanding of boundary layer characteristics under natural conditions. Our results, in addition to those of previous studies, provide information about links between plastron function and environment, and where limitations to the plastron may exist in relation to temperature, aquatic P_{O_2}, and convection.

3. Methods and materials

Animals

Aphelocheirus aestivalis were collected from the Warnow River and a tributary of the Schweriner See in northern Germany in July and August 2015. They were kept in aquaria at approximately 18°C with 12 h day night cycle. Prior to experiments bugs were blotted with tissues and weighed to 0.1 mg with an analytical balance (1201 MP2, Sartorius GmbH, Göttingen, Germany).

Plastron P_{O_2}

Plastron and water P_{O_2} were measured with two, temperature compensated, fibre-optic O_2-sensing optodes (sensor model B2; meter model TX-3; PreSense GmbH, Regensburg, Germany) that were supported by 3D micromanipulators above a 12 L aquarium filled with air equilibrated water. Water was circulated with an air pump (Schego optimal, Schemal and Goetz GmbH & Co KG, Germany) pumping air at 250 L h^{-1} though a circular sintered glass gas diffuser in the bottom of the aquarium, and a polystyrene sheet was suspended approximately 5 cm above the surface to help maintain temperature. A refrigerated water bath (model F3, Haake Mess-Technik GmbH, Germany) circulated water through a U-shaped metal tube within the aquarium that regulated water temperature which was measured with a mercury thermometer (model 12.80, Labotherm-N, Germany). A horizontal dissecting microscope was mounted in front of the aquarium to view the bugs and optodes.

Preparation of the bugs for P_{O_2} measurement

Bugs were gently blotted with tissues before a 2 mm drop of cyanomethacrylate gel (Sekunden-gel Kleber, IDEN Berlin, Germany) was placed in between the wing buds. The bugs were then glued to a small wire stand with their ventral side facing upwards. Stands were made of thin

copper wire that had a circular base approximately 3.5 cm in diameter with wire rising from the centre (Fig. 1). The centre projection had a small bend in the end which was glued to the bug, with the head facing the middle between the other two projections. To restrict movement and stop the bug contacting the optode with its legs, the abdomen was placed through a 6 – 8 mm slit in a 20-mm square piece of 2 mm mesh fabric to the base of the third pair of legs and the mesh secured to the other two projections in front of the head of the bug.

Once the bug was secured, a ~20 mm piece of PVC tubing (I.D. 0.25 mm, O.D. 0.6 mm; called the “plastron tube”) was glued at one end with cyanomethacrylate gel over a spiracular opening on a sternite perpendicular to the ventral surface. Care was taken to make sure glue was not placed over the opening of the tube, spiracle, or spread across the plastron. The bugs were then placed into the aquarium and the water level was adjusted such that they were approximately 10 mm under water, with the top of the plastron tubes above the water. If a water droplet touched the open end of the plastron tube, it was drawn into it, preventing measurement of P_{O_2}. Therefore, a plastic shield around the preparation prevented droplets from popping bubbles from hitting the open tube. The tube was then cut at an angle and orientated vertically, which allowed insertion of the optode. Orientation of the tube could be manipulated by bending the wire at the base of the stand. The tip of the optode was lowered into the opening of the plastron tube until the first protective sheath of the optode fibre was inside the opening. Then a small amount of high viscosity vacuum grease (Beckman Instruments, Part no. 270-456248-A, Palo Alto, CA, USA) was placed around the opening of the tube, sealing the gas inside the tube and plastron from the atmosphere. Lower viscosity greases were sucked in by the negative pressure within the plastron. Once sealed, there was a 10 – 15 min equilibrium period where the P_{O_2} within the plastron declined in an exponential curve from atmospheric level, after which some measurements took place for up to 6 h.

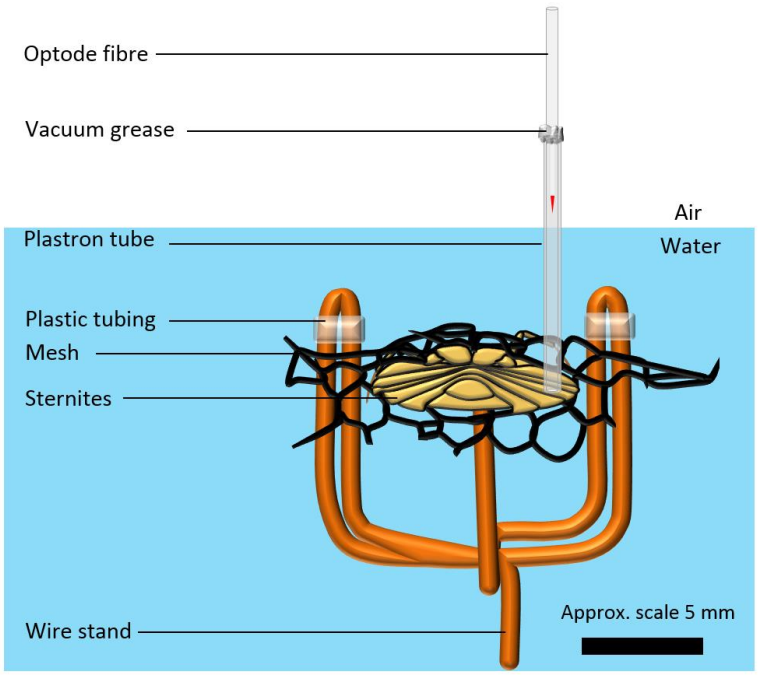

Figure 1. *Aphelocheirus* mounted on the top of a wire stand ready for measurement of plastron P_{O_2}. The bug is being viewed from the posterior slightly above the coronal plane where the sternites can be seen. The bug is glued to the wire stand between the wing buds from the centre projection. The plastron tube is glued to the surface hairs of the plastron, establishing a gas connection between the tube and the plastron gas. The optode fibre sealed into the tube measures P_{O_2} equilibrating with the plastron gas.

Temperature and circulation treatments

Once bugs were in the aquarium they were cycled through three temperature treatments, 15, 20 and 25°C. Water temperature required 30 – 40 min to stabilize after each adjustment. The plastron P_{O_2} for a given treatment was calculated as the mean value recorded over an approximately 10 min period. Leg movements of the bugs were used to describe whether they were either quiescent or active during the period. Activity would also result in a P_{O_2} trace with peaks and troughs, whereas P_{O_2} would remain stable if bugs were inactive (Fig. 2). During each temperature treatment, plastron P_{O_2} was measured in convected water and then in stagnant water by turning off the air pump.

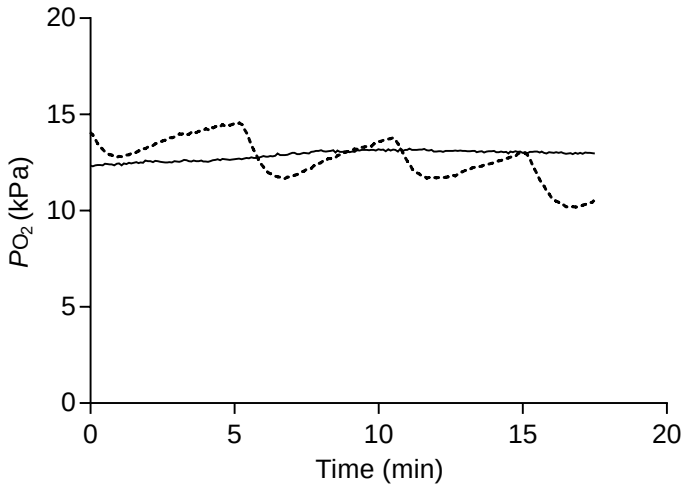

Figure 2. Continuous plastron P_{O_2} measurements from *Aphelocheirus* showing a quiescent bug (solid line) and the same bug with bouts of activity (dashed line) in circulated water, both at ~20°C. Declines in the active trace indicate activity such as leg movements, followed by slow rises during inactivity.

Swimming velocity

Swimming velocity was determined at the same three temperatures by placing a male and a female bug into a clear plastic aquarium (42 (L) × 26.5 (W) × 19 (H) cm) containing water 2 cm deep. A 1 × 1 cm grid was under the bottom of the aquarium and a video camera (GX-PX1, JVC, Yokohama, Japan) set to 30 frames s^{-1} was fixed 50 cm above. The swimming bugs were then filmed for 5 min. If the bugs stopped swimming they were gently touched with a piece of plastic. The same five pairs of bugs were exposed to each treatment. Between experiments they were placed in to a small amount of water within beakers with a small piece of paper towel which they could cling to.

Video data were analysed by removing every 10^{th} video frame with a media player (VLC media player, Version 2.2.3, USA) then tracking the bugs in ImageJ (Version 1.50i, Wayne Rasband, NIH, USA) with the MTrackJ plugin (Meijering et al., 2012). The 3 s after the bugs were placed into the aquarium and any data where encouragement of the bugs to swim influenced velocity measurements were ignored. The mean values for the ten highest velocity measurements over the 0.33 s between frames for each bug were used to produce a grand mean for each treatment temperature, and the single highest measurements for each bug were pooled to produce a mean peak value for each treatment.

Limnology

Surface water velocities at Warnow River and the tributary of the Schweriner See were estimated by placing a 3 × 3 cm piece of water-filled urethane foam at the water's surface and recording the time taken to travel 3 m with a stopwatch. P_{O_2} measurements were taken with an optode that was housed in an apparatus that could sample water from within 1-2 cm of where the bugs reside in the gravel substrate or plants. River water was sucked with a 100 ml syringe into a 23 cm long rigid tube (ID = 2 mm, OD = 6 mm), which had a piece of fabric over the opening. An optode was installed in the tube and led to the data acquisition unit (TX-3) that was connected to a laptop computer and powered with a 12 VDC battery. Water temperature was measured with the temperature probe associated with the TX-3 instrument. Measurements were taken on the 12th of August 2015, with P_{O_2} measurements taken at approximately 8 am at the Schweriner See tributary, and 1:30 pm at the Warnow River.

Statistics

Linear regressions, ANOVA, *F*-tests, *t*-tests and Tukey's post-hoc tests were conducted with Graphpad Prism 6 (GraphPad Software Inc., La Jolla, CA, USA). ANCOVA (Zar, 1998) and Johnson-Neyman tests (White, 2003) were conducted with a Bonferroni correction applied to account for multiple comparisons. Reported statistics are means and 95% confidence intervals and bands.

4. Results

Animals

Mean mass of bugs used for plastron P_{O_2} measurements was 51.5±3.4 mg (N=18). Females were significantly larger (55.0±4.3 mg, N=11) than males (46.0±2.3 mg, N=7, *t*-test, P<0.05).

Plastron P_{O_2}

Continuous plastron P_{O_2} traces showed effects of activity, cessation and initiation of water circulation, and changes in temperature on plastron P_{O_2} (Fig. 3). The trace in Figure 3 shows the plastron P_{O_2} of an inactive bug initially at 25°C. P_{O_2} is stable at 12.5 kPa until ~5.5 min when water circulation is turned off and plastron P_{O_2} declines rapidly, becoming more stable between 11 – 14 min at 4 kPa. Movement of the bug at 14 min is associated with another decline and stabilisation of P_{O_2} at ~ 2.7 kPa, before convection is resumed and water temperature is set to 20°C. Plastron P_{O_2} rapidly increases, slowed briefly when the bug is momentarily active. Two bouts of activity at 28 and 37 min are indicated by rapid declines in plastron P_{O_2} by 2 – 3 kPa. At

60 min water temperature is 20°C and the plastron P_{O_2} of the now inactive bug becomes stable at 13.1 kPa.

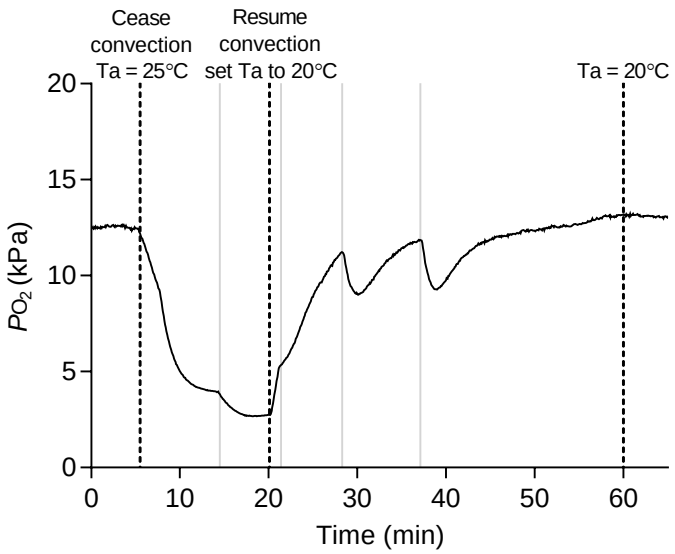

Figure 3. Example of a continuous plastron P_{O_2} trace from *Aphelocheirus*. Initially, this bug is inactive in convected water. Water circulation ceases at 5.5 min associated with a steep decline in plastron P_{O_2} that stabilises at ~2.7 kPa prior to resumption of convection at 20 min, when water temperature is adjusted to 20°C. Grey lines indicate when the bug was momentarily active resulting in a decline in plastron P_{O_2}.

Mean plastron P_{O_2} of inactive bugs in convected water was 16.8±1.3 kPa at 15.1±0.1°C (*N*=14), 14.2±1.2 kPa at 20.3±0.2°C (*N*=23) and 10.6±2.1 kPa at 25.1±0.2°C (*N*=15), with a linear slope of -0.6±0.2 kPa °C^{-1} (Fig. 4). 15°C and 20°C treatments were not significantly different from each other, however the 25°C treatment was significantly lower than the 15°C and 20°C treatments (ANOVA, Tukey's post-hoc, *P*<0.05). Active bugs in convected water showed mean values of 9.3±2.3 kPa at 15.2±0.2°C (*N*=13), 9.2±2.1 kPa at 20.3±0.3°C (*N*=8) and 7.1±3.1 kPa at 25.2±0.2°C (*N*=6), with a slope of -0.2±0.4 kPa °C^{-1}. Bugs in stagnant water were generally inactive (21 of 26 individuals were inactive during measurements) and had a much lower plastron P_{O_2}, with mean values of 2.9±1.4 kPa at 14.9±0.2°C (*N*=7), 2.2±0.7 kPa at 20.1±0.1°C (*N*=10) and 1.8±0.3 kPa at 25.1±0.1 °C (*N*=9), with a linear slope of -0.1±0.1 kPa °C^{-1}. No significant differences in plastron P_{O_2} were found between the three temperatures, in either active bugs in convected water or inactive bugs in stagnant water (ANOVA, Tukey's post-hoc, *P*>0.05). Slope of decline of plastron P_{O_2} with rising temperature in inactive bugs in convected water was significantly different from zero (*F*-test, *P*<0.0001), active bugs in circulated water, and those in

stagnant water (ANCOVA, Table 1). Slopes for active bugs and those in stagnant water were not significantly different from each other or zero (*F*-test, *P*>0.05). Regression elevation of plastron P_{O_2} were significantly higher in inactive bugs in circulated water than active bugs in circulated water (Johnson-Neyman test, significant below 24.6°C) and elevation was significantly lower in bugs in stagnant water than both other groups over the experimental range of temperatures (ANCOVA, J-N test, Table 1).

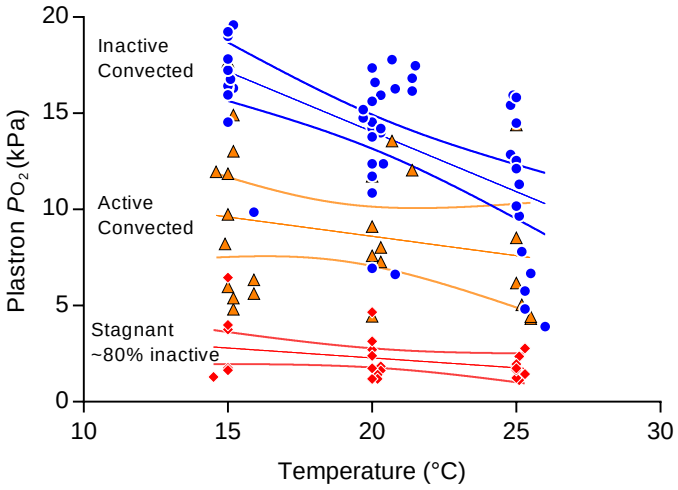

Figure 4. Plastron P_{O_2} of *A. aestivalis* when exposed to the 15, 20 and 25°C treatments. Data separated into inactive (*N*=52, blue) and active (*N*=27, orange) bugs in convected water, and bugs in stagnant water (*N*=26, red, 21 of 26 bugs inactive). The linear regressions are P_{O_2} = -0.6 *T*+26.5 (R^2=0.36) for inactive bugs, P_{O_2} = -0.2 T+2.6 (R^2=0.05) for active bugs, and P_{O_2} = -0.1 T+4.3 (R^2=0.11) for bugs in stagnant water. 95% CI bands for the regressions are shown. Water was air saturated, with P_{O_2} values of approximately 20.9 kPa at 15°C, 20.7 kPa at 20°C and 20.6 kPa at 25°C.

Table 1. ANCOVA comparisons between regressions of plastron P_{O_2} and temperature. If slopes are significantly different, the region of non-significance according to the Johnson-Neyman test† are provided.

Regression comparison	Slope	Elevation, or region of non-significance	*F*-value
Inactive vs active	*P*=0.01*	above 24.6°C†	$F_{1,75}$=6.934
Inactive vs stagnant	*P*<0.001*	above 30.6°C†	$F_{1,74}$=18.21
Active vs stagnant	*P*=0.40	*P*<0.001*	$F_{1,49}$=69.67

* Statistically significant

† Region of non-significance according to Johnson-Neyman test.

Nine paired sets of data from inactive bugs in circulated water were extracted from the full data set (Fig. 4) and produced values of 16.6±2.0 kPa at 15°C, 14.5±2.2 kPa at 20°C and 11.9±2.4

kPa at 25°C. All treatments are significantly different from one another (Pairwise ANOVA and Tukey's post-hoc, $P<0.05$, Fig. S1).

Swimming velocity

The grand mean of the ten highest recorded swimming velocities for each bug ($N=8$) were 8.1±1.2 cm s^{-1} at 15±0.4°C, 8.2±2.1 cm s^{-1} at 20.0±0.2°C, and 9.7±1.2 cm s^{-1} at 25.2±0.2°C (labelled "mean" in Fig. 5). The mean peak velocities produced from the single highest measurement from each bug were 10.3±1.6 cm s^{-1} at the 15°C treatment, 11.1±3.0 cm s^{-1} at 20°C, and 12.3±1.7 cm s^{-1} at 25°C (labelled "peak" in Fig. 5). No significant differences exist between treatments within the "mean" or "peak" mean values (Pairwise ANOVA, $P>0.05$)).

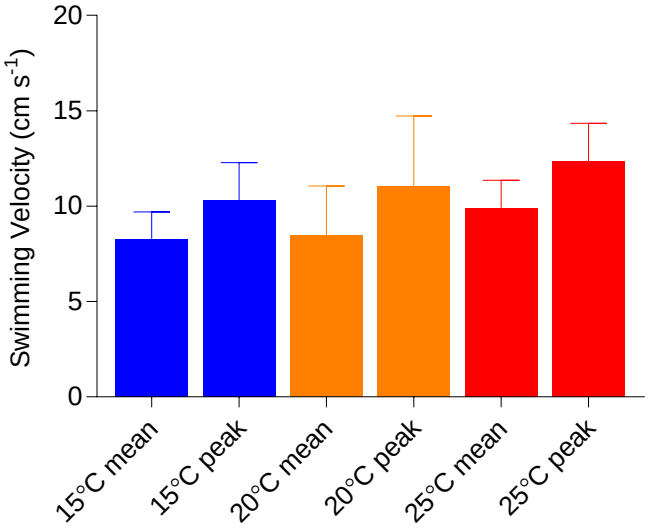

Figure 5. Paired mean maximum and peak swimming velocity measurements of *Aphelocheirus* (*N*=8 bugs). Mean maximum velocity values are calculated as the average of the highest ten velocity measurements for each bug, and peak velocity is the single highest measurement for each bug. Grand means shown with 95% CIs.

Limnology

Surface water velocities in the Schweriner See tributary were found to be 65 cm s^{-1} ($N=4$ for local sites of bug collection with 3 replicates each) with mean water depths of 16 cm ($N=6$), ranging from 10 to 20 cm. Water temperature was 19.2°C and the mean PO_2 was 17.5 kPa (range 17.3–17.7 kPa) within 1–2 cm of the substrate. Bugs were found in fast-flowing sections that formed between rocks with gravel substrate. In the Warnow River, where larger numbers of bugs were caught, mean water velocities were 67 cm s^{-1} ($N=3$ for local sites of bug collection with 3 replicates each), with a mean water depth of 13 cm ($N=3$) ranging from 9 to 20 cm. Water

temperature was 19.7°C and P_{O_2} 13.6 kPa (N=4). These bugs were in dense trailing aquatic plants (*Ranunculus aquatilis*) that covered a gravel substrate where water ran rapidly around rocks and obstacles.

5. Discussion

Metabolic rate, temperature and convection

This investigation shows that increased metabolic rate of *Aphelocheirus* results in a decreased P_{O_2} in the plastron gas, which increases the P_{O_2} difference between the water and plastron (ΔP_{O_2}) and increases the rate of O_2 diffusion from the water. The effect is evident when metabolic rate is increased with temperature in resting bugs (Fig. 4 and S1) and during activity (active data in Fig. 3 and 4). Measurements of plastron P_{O_2} can allow the metabolic rate of the insect to be estimated by using Eq. 1 and assuming boundary layer thicknesses measured in our previous study (Seymour et al. 2015). In particular, we assume that at 15, 20 and 25°C, respectively, air-equilibrated water P_{O_2} is 20.87, 20.74 and 20.56 kPa (the P_{O_2} changes associated with temperature are due to changes in water vapour pressure), and Krogh's coefficients of diffusion in water are 0.262, 0.277 and 0.290 pmol s^{-1} kPa^{-1} cm^{-1} (Seymour, 1994), plastron surface area is A=0.66 cm^2, and boundary layer thicknesses are 100 µm for circulated water with inactive and active bugs, or 500 µm for bugs in stagnant water (Seymour et al., 2015). The calculated O_2-consumption rates clearly increase with both rising temperature and activity (Fig. 6).

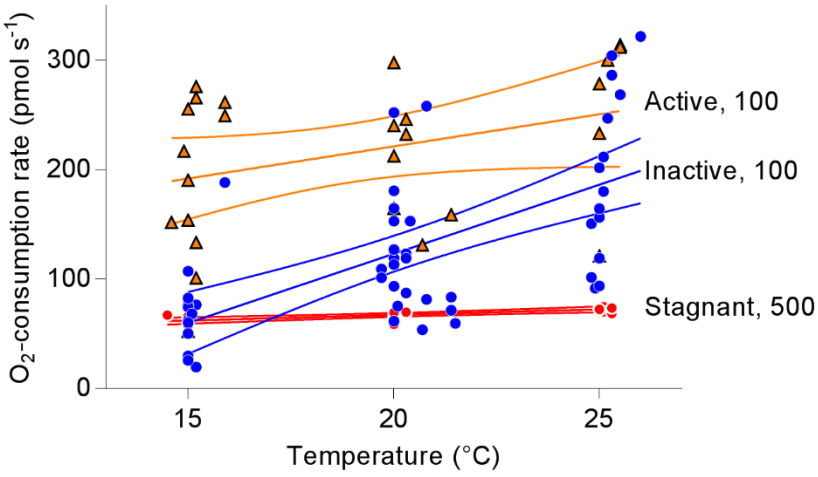

Figure 6. Metabolic rate calculated with Eq. (1) from measured plastron P_{O_2} data (Fig. 4) with assumed boundary layer thickness listed next to each group, with 100 µm indicating convected water, and 500 µm stagnant water. 95% CI bands shown, see text for details.

The relationship between increasing temperature and plastron P_{O_2}, is probably not linear as shown. Metabolic rate is expected to increase exponentially with temperature in ectotherms and therefore plastron P_{O_2} should decline curvilinearly with increasing metabolic rate. Moreover, higher temperatures reduce the viscosity of water and would be expected to increase conductance into the plastron by increasing convection velocity and reducing boundary layer thickness, and therefore permit higher metabolic rates. Also the high variability is associated with an inability to control the micro-convective environment surrounding the bugs, influencing the boundary layer thickness. Small differences in orientation of the bugs, how the fabric mesh was placed over the bugs, and position within the aquarium, could all contribute to variation.

Despite the variability, we can calculate the temperature coefficient (Q_{10}), the factor by which metabolism increases with a 10°C temperature rise. For all data, the values are 3.1 between 15 and 20°C, 2.6 between 20 and 25°C, and 2.8 between 15 and 25°C, and for the paired data, the values are 2.5 between 15 and 20°C, 2.2 between 20 and 25°C, and 2.3 between 15 and 25°C (Figs. 6 and S2). Verberk and Bilton's (2015) data show a Q_{10} of 2.3 between 5 and 10°C, 3.0 between 10 and 15°C and 2.6 between 5 and 15°C.

Bugs in stagnant water have both low plastron P_{O_2} and low metabolic rate unlike those in convected water (Fig. 4 and Figure). The lack of water convection over the surface of the plastron causes the boundary layer thickness to increase (Seymour et al., 2015). The inability of bugs to be able to move in our experiments is however an unnatural condition. If a bug found itself unrestrained in stagnant water simply moving would thin the boundary layer allowing a higher metabolic rate (Seymour et al., 2015). The plastron P_{O_2} measurements from this study at 20°C (2.2±0.7 kPa) do not differ significantly from those measured previously (2.0±0.9 kPa, Seymour et al., 2015). These P_{O_2} values are apparently near levels that cause O_2-diffusion-limitation in the tracheal system of *Aphelocheirus*. Thorpe and Crisp (1947a) calculated the decline in P_{O_2} though the O_2 cascade from the water through the plastron, tracheal system, and to the tissues. Despite underestimating the decline through the boundary layer their estimate of P_{O_2} decline from the plastron to the tissues of 2.4 kPa is reasonable and align with our plastron P_{O_2} measurements in stagnant water (Seymour et al., 2015). The point at which metabolic rate becomes limited by P_{O_2} is called the critical P_{O_2} ($P_{O_{2crit.}}$). These estimates of $P_{O_{2crit.}}$ for *Aphelocheirus* are similar to that of water boatmen (2.1 kPa) (Matthews and Seymour, 2010).

Continuous measurements of plastron P_{O_2}, shown in Figures 2 and 3, highlight how changes in convection and activity influence plastron P_{O_2}. Bouts of activity cause a rapid decline in plastron

P_{O_2} that returns more slowly to an equilibrium P_{O_2} when the insect becomes inactive again. Cessation of water convection also contributes to a rapid decline in plastron P_{O_2} and the boundary layer becomes thicker. The equilibrium times between the plastron tube and plastron in this study (10 – 15 min), after initial set up, were longer than those of our previous study (1.5 – 4 min), which used a small bubble on the tip of a tube placed over the end of the optode fibre, which was pushed down onto the plastron to make a gas connection (Seymour et al., 2015). This is explained by the difference in length of the tube on the optode used in this study (~20 mm) containing ~2.8 times more air compared to that in the previous study (5 mm). The longer tube results in a longer equilibrium time.

The boundary layer thickness surrounding the plastron is determined by the O_2 demand of the respiratory surface and convection of the fluid next to the surface. In *Aphelocheirus*, the plastron can be convectively ventilated by either being in moving water or moving through it. The maximum swimming velocity of *Aphelocheirus* is between 11 and 13 cm s^{-1} with no significant differences between temperatures (Fig. 5). The lack of increase in swimming velocity with temperature is contrary to predictions. Locomotion velocity in other insects increases with temperature, consistent with the relationship between temperature, metabolic rate, and the kinetic properties of muscles (Gibert et al., 2001; Hurlbert et al., 2008; Marden and Kramer, 1994). However, *Aphelocheirus* is generally observed crawling on the substrate, and although water viscosity decreases with rising temperatures, which could enable higher swimming velocities, bugs may swim at a similar velocity but at a reduced energetic cost. Swimming velocities of *Aphelocheirus* are comparable to that of similarly sized (6.9 – 11.9 mm) aquatic beetles with swimming velocities between 6.7 – 12.5 cm s^{-1} (Hygrobiidae and Dytiscidae) (Ribera et al., 1997). Our earlier work showed that the boundary layer is 500 µm thick in stagnant water and declines to 200 µm with estimated water velocities of ~0.25 cm s^{-1}, and to 100 µm at ~0.58 cm s^{-1} (Seymour et al., 2015). These data indicate that the boundary layer thickness would decline below 100 µm at maximum swimming velocities enabling the high metabolic rates associated with swimming.

Surface water velocities can further exceed swimming velocity, with rates between 10 – 67 cm s^{-1} recorded at the locations sampled from our study. However, *Aphelocheirus* resides within the fluvial hydrodynamic boundary layer, a layer where water velocity is reduced in comparison to the free flowing water above the substrate or surface. The thickness of the hydrodynamic boundary layer is arbitrarily defined as the distance from a surface to a distance above the surface where the water velocity is 99% of the free flowing fluid (Vogel, 1994). The thickness of this layer is

dependent on structure of the surface and water velocity (Hoerner, 1965), but flow above stony substrates is complex and not predictable from theories based on laminar flow next to smooth surfaces (Carlson and Lauder, 2011). Nevertheless, it is clear that the velocities near *Aphelocheirus* are much lower than measured at the surface. Stony substrates characterise the stream at the Schweriner See, and in the Warnow River, bugs were found in long trailing aquatic plants. Hydrodynamic boundary layers that form over plant patches vary depending on morphology of the plants; however, plants with long streamlined leaves have higher water velocities around them than those with large leaf surface areas and bushy structures (Sand-Jensen and Mebus, 1996). By residing within the hydrodynamic boundary layer, *Aphelocheirus* can still have sufficient water flow to convect the gas boundary layer over the plastron as well as avoiding high flow velocities that exceed its maximum swimming speed that could wash the insect away.

Respiratory limitation and environment

Predictions about environmental conditions in which *Aphelocheirus* may exist without O_2 limitation can be made with information gained from this and previous studies. Further utilisation of Fick's law allows estimates of water temperatures, water P_{O_2}, and boundary layer thicknesses that enable aerobic metabolism and provide a predicted ecological envelope. The ambient water P_{O_2} required to maintain a given O_2-consumption rate can be calculated according to $P_{O_{2water}} = P_{O_{2plastron}} + \dot{M}_{O_2}/(A/X)/K_{O_2}$, a rearrangement of Eq. 1. Here $\dot{M}_{O_2}$ is based on actual measurements, with a resting $\dot{M}_{O_2}$ of 30 pmol s^{-1} and a maximum rate ten times higher at 300 pmol s^{-1} at 20°C (Seymour et al., 2015) and assuming a Q_{10} of 2.5 across a temperature range of 5–35°C (Verberk and Bilton, 2015). K_{O_2} values are given above. Plastron P_{O_2} is assumed to be constant at either 2 kPa, the measured $P_{O_{2\,crit.}}$ for resting bugs (Matthews and Seymour, 2010; Seymour et al., 2015; Thorpe and Crisp, 1947b) or 5 kPa for bugs at their maximum metabolic rate during swimming. Conductance of the tracheal system can increase with activity (Wigglesworth and Lee, 1982), and 5 kPa is approximately the $P_{O_{2\,crit.}}$ for jumping grasshoppers, *Melanoplus differentialis* and *Trimerotopic pallidipennis* (Harrison et al., 2006), a similar activity to swimming. Water P_{O_2} can then be calculated over the temperature range at different boundary layer thicknesses (X = 100, 200, 300, 400 and 500 µm), where surface area A = 0.66 cm (Seymour et al., 2015). These results are shown in Figure 7.

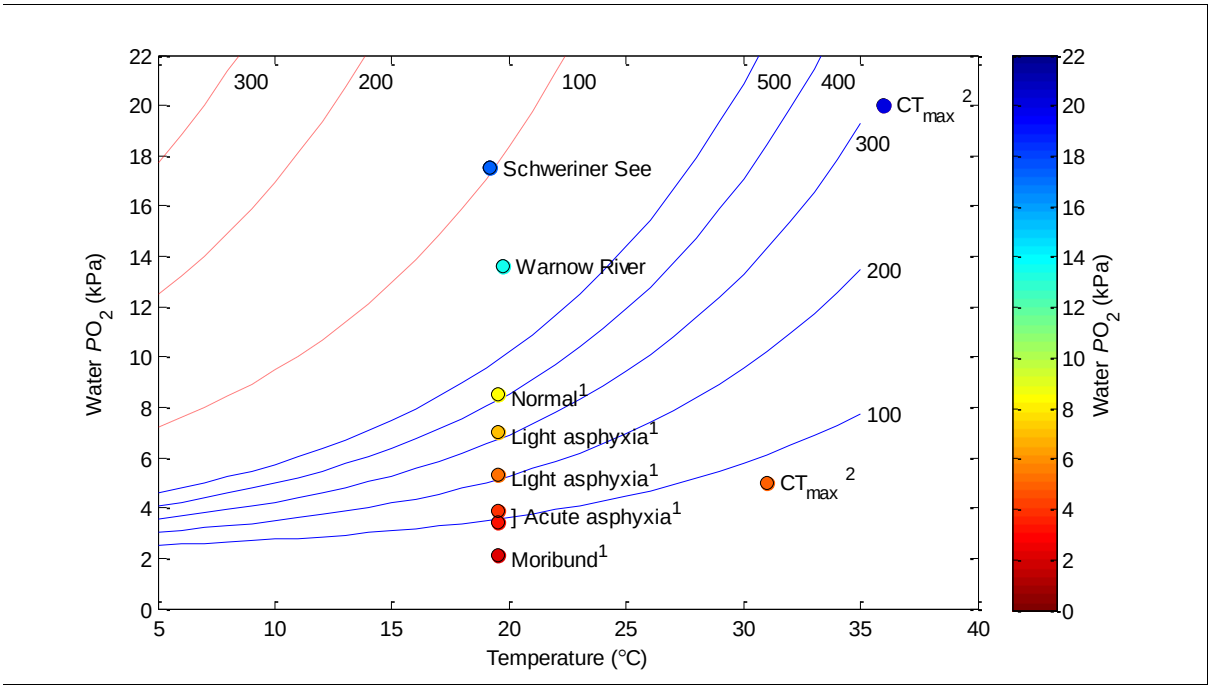

Figure 7. Calculated minimum water P_{O_2} required for Aphelocheirus to maintain O_2-consumption rate without limitation (indicated by lines) with rising temperatures and boundary layer thickness (noted at the right end of each line in µm). Any P_{O_2} above a line allows metabolism without diffusion limitation. Blue solid lines indicate resting O_2-consumption rate and a critical plastron P_{O_2} of 2 kPa. Red dashed lines represent the maximum O_2-consumption rate and a critical plastron P_{O_2} of 5 kPa. Schweriner See and Warnow River points indicate mean water temperatures and P_{O_2} recorded in the field from this study. [1] Symbols for behavioural observations of *Aphelocheirus* exposed to selected P_{O_2}: Normal, light and acute asphyxia, and moribund (Thorpe and Crisp, 1947a). [2] Maximum critical temperatures (CT_{max}) recorded for *Aphelocheirus* at 5 and 20 kPa P_{O_2} (Verberk and Bilton, 2015).

Each curve in Figure 7 represents the minimum water P_{O_2} at a given temperature and boundary layer thickness required to maintain the resting and maximum O_2-consumption rates. Measurements of mean water temperature and P_{O_2} from the Schweriner See tributary and Warnow River are compared to these results. These data indicate that at both locations the water P_{O_2} is sufficient to maintain resting metabolism even in stagnant water, e.g. X = 500 µm, as both points are above the resting metabolism curves. Maximum metabolic rate in well convected water (X = 100 µm) in Schweriner See bugs can also be supported, however, maximum metabolic rate may be limited in Warnow River bugs, because P_{O_2} is insufficient to satisfy a tenfold rise in metabolism.

Thorpe and Crisp (1947b) placed three *Aphelocheirus* into 200 mL jars and undertook several experiments where bugs were exposed to different P_{O_2} levels at 18 – 21 °C. They observed the bugs' behaviour during the experiments (75–160 min) and arbitrarily assessed their behaviour every few minutes. Figure 7 shows these P_{O_2} levels and the poorest behavioural conditions

observed over the duration of each experiment. Condition of the animals deteriorates progressively from “normal” at 8.5 kPa to “moribund” at 2.1 kPa. These data correlate well to estimates of resting bugs in moderately convected water. However, the actual boundary layer thickness these bugs experienced is not known.

Modelling in this study has only considered factors associated with Fick’s law and their relationship to temperature. Between 5 and 35°C, the Krogh’s coefficient, the product of capacitance and diffusivity, increases by 43% (Seymour, 1994) and O_2-consumption rate increases by ~1460%. However, water viscosity has not been considered and declines by ~50%, therefore at a constant water velocity, boundary layer thickness is reduced. Hydrodynamic boundary layer models, opposed to diffusion boundary layers, take into consideration water viscosity, water velocity, characteristic length (distance from the leading edge of a flat plate or insect length), and whether flow is turbulent or laminar (Levich, 1962; Statzner, 1988). Additionally, surface structure and morphology of the animal over which a fluid flows influences boundary layer thickness. These complexities make boundary layer modelling difficult (Pinder and Feder, 1990; Vogel, 1994). In an idealised situation with laminar flow, a hydrodynamic boundary layer would decline by 31% between 5 and 35 °C, according to $5(VL/U)^{1/2}$ where V is kinematic viscosity, L is characteristic length and U is water velocity (Jennissen et al., 1999). If this is applied to Figure 7, a boundary layer of 100 µm at 5 °C, at the resting O_2-consumption rate, declines to 69 µm at 35 °C with the increase in the water P_{O_2} required to sustain aerobic metabolism declining from 3.1 times greater at 35 °C, to 2.3 times. At maximum metabolic rate, the difference changes from 8.2 times to 5.8 times. The model in Figure 7 is based on data in the middle of the temperature range (20°C), so the size of the error associated with not taking into account viscosity is reduced in comparison to data based at either extreme of the temperature range.

The O_2- and capacity-limited thermal tolerance (OCLTT) hypothesis proposes that thermal tolerance is set by a mismatch between O_2 supply and O_2 demand at temperature extremes, therefore influencing the temperature dependant performance curve (Pörtner, 2001; Verberk et al., 2016). This makes the OCLTT attractive to understand current and future impacts of climate change, both at an individual and ecosystem level (Bozinovic and Pörtner, 2015). However, the generality of the hypothesis has been debated and much of the support comes from aquatic arthropods (Bozinovic and Pörtner, 2015; Clark et al., 2013; Verberk et al., 2016). Verberk and Bilton (2015) used *Aphelocheirus* and closely related *Ilyocoris cimicoides* to test if the OCLTT hypothesis is associated with respiratory control. *Ilyocoris* uses a compressible gas gill and

therefore can take up O_2 from the atmosphere. They exposed both species to 5, 20 and 60 kPa aquatic P_{O_2} and measured the critical thermal maximum (CT_{max}) under each treatment. In *Aphelocheirus*, there were significant differences in $CT_{max.}$ between all three treatments, being 36°C at 20 kPa, and slightly higher at 60 kPa, but declining to 31°C at 5 kPa. No significant differences between treatments were observed in *Ilyocoris*, however, when denied access to air a similar pattern to that of *Aphelocheirus* was observed. These data suggest that a lack of respiratory control in *Aphelocheirus* makes them more susceptible to rising temperature and a mismatch between O_2 delivery and O_2 demand. The $CT_{max.}$ at 5 kPa and 20 kPa are plotted on Figure 7. This figure shows that at 5 kPa resting *Aphelocheirus* would become O_2 limited at approximately 27°C, even in well convected water. At 20 kPa and 36°C, mild levels of boundary layer convection could maintain resting respiration without O_2 limitation. Resting metabolic rate of *Aphelocheirus* can be sustained in stagnant water of 5 kPa P_{O_2} only at temperatures below 5°C. At the 31°C CT_{max}, fast convection reducing the boundary layer below 100 µm would be required. Mean flow rate through the chambers used by Verberk and Bilton (2015) was 0.76 cm s^{-1}, although due to non-uniform flow, the bugs may have experienced higher flows. It seems likely that exposure to 5 kPa may be lethal at much lower temperatures, but over a longer period than characteristic of short-term $CT_{max.}$ measurements. It is acknowledged that the methodology can have significant impacts on comparisons of results between studies relating to $CT_{max.}$ and O_2 limitation (Boardman and Terblanche, 2015; Verberk et al., 2016). In any case, $CT_{max.}$ temperatures would never be reached by *Aphelocheirus* under current climate change scenarios, since their present distribution is limited to cool waters (Lemb and Maier, 1996; Seymour et al., 2015; Thorpe and Crisp, 1947b; Verberk and Bilton, 2015).

6. Acknowledgements

This work was supported by the Australian Government Research Training Program Scholarship; the Alexander von Humboldt Foundation; the University of Adelaide; and the Humboldt-Universität Berlin. We thank W. C. E. P. Verberk and the other reviewers for their valuable comments and suggestions for this article.

7. Supplementary material

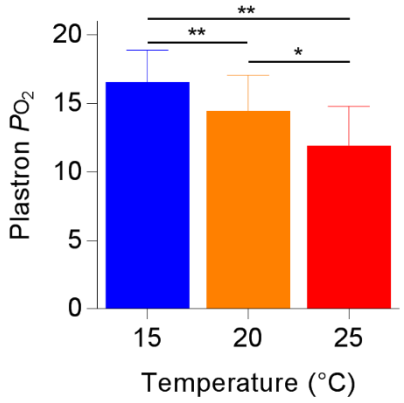

Figure S1. Pairwise plastron P_{O_2}, while inactive, in convected air equilibrated water at treatment temperatures 15°C, 20°C and 25°C (*N*=9). All temperatures are significantly different from one another (Pair-wise ANOVA, Tukey's post-hoc, $P<0.05$). Asterisks indicate statistical significance between pairs, * $P<0.05$, ** $P<0.01$.

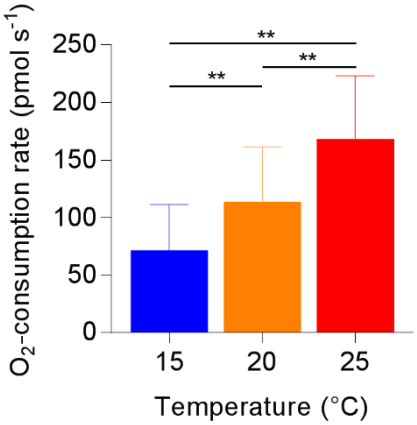

Figure S2. Predicted metabolic rate from paired plastron P_{O_2} (Fig. S1) data from inactive bugs using the same model parameters as Fig. 6, with circulated water and a 100 µm boundary layer. At the different treatment temperatures predicted metabolic rates are significantly different from one-another (Pairwise ANOVA, $P<0.05$). Asterisks indicate statistical significance between pairs, ** $P<0.01$. Means and 95% CIs shown.

Chapter Three: Cutaneous respiration by diving beetles from underground aquifers of Western Australia (Coleoptera: Dytiscidae)

Statement of Authorship

Title of Paper	Cutaneous respiration by diving beetles from underground aquifers of Western Australia (Coleoptera: Dytiscidae)
Publication Status	☑ Published ☐ Accepted for Publication ☐ Submitted for Publication ☐ Unpublished and Unsubmitted work written in manuscript style
Publication Details	Jones, K.K., Cooper, S.J.B., Seymour, R.S., 2019. Cutaneous respiration by diving beetles from underground aquifers of Western Australia (Coleoptera: Dytiscidae). Journal of Experimental Biology 222, jeb196659

Principal Author

Name of Principal Author (Candidate)	Karl K. Jones
Contribution to the Paper	Undertook field work, experiments, statistical and data analyses, and wrote the initial manuscript draft, and reviewed and edited subsequent drafts.
Overall percentage (%)	80%
Certification:	This paper reports on original research I conducted during the period of my Higher Degree by Research candidature and is not subject to any obligations or contractual agreements with a third party that would constrain its inclusion in this thesis. I am the primary author of this paper.

Signature		Date	31/1/2019

Co-Author Contributions

By signing the Statement of Authorship, each author certifies that:

i. the candidate's stated contribution to the publication is accurate (as detailed above);

ii. permission is granted for the candidate in include the publication in the thesis; and

iii. the sum of all co-author contributions is equal to 100% less the candidate's stated contribution.

Name of Co-Author	Steven J. B. Cooper		
Contribution to the Paper 10%	Undertook field work, and reviewed and edited manuscript drafts.		
Signature		Date	4/2/2019

Name of Co-Author	Roger S. Seymour		
Contribution to the Paper 10%	Conducted field work, and assisted with experimental setup and design, and reviewed and edited manuscript drafts.		
Signature		Date	1/2/2019

1. Abstract

Insects have a gas filled respiratory system, which provides a challenge for those that have become aquatic secondarily. Diving beetles (Dytiscidae) use bubbles on the surface of their bodies to supply O_2 for their dives and passively gain O_2 from the water. However, these bubbles usually require replenishment at the water's surface. A highly diverse assemblage of subterranean dytiscids has evolved in isolated calcrete aquifers of Western Australia with limited/no access to an air-water interface, raising the question of how they are able to respire. We explore the hypothesis that they use cutaneous respiration by studying the mode of respiration in three subterranean dytiscid species from two isolated aquifers. The three beetle species consume O_2 directly from the water, but they lack structures on their bodies that could have respiratory function. They also have a lower metabolic rate than other insects. O_2 boundary layers surrounding the beetles are present, indicating that O_2 diffuses into the surface of their bodies *via* cutaneous respiration. Cuticle thickness measurements and other experimental results are incorporated into a mathematical model to understand if cutaneous respiration limits beetle size. The model indicates that the cuticle contributes considerably to resistance in the O_2 cascade. As the beetles become larger their metabolic scope narrows, potentially limiting their ability to allocate energy to mating, foraging and development at sizes above approximately 5 mg. However, these beetles' ability to utilise cutaneous respiration has enabled the evolution of the largest assemblage of subterranean dytiscids in the world.

2. Introduction

Insects evolved in a terrestrial environment, indicated by their gas filled respiratory system (Pritchard et al., 1993). The tracheal system is a network of branching tubes that run from small openings (spiracles) on the outside of the insect's body through to the tissues to bring O_2 into close proximity with the mitochondria and allow CO_2 to move out. O_2 is able to diffuse through air 250,000 times faster than through water (Dejours, 1981), and in combination with gas convection, the tracheal system of flying insects supplies the highest known mass-specific metabolic rate of any animal (Snelling et al., 2017). However, insect species in several groups, including Ephemeroptera, Plecoptera, Megaloptera, Trichoptera, Odonata, Diptera, Coleoptera and Hemiptera, have become aquatic secondarily, providing challenges for the gas filled respiratory system (Foottit and Adler, 2009; Hutchinson, 1981).

Solutions to the challenge of having a gas filled respiratory system underwater include, air stores, which are bubbles taken underwater from which O_2 can be consumed during a dive, and gas gills, bubbles with a surface exposed to the water through which O_2 can diffuse, thus extending the dive. There are two types of gas gill: compressible and incompressible (plastrons). Compressible gas gills require replenishment at the surface due to both O_2-consumption by the insect and N_2 and CO_2 loss from the bubble to the water (Ege, 1915; Jones et al., 2015; Rahn and Paganelli, 1968; Seymour and Matthews, 2013). However, plastrons can be sustained indefinitely due to structures that prevent collapse of the bubble-water interface (Jones et al., 2018b; Marx and Messner, 2012; Seymour and Matthews, 2013; Thorpe and Crisp, 1947a).

In addition to air stores and gas gills, many aquatic insects use cutaneous respiration. In some insects, diffusion occurs simply across the body surface, while in others diffusion is assisted by elaborations of the cuticle that increase the conductance of O_2 into the insect, as is the case with tracheal gills and setal tracheal gills (Bäumer et al., 2000; Eriksen, 1986; Kehl and Dettner, 2009; Morgan and O'Neil, 1931; Rasmussen, 1996; Thorpe and Crisp, 1947b; Verberk et al., 2018; Wichard and Komnick, 1974). Species that utilise cutaneous respiration contend with two significant resistances to diffusion in the O_2 cascade from the water to the tissues, the boundary layer (a water layer above a respiratory surface deficient in O_2 that provides resistance to diffusion) and the cuticle. In plastron breathers, the boundary layer can provide the greatest resistance in the O_2 cascade (Seymour et al., 2015). Consequently, plastron breathers are restricted to a small size, and have lower metabolic rates than insects in general, with *Aphelochirus* being the largest known species at 40 mg (Seymour and Matthews, 2013). This size limitation is associated with the relationship between metabolic rate, surface area and

boundary layer thickness. The O_2 diffusion rate is, in part, affected by the quotient of surface area over boundary layer thickness, and as the insect becomes larger, the surface area relative to O_2 demand decreases, requiring the insects to have a thinner boundary layer to satisfy O_2 demand or have a lower metabolic rate to avoid O_2 limitation, or both.

It is, therefore, anticipated that cutaneously respiring insects, without cuticular elaboration, would have lower metabolic rates and be smaller again than plastron breathers due to the additional resistance of the cuticle to O_2 diffusion. This hypothesis could be tested with subterranean aquatic beetles, as several pieces of evidence indicate that they use cutaneous respiration. Observations of two subterranean aquatic beetles indicate they lack plastrons, have little or no gas underneath the elytra to act as an air store and they do not use gas gills (Ueno, 1957). However, subterranean aquatic beetles do have rich tracheation of the elytra and tolerate long periods of submergence, and are likely, as in some other subterranean species, to have low metabolic rates (Ordish, 1976; Smrž, 1981; Ueno, 1957). Additionally, the beetles may become trapped in interstitial spaces without air-water interfaces and would be unable to replenish their air stores (Ueno, 1957). Other than a small number of observations of these beetles' behaviour and habits (Ordish, 1976; Ueno, 1957), and quantification of the level of tracheation in the elytra of six subterranean diving beetles (Dytiscidae) (Smrž, 1981), no studies have thoroughly investigated respiration in subterranean aquatic beetles.

In Western Australia, there are more than 100 species of subterranean diving beetles described from approximately 50 isolated calcrete aquifers, representing the largest assemblage of subterranean diving beetles in the world (Balke et al., 2004; Watts and Humphreys, 2009). Each aquifer contains species of different size classes, but all species are less than 5 mm long (Balke et al., 2004; Watts and Humphreys, 2009). Most species (~75%) within each aquifer have evolved independently from separate surface dwelling ancestors, with aridification of the Australian continent, after the Pliocene, likely to be the driver of their isolation in aquifers and evolution underground (Cooper et al., 2002; Guzik et al., 2009; Leys et al., 2003). However, there is also evidence that some species diversified underground from a subterranean ancestor (Cooper et al., 2002; Leijs et al., 2012; Leys and Watts, 2008; Leys et al., 2003). The aquifers are completely enclosed and it is likely that much of each aquifer does not have an air-water interface. The lack of an air-water interface, the small size of the beetles and the apparent lack of setal tracheal gills found in some small surface dytiscids (Kehl, 2014), makes these diving beetles good candidates for cutaneous respiration.

In this study, we tested whether Australian subterranean dytiscids do use cutaneous respiration and investigated the hypothesis that cutaneous respiration limits them to small size (<5 mm). We examined respiration in three subterranean dytiscids, *Paroster macrosturtensis* (Watts and Humphreys 2006) and *Paroster mesosturtensis* (Watts and Humphreys 2006), which are sympatric sister species from the Sturt Meadows calcrete aquifer, and an independently evolved species *Limbodessus palmulaoides* (Watts and Humphreys 2006) from the Laverton Downs aquifer in Western Australia (Guzik et al., 2009; Guzik et al., 2011; Watts and Humphreys, 2006). We tested if their mode of respiration is similar to surface dwelling species that use air stores and a small compressible gas gill (Calosi et al., 2007) or whether they use cutaneous respiration. We carried out closed-system respirometry to obtain O_2-uptake measurements from all three species. In *P. macrosturtensis,* we determined the relationship between aquatic PO_2 and O_2-uptake. Fibre-optic O_2-sensing probes (optodes) were then used to measure O_2 boundary layers surrounding all three subterranean species, and scanning electron microscopy (SEM) showed they lacked structures such as pores or setae that could have respiratory significance. These results indicated the beetles use cutaneous respiration. Cuticle thickness was measured in the subterranean species as well as six surface dytiscids to determine the relationship between cuticle thickness and size. The experimental data and measurements were then integrated into a respiration model based on Fick's general diffusion equation to assess conclusions made from experimental data and understand how cutaneous respiration limits beetle size.

3. Methods and materials

Animals

P. macrosturtensis and *P. mesosturtensis* were collected during October 2015 and September 2016 from Sturt Meadows Station, and *L. palmulaoides* was collected during September 2016 from Laverton Downs Calcrete, Western Australia (WA). Beetles were captured with a 75 mm diameter plankton net attached to a fishing rod placed down boreholes into the calcrete aquifers (Borehole depth 4.03 – 9.31 m, water depth 0.50 – 5.71 m at Sturt Meadows). After capture, beetles were placed in aquifer water, into 200 ml plastic containers with some sand, small rocks, and plant roots that were retrieved in the plankton net. The containers were maintained between 20 – 28°C and transported back to Adelaide by road before being placed in a constant temperature (CT) room at 24.5 – 25.5°C in darkness. Beetles were placed into plastic aquaria (22 cm L x 13 cm W x 14 cm H) with reverse osmosis (RO) water mixed with rock salt (Australian Sea Salt Rocks, Hoyts Food Industries P/L, Moorabbin, VIC, Australia) to a salinity of 19 – 22 ppt, and a ~5 mm layer of calcium carbonate sand and some calcrete stones were placed on the

bottom of the aquaria. Water was lightly aerated with air pumped at 1 – 2 bubbles per second from a tube (4 mm I.D.). Beetles were fed two to three times a week with either small pieces of freshly killed amphipods (*Austrachiltonia australis*) or blackworm (*Lumbriculus sp.*). Beetles were weighed with an analytical balance (Mettler 163, Mettler, Greifensee, Switzerland; precision 0.01 mg) after each experiment or measurement.

Microscopy

Several species of small dytiscids have been identified as having structures such as setae or pores on the surfaces of their bodies that have, or may have, respiratory function (Kehl and Dettner, 2009; Madsen, 2012; Verberk et al., 2018). To determine if these structures were present on the subterranean species we used SEM. Specimens that had been kept in 100% ethanol were air dried, mounted on stubs, sputter coated with platinum, and viewed by scanning electron microscope (Quanta 450, FEI, Tokyo, Japan).

To understand how the structure of the cuticle relates to O_2 diffusion, we histologically examined thin sections of the cuticle. For sectioning of the ventral and elytral cuticle, the heads of beetles were removed before the abdomens were placed in electron microscopy fixative (4% paraformaldehyde/1.25% glutaraldehyde in PBS, + 4% sucrose, pH 7.2) for at least 24 h. Samples were then washed in buffer (PBS + 4% sucrose, 10 min), post fixed with 2% OsO_4 for 1 h, placed through ethanol series (2x 70%, 2x 90%, 3x 100%, 15 min each), then propylene oxide (15 min), a 1:1 mixture of propylene oxide and epoxy resin for ~3 h, then two changes of 100% resin for ~5.5 and 16 h, before samples were placed in fresh resin and polymerized at 70°C for at least 24 h. 1 – 2 µm thick sections were made through the transverse plane midway along the abdomen using a microtome (Leica EM UC6, Leica Mikrosysteme GmbH, Vienna, Austria), and samples were stained with a 1% Toluidine blue and 1% borax mixture. Although samples were prepared for transmission electron microscopy, they were viewed under a light microscope. Four cuticle thickness measurements from each sample produced a mean value for that sample. Some beetle specimens had been prepared and stored differently prior to fixation, including freshly killed specimens, those stored in 70% and 100% ethanol, and air dried specimens. Data were pooled for each species for comparisons among species.

Cuticle samples from freshly killed surface species were also taken and prepared in the same manner as above to produce an allometric relationship of cuticle thickness with mass. Species included were *Necterosoma dispar* (Germar 1848), *Rhantus suturalis* (W.S. Macleay 1825), *Sternopriscus clavatus* (Sharp 1882), *Platynectes decempunctatus* (Fabricius 1775),

Onychohydrus scutellaris (Germar 1848) and *Hyderodes shuckardi* (Hope 1838) (Watts and Hamom, 2014). *N. dispar*, *R. suturalis* and *S. clavatus* were collected near Forreston in the Adelaide Hills, *P. decempunctatus* from near Strathalbyn, and *O. scutellaris* and *H. shuckardi* from near Penola, South Australia, between February and May 2017. For larger surface species, cuticular samples were taken from the centre of an elytron and the fourth abdominal sternite, and in smaller species, from the centre third of an elytron and the second to fourth sternites.

The simple structure of the ventral cuticle formed by a number of parallel laminae contrasts with the elytral cuticle. The elytral cuticle in small species consists of a layer of parallel laminae with a layer of soft tissue on the ventral surface. However, in larger species, from *P. decempunctatus* (28 mg) up, there are haemolymph spaces that are encompassed within the cuticular laminae to varying degrees (Noh et al., 2016). Cuticle thickness was measured on the ventral surface perpendicular to the cuticular laminae from the outside surface through to the soft tissue, and in the elytra, from the outside surface including, or excluding, the soft tissue or haemolymph spaces.

Boundary layer thickness

If O_2 is taken up from the water through a surface such as the cuticle or a gas gill bubble, O_2 diffusion will be evident by a decrease in P_{O_2} from the free water through a layer next to that surface, called the boundary layer, and the effective thickness can be measured by the distance from the beginning of the P_{O_2} decrease to the surface. Boundary layer thickness in the subterranean dytiscids was detected and measured with a fast-responding fibre-optic O_2 sensing optode (Sensor model, PSt 1 taper tip, tip dia. <50 µm; meter model TX-3; PreSense, Germany)) mounted in a 3D micromanipulator (Seymour et al., 2015). Individuals of the three subterranean species were glued with cyanomethacrylate gel either dorsally or ventrally to a small wire stand that was placed into a clear Perspex container (110 mm L × 90 mm W × 25 mm H) containing stagnant water at 15 mm total depth. If placed with the ventral surface upwards, a small amount of glue was used to restrain the legs as movement would disrupt the boundary layer and P_{O_2} measurements. A dissecting microscope was mounted horizontal and perpendicular to the Perspex container to view the beetle ~1 cm below the surface. The optode was lowered to the surface of the beetle and progressively raised at 50 µm steps until 200 µm above the surface of the beetle, then in 100 µm steps until 500 µm, and 250 µm steps to 1,000 µm. The optode was left for measurements at each position for 30 s, after which a 30 s recording period took place before the optode was moved to the next measurement position. Optodes were calibrated weekly

with sodium sulphite and air equilibrated water at the measurement temperature. In a pilot study, we attempted to detect boundary layers above the cuticle of the large surface dytiscid *O. scutellaris*. However, no P_{O_2} differences consistent with the presence of a boundary layer were detected on the elytron, metacoxa, metafemur or sternites. This study provided evidence that optode measurements in the subterranean beetles were unlikely to be caused by changes in sensor readings when approaching the surfaces of the beetles, or by microbial growth.

Respirometry

Two methods of respirometry were used to measure O_2-consumption rate in the beetles. The first involved a closed chamber containing water and a small amount of air in which P_{O_2} was measured both in the water and air with an optode (Sensor model, B2 flat tip; PreSense, Germany). Only the O_2-consumption of *P. macrosturtensis* was measured with this method when it was unknown if the beetles returned to the surface to collect air. Once it was established that the beetles could remain underwater for long periods, a second method was used involving a closed respirometry chamber, filled with water only, where P_{O_2} was measured with a Clark-type O_2 electrode. This chamber was subsequently used for *P. macrosturtensis*, *P. mesosturtensis* and *L. palmulaoides*.

The first setup consisted of a glass vial 41 mm long, 18 mm in diameter with a 7 mm diameter opening. Nylon mesh surrounded the inner sides and bottom of the jar to prevent beetles getting stuck to the glass and allow them to get to the surface if needed. The jar was filled with 25°C, air-equilibrated RO water adjusted to a salinity of 22 ppt using NaCl. Individual beetles were placed into the chambers in a drop of water, minimising the introduction of bacteria and preventing the beetle from getting stuck on the meniscus. Chambers were then sealed with a rubber stopper, with excess water pushed through a 1 mm hole in the stopper. The chamber was then dried on the outside and weighed with the analytical balance. Afterwards, approximately 0.2 ml of water-saturated air at 25°C was injected into the chamber, pushing excess water out. The chamber was dried and weighed again. A water-filled Pasteur pipette was then inserted into the chamber, through the hole in the stopper. The chamber was then placed into a water bath regulated by a thermocirculator (Thermomix 1419, type 850094, B. Braun, Germany), and sat for 4-5 min to allow temperature to equilibrate. An optode was inserted through the tight-fitting pipette to measure P_{O_2}, effectively sealing the chamber with water. The optode inserted into the bubble, and then water, recorded the initial P_{O_2} in each medium for 2 min after the P_{O_2} traces became stable (~2-4 min). Each chamber was left for approximately 3 h after which the optode was

placed back into the air bubble, and then the water, which was gently mixed producing a uniform distribution of O_2 for final P_{O_2} measurements (2 min stable trace). The beetle was then removed from the chamber, dried with paper towel and weighed live. The experimental water was returned to the chamber, topped up with fresh RO water and closed. The pipette and optode were inserted into the chamber, which was returned to the water bath. The water-filled chambers were used to assess background respiration and sensor drift and left for approximately 3 h between initial and final P_{O_2} measurements. If background respiration and drift exceeded ±10% O_2-uptake, data were excluded. Air and water volumes in the chambers were determined from the mass measurements of the chambers with water, and air and water minus beetle wet mass (if present), and the dry mass of the chambers, the stopper seal, and mesh.

The second respirometry setup, used while at Sturt Meadows Station, consisted of four closed water-filled high density polyethylene chambers with a glass front (0.67 mL, model 1271, Diamond General, Ann Arbor, MI, USA), each with a Clark-type O_2-electrode (model 730, Micro-electrodes, Bedford, NH, USA) (Mueller and Seymour, 2011). Temperature was regulated by circulating water at the experimental temperature through a water bath and water jackets surrounding the respiratory chambers. The electrodes were connected to an O_2-analyzer (ReadOx-4H, Sable Systems, Las Vegas, NV, USA), a data acquisition unit (PowerLab ML750, ADInstruments Pty Ltd, Castle Hill, Australia) and a laptop computer, and were calibrated with sodium sulphite every 1 – 4 days (zero drifted ≤ 1% per day), and air equilibrated water daily. In the back of each chamber was a miniature magnetic stirrer that rotated at ~2 Hz.

For air equilibrated $\dot{M}_{O_2}$ measurements, chambers were 2/3^{rds} filled with water and the stable P_{O_2} recorded for 5 min providing an initial measurement for drift calculation. Drift was assumed to be linear (Seymour and Roberts, 1995). Individual *P. macrosturtensis* or *L. palmulaoides*, or four *P. mesosturtensis*, were then pipetted into the open chambers, which were closed and filled with the treatment water ensuring no air bubbles remained. Four *P. mesosturtensis* were placed into each chamber because of their small size. Beetles were left for approximately 2 h with the stirrer on to maintain homogenous P_{O_2} before the beetles were removed and the experimental water put aside. Chambers were again 2/3^{rds} filled with air-equilibrated water for a second stable 5 min period to calculate drift over the time beetles were in the chambers. The water that contained the beetles was then returned to the chamber for 30 min to measure background respiration, followed by another stable 5 min period with clean water for drift calculation during background respiration measurement.

Oxygen saturation in boreholes where beetles are found can vary widely both between and within boreholes (Fig. S1). Due to this variation, the relationship between $\dot{M}O_2$ and declining PO_2 was measured in *P. macrosturtensis* to understand how these conditions might affect metabolism. Individual *P. macrosturtensis* were exposed to four individual PO_2 treatments in the 0.67 ml chambers, nominally ~20 kPa, ~15 kPa, ~10 kPa and ~5kPa. This was done to avoid excessive build-up of CO_2 and bacterial contamination that would have occurred in one long respirometry run. Beetles were placed into the chambers for 1.5 h, then removed and background respiration measured for 30 min. Before and after each measurement, PO_2 was measured for 5 min periods, as above, to determine drift.

$\dot{M}O_2$ was calculated in both respirometry methods with Eq. 1.

$$\dot{M}O_2 = \beta O_2 \times V \times \dot{P}O_2 \quad (1)$$

where $\dot{M}O_2$ (μmol h^{-1}) is the rate of O_2-consumption, βO_2 is the capacitance of the medium for O_2 (μmol ml^{-1} kPa^{-1}), V is the volume of medium (ml) and $\dot{P}O_2$ is the rate of decrease of PO_2 in the medium (kPa h^{-1}). The βO_2 at 25°C in the air was 0.4032, and in the water, accounting for salinity, 0.01130 at 19 ppt, 0.01117 at 21 ppt, and 0.01110 at 22 ppt assuming a linear change in capacitance from 0 to 35 ppt salinity (Dejours, 1981)). The volume (V) of water was ~6 ml and air ~0.19 ml in the air+water chambers, and 0.67 ml in water-only chambers. $\dot{P}O_2$ decline in air+water chambers was determined from the initial and final PO_2 measurements in air, and water, and the amount of time between the measurements. Total $\dot{M}O_2$ in the air+water chambers was calculated by adding the $\dot{M}O_2$ calculated for each medium. $\dot{P}O_2$ in water-only chambers was determined directly from the linear slope of the PO_2 trace.

The rate of PO_2 decline (or $\dot{M}O_2$ decline in the air+water chambers) of the background measurement was subtracted from the total respiration rate of the chamber with the beetle in it to determine the beetles' $\dot{M}O_2$. Background respiration was 4.1±3.1% of the total (N=7) in the air+water chambers with *P. macrosturtensis*, and 6.4±4.4% (N=7) in the water-only chambers, and 20.1±7.1% (N=27) for the critical PO_2 measurements. For *P. mesosturtensis*, background respiration was 29.6±24.5% (N=5), and for *L. palmulaoides* it was 40.7±20.6% (N=6).

Activity of the beetles, e.g. crawling or moving legs or body, was assessed in beetles within the water-filled respirometry chambers as the cumulative duration of activity of one or more beetles within the chamber over a 10 min period. A stopwatch was used while observing the beetles and activity reported as the percentage of time active during the 10 min period.

Wet mass of *P. macrosturtensis* was recorded from air+water chamber experiments conducted in the lab. However, all other experiments took place at the field station at Sturt Meadows, where a balance was unavailable. There, beetles were dried with silica gel beads and weighed with the analytical balance once back in the lab. Wet mass was reconstructed from dry mass using the water content of living beetles, which was found to be 66.5% of wet mass.

The subterranean beetles hold a small amount of gas within the sub-elytral cavity but are slightly negatively buoyant. The O_2 within this gas was not included in calculations of O_2-consumption rate because it represents only 1% of the O_2 in the water only chambers and <0.1% in the air+water chambers.

Field measurements - Video recording of beetles in bore holes

Video recording of the beetles in the boreholes was undertaken to quantify the beetles' activity, and pattern of occurrence, which may be related to O_2 levels or resource availability within the boreholes. To record the beetle's activity, we mounted a bore camera (USB Endoscope Camera, 20m, 14.5 mm dia., with four LEDs), angled at ~45° downward on a weight on the end of a tape measure. The camera was orientated so the view was not obstructed by the side of the borehole, and was placed at the water surface, 0.5 m depth and at the bottom of each hole (*N*=11 bores holes surveyed). Water depth at the bottom varied between holes. The three beetle species found at Sturt Meadows, *P. macrosturtensis*, *P. mesosturtensis* and *P. microsturtensis* were not distinguished in the video recordings as parallax and distortion made it difficult to discern size and shape differences between species. Recordings at each point within the borehole were made for 600 s and observed using VLC Media player (VLC media player, version 2.2.3, USA). The number of occurrences of beetles was counted. An occurrence counted as a beetle entering the camera view. The proportion of time beetles were active in boreholes was determined by measuring how long beetles were in view of the camera and recording when and how often beetles were active.

Statistics

Wilcoxon matched pairs, ANOVA and Tukey's pots-hoc tests were conducted with GraphPad Prism 7.02 (GraphPad Software Inc., La Jolla, CA, USA), and ANCOVA were conducted according to Zar (1998). Linear, one-phase association, power and polynomial regressions were performed with Excel or GraphPad Prism. Statistics reported are means and 95% confidence intervals.

4. Results

Microscopy

The dorsal surfaces of the head, pronotum and elytra of *P. macrosturtensis* and *P. mesosturtensis* were very similar (Fig. 1A and B). Both species had very sparse setae with the dominant structures being hexagonal reticulations on all three surfaces viewed. *L. palmulaoides* also had sparse setae, but the pronotum and elytra were smooth with no visible reticulations, and the head showed irregular hexagonal reticulations (Fig. 1C). The ventral surface of *P. macrosturtensis* was also viewed and was similar to the dorsal surface.

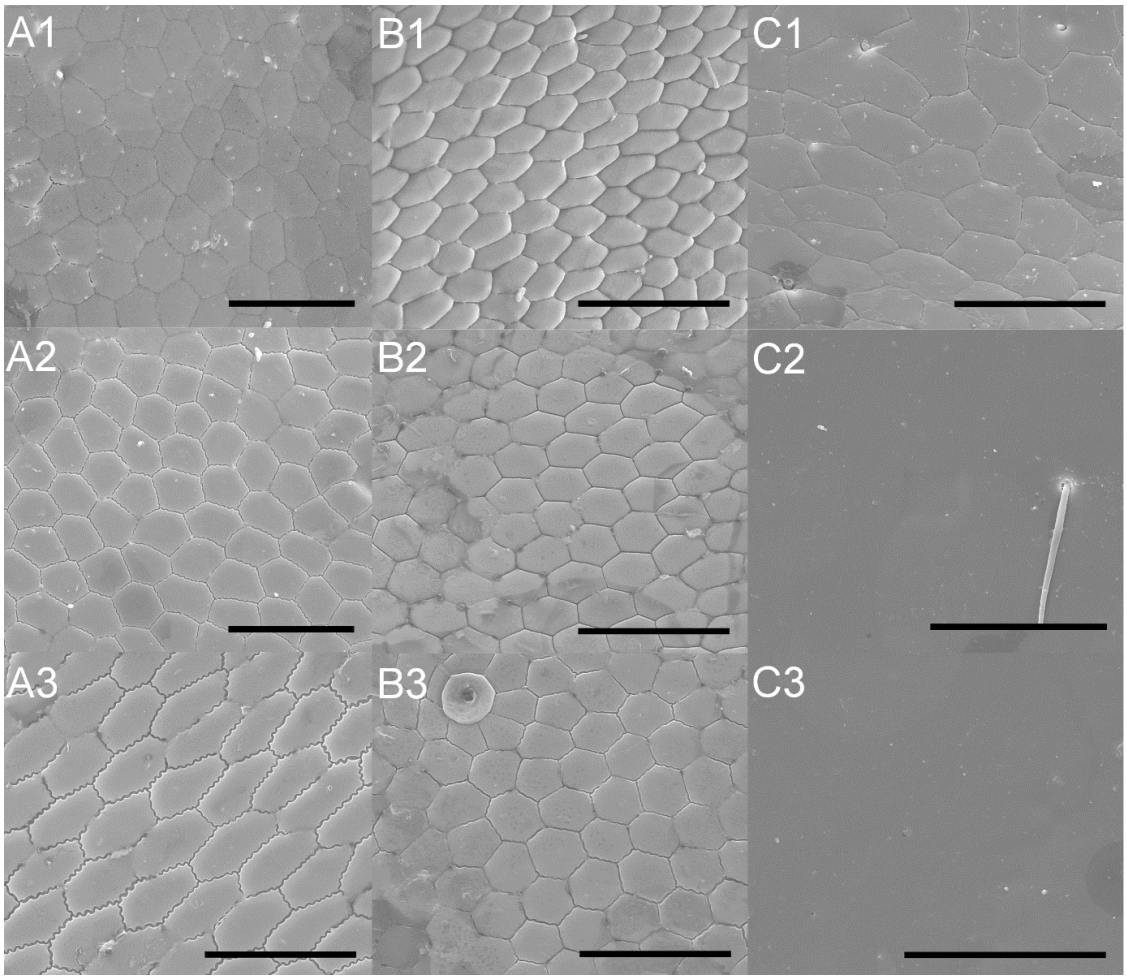

Figure 1. SEM images of *P. macrosturtensis* (A), *P. mesosturtensis* (B), and *L. palmulaoides* (C), showing dorsal surfaces of the head (1), pronotum (2) and elytron (3). All scale bars 20 µm.

Cuticle structure and thickness

Cuticle structure varied between dorsal and ventral surfaces, as well as between the elytral cuticles of different species. The ventral cuticle consisted of a number of parallel cuticular laminae next to the soft tissue of the abdomen in all species (Fig. 2E and F). However, the elytral

cuticle in the small dytiscids (subterranean species, *S. clavatus* and *N. dispar*) consisted of a layer of parallel laminae with a thin layer of soft tissue on the ventral surface of the elytra (Fig. 2D). Tracheae were visible within the soft tissue, which in the sections were small circular structures that correspond with the tracheae seen in the elytra of living *P. macrosturtensis*. In the larger species (*O. scutellaris*, *H. shuckardi*, *P. decempunctatus* and *R. suturalis*), haemolymph spaces were seen between a dorsal and ventral layer of cuticular laminae separated by trabeculae, pillar-like structures consisting of the chitinous laminae, except in *P. decempunctatus* where they were absent or poorly developed (Fig. 2A–C, (Noh et al., 2016; Van de Kamp and Greven, 2010)). Observations of beetle elytra in another study suggest the tracheae are within the haemolymph spaces (Iwamoto et al., 2002).

The cuticle thickness of all surface dytiscids was significantly greater than in the subterranean species (Table 1, Fig. 3). The dorsal and ventral thickness data were pooled to produce an allometric regression of cuticle thickness. Dorsal measurements that excluded the soft tissue and haemolymph spaces were used. These values were the most relevant to O_2 diffusion through the cuticle due to the presence of tracheae within the soft tissue and likely within the haemolymph spaces. The pooled data of both surface and subterranean species showed that cuticle thickness increased with mass to the exponent 0.31±0.05 (Fig. 3).These data were not phylogenetically adjusted because of the small number of taxa used in the analysis. The ability to detect phylogenetic signal in a trait is much lower where analyses have less than 20 taxa (Blomberg et al., 2003). Additionally, a phylogenetically adjusted regression may differ from the observed regression, which would result in diffusion models based on the corrected data being less representative of the actual system.

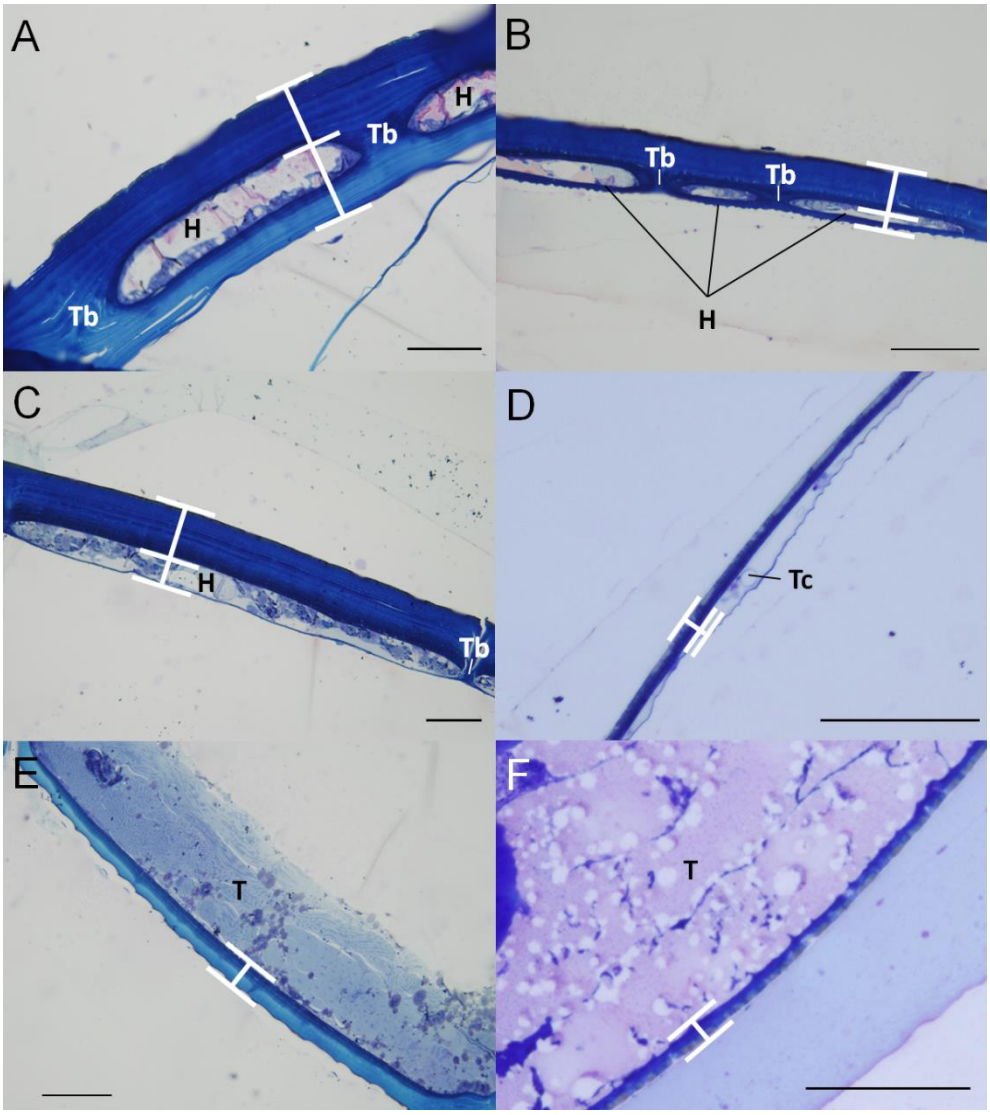

Figure 2. Sections of dytiscid cuticle showing differing levels of integration of the haemolymph spaces (H) and trabeculae (Tb) in the elytra of large dytiscids (above ~25 mg) and the trachea (Tc) in the soft tissue of small dytiscids (below ~10 mg), and the simple ventral cuticle with soft tissue (T) on the dorsal side. A – D, elytra, dorsal surface orientated towards top of figure, E and F ventral cuticle, ventral surface orientated towards bottom of figure. White bars show examples of how cuticle thickness was measured in the different species by measuring the perpendicular distance between the surfaces of the cuticle. A, *O. scutellaris*; B, *R. suturalis*; C, *H. shuckardi*; D, *P. macrosturtensis*; E, *S. clavatus*; F, *P macrosturtensis*. All scale bars 100 µm.

Table 1. Dorsal (Elytral, excluding and including haemolymph spaces and soft tissue (H/ST)) and ventral cuticle thickness, and mass of dytiscids. Mean and 95% CI shown with *N* in parentheses.

Species	Mass (mg)	Dorsal (µm) Excl. H/ST	Dorsal (µm) Incl. H/ST	Ventral (µm)
P. mesosturtensis	0.55*	**7.2±0.3 (7)**	11.1±0.5 (7)	**8.4±0.7 (6)**
L. palmulaoides	2.32*	**6.4±0.7 (8)**	12.2±2.1 (6)	**6.5±0.5 (7)**
P. macrosturtensis	2.72*	**7.5±0.5 (13)**	12.2±2.4 (12)	**7.7±0.7 (11)**
S. clavatus	3.95±0.46 (8)	**42.9±3.6 (8)**	51.0±2.8 (7)	**33.0±2.4 (7)**
N. dispar	7.7±0.5 (6)	**43.0±4.0 (6)**	50.2±3.5 (6)	**38.6±5.2 (6)**
P. decempunctatus	28.54±2.24 (8)	**35.0±3.7 (8)**	44.6±5.2 (8)	**32.9±2.4 (8)**
R. suturalis	101.11±8.38 (8)	**34.8±3.1 (8)**	60.8±4.1 (8)	**34.7±3.4 (8)**
H. shuckardi	627.45±37.79 (8)	**76.9±6.9 (8)**	119.0±6.7 (8)	**70.7±7.4 (8)**
O. scutellaris	1319.42±119.77 (8)	**67.3±7.0 (7.0)**	171.2±19.3 (8)	**103.6±23.3 (8)**

* Wet mass values calculated from dry mass. Bold values used for cuticle thickness regression in Fig. 3. Thickness of the cuticle including the soft tissue in subterranean species may be artificially reduced due to some samples being dried or stored in ethanol before fixation.

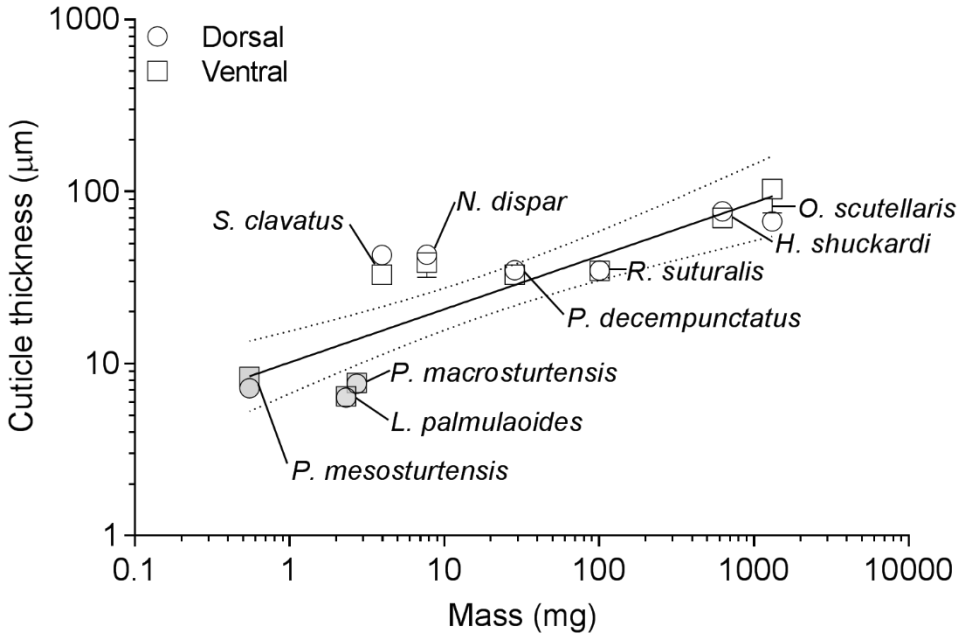

Figure 3. Allometric regression of dorsal cuticle (circles), excluding the haemolymph spaces and soft tissue, and ventral cuticle thickness (squares) of dytiscids. Stygobitic species indicated by grey symbols. Values are means with 95% CIs. Many error bars are shorter than symbols and are therefore not visible. Cuticle thickness = $10.162M_b^{0.31}$, regression showing 95% CI bands.

O_2 boundary layers

O_2 boundary layers were found on both the dorsal and ventral surfaces of *P. macrosturtensis*, *P. mesosturtensis* and *L. palmulaoides* (Fig. 4A). To reduce variation associated with small differences in the PO_2 of the water in which the beetles were placed, the difference (ΔPO_2) between the maximum PO_2 value recorded in each PO_2 trace and the PO_2 value at each measurement position was calculated (Fig. 4B). To approximate the effective boundary layer thickness, a one-phase association was applied to the ΔPO_2 data (Fig. 4B) where $\Delta PO_2 = Y_0 + (\text{Plateau}-Y_0)*(1-\exp^{(-k*X)})$, where Y_0 is the y-intercept, and the plateau constrained to 0 representing the PO_2 of the surrounding water. The effective boundary layer thickness was defined as where the ΔPO_2 (Y) is 5% different from zero where Y_0 equals 100%. The boundary layer thickness (*X*) was calculated by rearranging the one-phase association, where $X = (\text{Ln}(Y/Y_0))/-k$ (excluding the plateau which equals 0, Fig. 4B). For *P. macrosturtensis*, Y_0= -4.995 and k=0.004363 (Dorsal, R^2=0.80), and Y_0= -7.576 and k= 0.003739 (Ventral, R^2=0.88), for *L. palmulaoides*, Y_0= -9.067 and k= 0.004175 (Dorsal, R^2=0.88), and Y_0= -7.222 and k= 0.004689 (Ventral, R^2=0.92), and for *P. mesosturtensis* Y_0= -5.312 and k= 0.006659 (Dorsal, R^2=0.73), and Y_0= -4.113 and k= 0.006561 (Ventral, R^2=0.81). In *P. macrosturtensis* the dorsal and ventral boundary layers were 687 µm and 801 µm, respectively; in *L. palmulaoides* the dorsal and ventral boundary layers were 718 µm and 639 µm, respectively; and in *P. mesosturtensis* the dorsal and ventral boundary layers were 450 µm and 457 µm, respectively. The PO_2 within the boundary layer of *P. macrosturtensis* on the ventral surface was significantly lower than within the layer at the dorsal surface at distances less than 400 µm from the surface of the beetles (Two-way ANOVA, P<0.0001, Tukey's post-hoc, $P \leq 0.01$). In *L. palmulaoides* the PO_2 within the ventral boundary layer was significantly higher than the dorsal surface from 200 µm to the surface (Tukey's post-hoc, $P \leq 0.01$). In *P. mesosturtensis* there are no differences between dorsal and ventral boundary layers until at the surface where the ventral PO_2 is significantly higher than the dorsal (Tukey's post-hoc, $P \leq 0.01$).

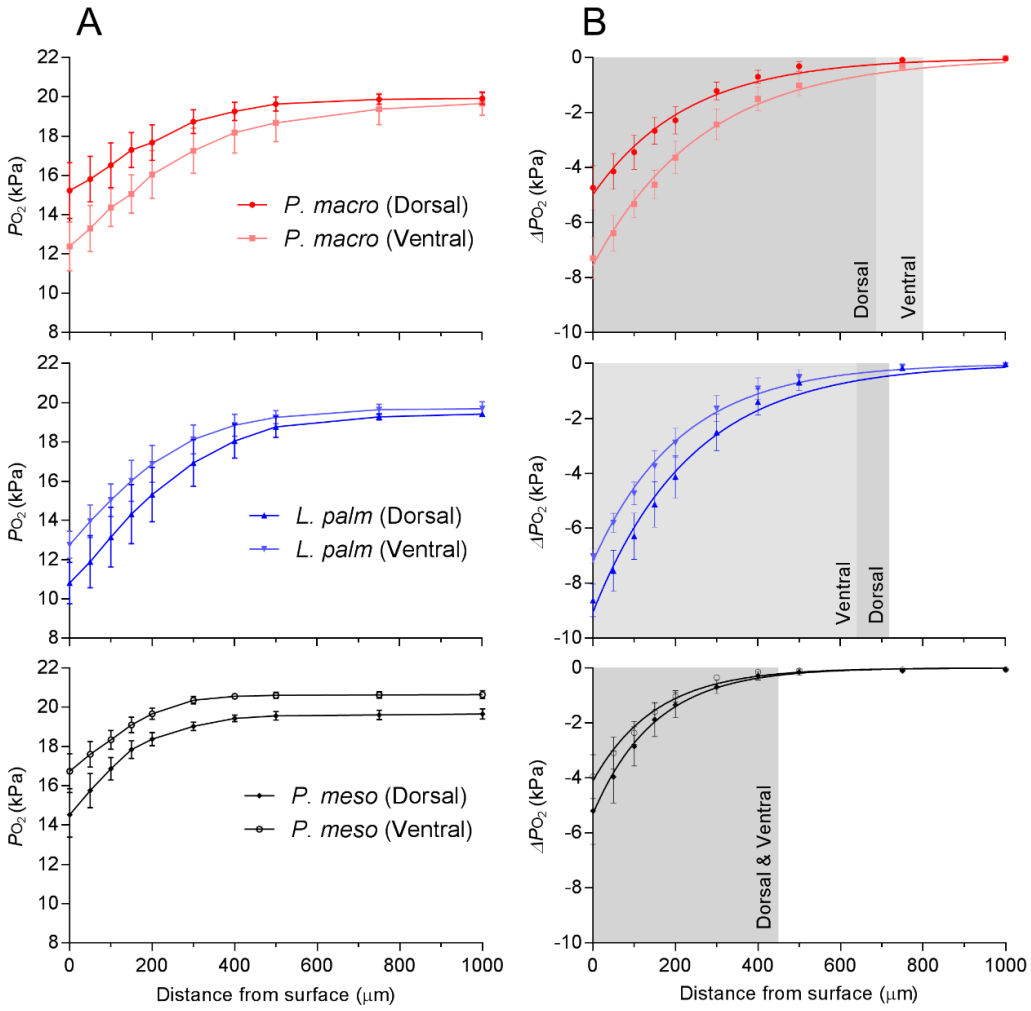

Figure 4. (A) Mean P_{O_2} transects from the dorsal and ventral surfaces of *P. macrosturtensis*, *L. palmulaoides*, and *P. mesosturtensis* in stagnant water, and (B) mean P_{O_2} difference between the maximum P_{O_2} recorded in a transect and the P_{O_2} at a particular distance from the beetle's surface. A one-phase association shows the approximate effective boundary layer profile where the thickness is defined as where the ΔP_{O_2} is 5% different from 0, and 100% is the y-intercept (Y_0, see text). Six individuals of each species were used, three each for dorsal and ventral measurements, with five transects per individual. Mean water temperature during all P_{O_2} transects was 25.3±0.4°C. Shown are means and 95% CIs.

Respirometry

Mass-specific O_2-consumption rate was not significantly different between all three subterranean species in the water-only chambers (Table 2, ANOVA). However, *P. macrosturtensis* in the air+water chambers had a significantly higher mass-specific metabolic rate than *L. palmulaoides* (Table 2, ANOVA $P<0.05$, Tukey's Post-hoc). Whole animal O_2-consumption rates were significantly different between all species and experimental setups except for *L. palmulaoides* and *P. macrosturtensis* both in the water-only chambers (Table 2, ANOVA, $P<0.0001$, Tukey's

post-hoc). Mean percentage of time individual beetles were active in the water-only chambers over a 10 min period was 15% in *P. macrosturtensis* (*N*=8) and 3% in *L. palmulaoides* (*N*=6). Mean percentage of time one or more beetles were active with *P. mesosturtensis* within the chambers was 1% (*N*=2). Beetles would occasionally cling to the magnetic flea in the chamber, however, while not moving this may have elevated these beetles metabolic rate above resting metabolism.

As *P. macrosturtensis* was exposed to progressively lower P_{O_2}, O_2-consumption rate declined indicated by a linear regression (solid orange line, Fig. 5), and a decline in the upper bounds of O_2-consumption rate measured at a given P_{O_2} (dashed black line, *N*=11 beetles, dry mass 1.08±0.13 mg, calculated wet mass 3.23±0.4 mg).

Table 2. Whole animal and mass-specific O_2-consumption rates for subterranean dytiscids.

Species (*N*)	Dry mass (mg)	Wet mass (mg)	Whole animal O_2-consumption rate (nmol h^{-1})	Mass specific O_2-consumption rate (nmol h^{-1} mg^{-1})
*P. macrosturtensis** (7)	–	2.52±0.16	26.5±3.1	10.6±1.7
P. macrosturtensis (7)	0.91±0.24	2.71±0.72	20.1±3.3	7.9±1.6
P. mesosturtensis† (5)	0.19±0.02	*0.55±0.05*	4.2±1.0	7.7±2.2
L. palmulaoides (6)	0.78±0.21	*2.32±0.62*	15.1±2.8	7.1±1.9

* O_2-consumption rate measured in air+water chambers (water temperature 25.1±0.0°C). In water-only chambers water temperature was maintained between 24.4 – 25.6°C at the field station. Underlined mass values calculated from dry mass. † mean individual O_2-consumption rate and mass of four beetles within each chamber of *N*=5 experiments. Mean values are shown with 95% CIs.

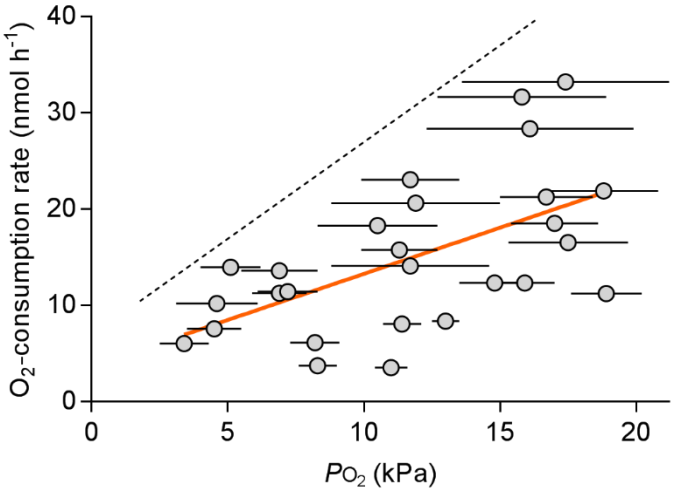

Figure 5. O_2-consumption rate of *P. macrosturtensis* when exposed to varying initial P_{O_2} levels in the water-only chambers. Each point represents the mean P_{O_2} and O_2-consumption rate while the beetles were in the chamber for a particular experiment (*N*=11 individual beetles, *N*=27 data points). Horizontal bars represent the P_{O_2} range over which O_2-consumption rate was measured. A linear regression of the decline in O_2-consumption rate is shown by the solid orange line (O_2-consumption rate = 0.959*P_{O_2}+3.673, R^2=0.33) and dashed line illustrates the trend of decline in the upper bounds of O_2-consumption rate measurements.

Field measurements

Eight of 11 boreholes surveyed with the borescope contained beetles. Water depth in the boreholes with beetles was 2.7±1.7 m (range 0.50 – 5.71 m). Mean number of beetle occurrences over 10 min was 4.8±4.4 (*N*=8) at the surface, 1.7±1.1 (*N*=6) at 50 cm water depth, and 2.1±2.4 (*N*=8) at the bottom of the boreholes. Two boreholes had total depths of 0.50 and 0.65 m and these records are included in the bottom category. The number of beetle occurrences at the surface was significantly higher than at the bottom (Wilcoxon matched pairs nonparametric test, *P*<0.05). Mean percentage of time individual beetles spent active while in the view of the camera, either swimming or crawling in boreholes, was 71±7% (*N*=50 observations determined from six boreholes), spending an average 9.9±7.8 s in view of the camera with 3.08 bouts of activity during this time.

5. Discussion

Cutaneous respiration in subterranean dytiscids

This study shows that small subterranean diving beetles rely entirely on cutaneous respiration, in which O_2 diffuses from the water through the O_2 boundary layer to the beetles' surface and then through the cuticular laminae. On the ventral surface, O_2 diffuses directly into the tissues, but on

the dorsal surface of the elytra, it goes into the thin layer of soft tissue or the tracheoles within that tissue, as well as the sub-elytral cavity. In all three species, the sub-elytral cavity is gas filled, so O_2 entering this space could diffuse to the spiracles on the dorsal side of the abdomen and into the tracheal system or diffuse directly through the tergites. SEM showed the tergites are not hardened like the elytra or sternites.

Unlike surface-dwelling dytiscids, the gas within the sub-elytral cavity does not appear to be exchanged with the air or water directly. These beetles rarely go to the surface and break the meniscus with the tip of the abdomen, and were never observed to have a small gas gill bubble at the tip of the abdomen, like in surface species. Additionally, *P. macrosturtensis* and *P. mesosturtensis* have tightly locked elytra (Watts and Humphreys, 2006). Consistent with the hypothesis that the beetles use cutaneous respiration, we observed that beetles could survive at least 12 days submergence without access to air, and they are slightly negatively buoyant. Another subterranean beetle, *Phreatodytes relictus* (Noteridae), has no gas underneath the elytra (Ueno, 1957), which shows that the sub-elytral gas is not necessary for respiration.

The strongest support for cutaneous respiration in *P. macrosturtensis, P. mesosturtensis* and *L. palmulaoides* is the presence of O_2 boundary layers surrounding the beetles, indicating O_2 diffusion into the surface of their bodies (Fig. 4). Boundary layer thickness on the dorsal and ventral surfaces are similar to each other in *P. mesosturtensis*, 450 µm and 457 µm, respectively. However, in *P. macrosturtensis* and *L. palmulaoides* the dorsal layers (687 µm and 718 µm, respectively) differ from the ventral (801 and 639 µm, respectively, Fig. 4). The difference in thickness between the dorsal and ventral boundary layers is unclear, but may be linked to differences in the cuticle thickness more widely across the body despite the similarities measured in thin sections. The thinner boundary layer found around *P. mesosturtensis* is due to this species' smaller size. In experiments, glue holding the beetles to the stand would increase O_2 demand through the other surfaces that are not covered, thus increasing the boundary layer thickness. Under natural conditions the boundary layers are likely to be thinner, because the beetles are often moving (a mean of 3.08 bouts of activity over the average duration of 9.9 s that beetles were in view of the borescope), and, at least at Sturt Meadows, there appears to be some slow water movement within the aquifer that would help ventilate the boundary layer.

Modelling external diffusion barriers

Fick's general diffusion equation (Eq. 2) can be used to model diffusion from the water to a respiratory surface, such as a gas gill (Rahn and Paganelli, 1968).

$$\dot{M}O_2 = KO_2 \times A/X \times \Delta PO_2 \quad (2)$$

where $\dot{M}O_2$ (pmol s^{-1}) is the rate of O_2-consumption, KO_2 (pmol s^{-1} kPa^{-1} cm^{-1}) is the Krogh's coefficient of diffusion, the product of capacitance and diffusivity, A (cm^2) is the surface area for gas exchange, X (cm) is the thickness of the boundary layer, and ΔPO_2 (kPa) is the PO_2 difference between the surrounding water and respiratory surface. This equation can be rearranged to calculate PO_2 through the O_2 cascade of the subterranean beetles to evaluate the extents of diffusion-limitations to respiration (Table S1). PO_2 at the surface of the beetles and on the inside of the cuticle, representing O_2 diffusion through the boundary layer and then through the cuticle, can be calculated with the experimentally determined O_2-consumption rates, under different convective conditions (stagnant and circulated water, Fig. 6A, Table S2). The model endpoint is when the O_2 reaches the gas within the tracheal system, sub-elytral space or soft tissues. The diffusion pathway under the chitin is complicated and uncertain, because it includes soft tissue and tracheae (Fig. 2). These structures are safely ignored, because the Krogh's coefficient in soft tissue is greater than 10 times higher than in chitin (Krogh, 1919), and the tracheal walls are very thin (Fig. 2D). In circulated water, mean ΔPO_2 to the beetles' surface is 1.3 kPa in *P. macrosturtensis*, 0.8 kPa in *P. mesosturtensis* and 0.9 kPa in *L. palmulaoides*, which increases to 9.4 kPa, 3.8 kPa and 6.4 kPa in stagnant water, respectively (Fig. 6A). Mean decline in PO_2 through the cuticle is 2.8 kPa in *P. macrosturtensis*, 1.9 kPa in *P. mesosturtensis* and 1.7 kPa in *L. palmulaoides*. In stagnant water *P. macrosturtensis* could become O_2-limited when the aquatic PO_2 declines to 14.5 kPa. This assumes the PO_2 on the inside of the cuticle declines below an assumed critical PO_2 ($PO_{2crit.}$) of 2.3 kPa, as found in the water bug *Agraptocorixa eurynome*, under which metabolism becomes limited (Matthews and Seymour, 2010). In *P. mesosturtensis*, limitation could occur at 8.0 kPa aquatic PO_2 and 10.4 kPa for *L. palmulaoides*. These O_2 levels are similar to the lowest values recorded at Sturt Meadows (Fig. S1). However, activity such as swimming or crawling, or water convection (Fig. 6A1) would thin the boundary layer enabling a higher metabolism without limitation under these PO_2 levels.

Differences between the model and experimental results arise when considering O_2 uptake per unit surface area. O_2-consumption rate is 36.5 pmol s^{-1} cm^{-2} in *P. macrosturtensis*, 24.6 pmol s^{-1} cm^{-2} in *P. mesosturtensis* and 26.4 pmol s^{-1} cm^{-2} in *L. palmulaoides*. These values result in a similar boundary layer thickness between *P. mesosturtensis* and *L. palmulaoides*, however, the experiments show the boundary layer is thinner in *P. mesosturtensis* (Fig. 4). The difference may be linked to the smaller size of *P. mesosturtensis*, in which diffusion is closer to radial than linear as assumed in Fick's diffusion equation for the other species. Nevertheless, despite the similarity

in size, *L. palmulaoides* is likely to be more tolerant of low P_{O_2} compared to *P. macrosturtensis* due to a better ratio of surface area to O_2-consumption rate and a thinner cuticle (Table 1, Fig. 6A).

The model can be adjusted to make predictions about O_2 limitation with increasing beetle size. This is achieved by taking the average relationship between length, width and height of the three subterranean diving beetles and increasing the size of a hypothetical beetle (assuming a lozenge shape, Table S1, S2 and Fig. S2). This model assumes circulated water and cuticle thickness increase with mass according to the equation determined in Figure 3. The O_2-consumption rate scaling began with a resting metabolic rate of 0.2 nmol h^{-1} at 0.04 mg up to 24.2 nmol h^{-1} and 4.82 mg (5 mm), which is approximately the size of the largest known subterranean dytiscid, with the metabolic scope being ten times resting metabolism. There is little effect of size on the P_{O_2} at the surface of the cuticle (Fig. 6B1). A thicker boundary layer would, however, decrease P_{O_2} at the surface of the beetle more, but given the animals would be moving when metabolic rates are high, this would not limit the system. In contrast, cuticle thickness has a greater effect on P_{O_2} than the boundary layer (Fig. 6B2). Although the estimated resting metabolism does not become limited at the maximum beetle size, the metabolic scope is reduced. A beetle such as *P. mesosturtensis* would be able to increase metabolic rate more than ten times above resting, however *P. macrosturtensis* and *L. palmulaoides* have a calculated metabolic scope of only four to five times resting, which are similar to the narrower metabolic scopes recorded between rest and ambulatory activity in several terrestrial beetle species (Bartholomew and Casey, 1977; Rogowitz and Chappell, 2000).

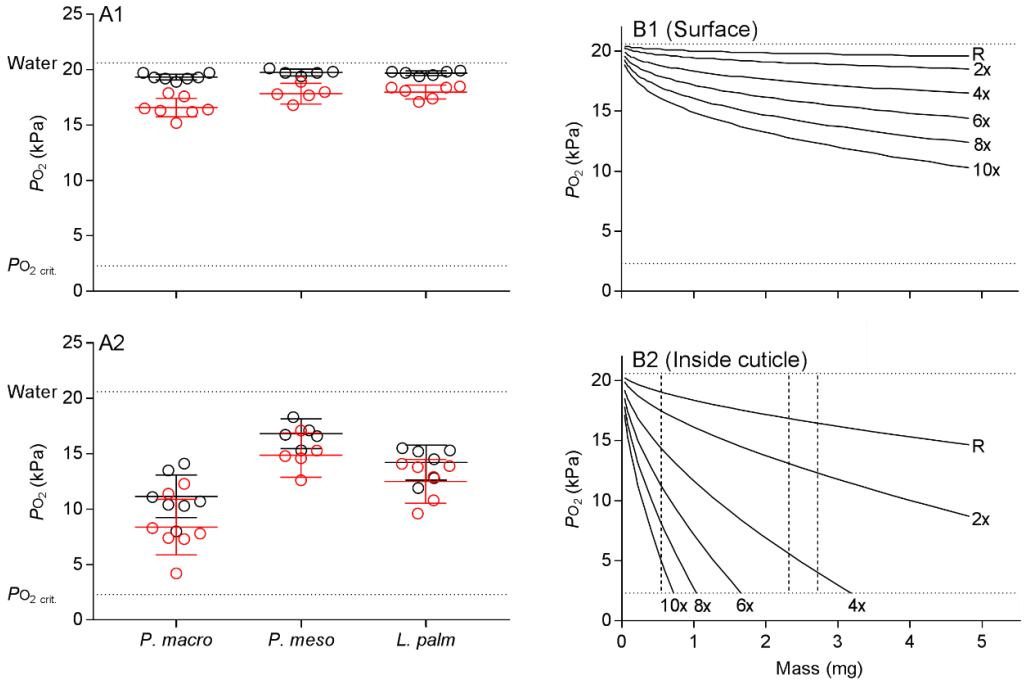

Figure 6. Calculated P_{O_2} through the O_2 cascade of subterranean dytiscids using Fick's general diffusion equation (Table S1 and S2). (A) Calculated P_{O_2} on the surface (black, top) of the beetles and on the inside (red, bottom) of the cuticle using the experimentally measured O_2-consumption rates from beetles in this study. A1 shows calculated P_{O_2} under convected conditions with 100 µm boundary layers. A2 represents stagnant water, with boundary layer thicknesses of 750 µm for *P. macrosturtensis*, 700 µm for *L. palmulaoides* layers and 450 µm for *P. mesosturtensis* (mean of dorsal and ventral boundary layers rounded to the nearest 50 µm). Means shown with 95% CIs. (B) Model estimates of P_{O_2} (solid lines) at the surface (B1) and on the inner side of the cuticle (B2) of a generalised subterranean diving beetle with increasing size. "R" shows the predicted resting metabolic rate regression estimated from lowest O_2-consumption rate measurements undertaken in air equilibrated water in water-only chambers, where estimated resting O_2-consumption rate is 13 nmol h^{-1} in *P. macrosturtensis*, 2.5 nmol h^{-1} in *P. mesosturtensis* and 11.5 nmol h^{-1} in *L. palmulaoides* (O_2-consumption rate = $4.68Mb^{1.04}$). Estimated resting metabolism is then multiplied by 2, 4, 6, 8 and 10 times, indicated at the end of each P_{O_2} line. Boundary layer thickness is 100 µm. The dashed vertical lines (B2) represent the mass of the three subterranean dytiscids used in the model. Beetle length (mm) = $2.96Mb^{0.33}$. In both A and B top dotted line shows the air saturated water P_{O_2} at 25°C (20.6 kPa) and the bottom dotted line is $P_{O_2\ crit.}$ (2.3 kPa) the critical P_{O_2} under which the metabolism becomes limited. The Krogh's coefficient for water is 0.290 pmol s^{-1} kPa^{-1} cm^{-1} (Seymour, 1994), and for cuticle 0.010 pmol s^{-1} kPa^{-1} cm^{-1}, adjusted to 25°C with a Q_{10} of 1.1 (Bartels, 1971; Krogh, 1919).

Metabolic scope and oxygen availability

When *P. macrosturtensis* is exposed to declining P_{O_2}, both metabolic scope and O_2-consumption rate tended to decrease, shown by the linear decline in O_2-consumption rate as well as a linear decline in the upper O_2-consumption rate values recorded (Fig. 5). Each point in Figure 5

represents the mean O_2-consumption rate of the beetle while it was in the chamber. However, because the beetles' activity cannot be controlled, they may be more or less active during the experiments producing a range of mean O_2-consumption rates at a given PO_2. Figure 7 shows the experimental results can be explained by varying levels of activity during each experiment where maximum metabolic rate declines linearly with PO_2 and is therefore O_2 limited, but resting metabolic rate remains unaffected. Experimentally measured values below the calculated values may indicate a lower resting metabolic rate than anticipated or that resting metabolic rate is affected at lower PO_2. The model results in Figure 7 would differ if the maximum proportion of the experiment the beetles could be active changed, or the metabolic scope changed. However, if maximum metabolic rate is O_2-limited and the beetles' activity is variable the same general trend would occur.

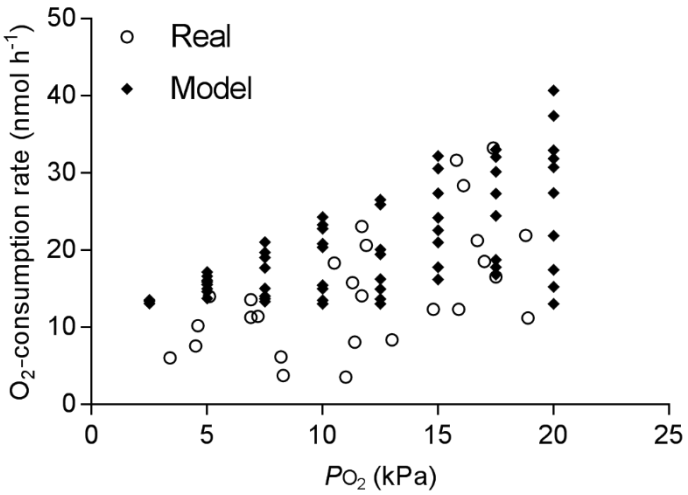

Figure 7. Measured O_2-consumption rates of *P. macrosturtensis* at different PO_2 values (Fig. 5, open circles) compared with a model calculating O_2-consumption rate with differing proportions of activity during each experiment (filled diamonds). The model parameters are that resting O_2-consumption rate is 13 nmol h^{-1}, comparable to the lowest values recorded for *P. macrosturtensis* in the water-only experiments, which is independent of PO_2 between 2.5 and 20 kPa. Maximum metabolic rate is assumed to be 10 times higher at 130 nmol h^{-1}, the metabolic scope observed in other aquatic insects (Seymour et al., 2015). This value declines linearly from 20 kPa PO_2 to the resting O_2-consumption rate at 2.5 kPa representing diffusion limitation at maximum metabolic rate. Each model point signifies the mean O_2-consumption rate given a randomly selected proportion between 0 and 0.25 of the experiment that a beetle is active and at the maximum metabolic rate, with the remainder of the time spent at resting O_2-consumption rate. Therefore, O_2-consumption rate = Max. O_2-consumption rate at a given PO_2 × proportion of time active + resting O_2-consumption rate × proportion of time inactive. At each PO_2 (20, 17.5, 15, 12.5, 10, 7.5, 5 and 2.5 kPa) ten model iterations are shown.

A considerable reduction in metabolic scope could limit the ability of particularly larger beetles to successfully occupy and utilise a subterranean habitat. Reduction in metabolic rate has been suggested as an adaptation to stressful environments, enabling a greater allocation of resources to growth, reproduction and development (Chown and Gaston, 1999). Conversely, if the metabolic scope becomes narrower in larger beetles this could limit these vital processes.. Additionally, declines in aquatic O_2 levels reduce the beetles' metabolic scope. The largest known subterranean dytiscids, *Limbodessus magnificus* and *Limbodessus hahni* at 4.8 mm long, equivalent to 4.3 mg (Fig. 6B, (Balke et al., 2004; Watts and Humphreys, 2009)), may represent the upper size limit of these beetles which still have a functional metabolic scope. If small subterranean dytiscids are found to have a greater metabolic scope than larger species, this would support the idea that a reduction in metabolic scope associated with cutaneous respiration limits subterranean beetle size.

Body size, metabolic rate and cuticle thickness

The metabolic rate of subterranean dytiscids is lower than plastron breathing insects and resting insects generally (Fig. 8). The low metabolic rate in plastron breathers is associated with the significant resistance to O_2 diffusion that the boundary layer provides (Seymour and Matthews, 2013). The subterranean beetles have, in addition to the boundary layer, resistance of the cuticle, which corresponds with a further reduced metabolism. However, there are other factors that could contribute to a lowered metabolic rate. Subterranean dytiscids have reduced wings and are unable to fly (Watts and Humphreys, 2006), and insects that undertake low energy activities have lower resting metabolism compared to those that undertake highly energetic activities like flying (Reinhold, 1999). Low metabolism has also been associated with low and variable O_2 levels in subterranean aquatic isopods and amphipods (Hervant et al., 1998; Malard and Hervant, 1999), and resource limitation in subterranean environments (Hüppop, 1985). It is unclear whether the beetles in the Sturt Meadows and Laverton aquifers are resource-limited, but they are exposed to variable O_2 levels. In the Sturt Meadows aquifer, the percentage of the atmospheric O_2 saturation level ranges from ~50 to 100% in boreholes known to have beetles (Fig. S1), and O_2 saturation can vary by more than 40% within an individual borehole. This variability within and between bore holes has also been recorded in other aquifers containing dytiscids (Watts and Humphreys, 2006).

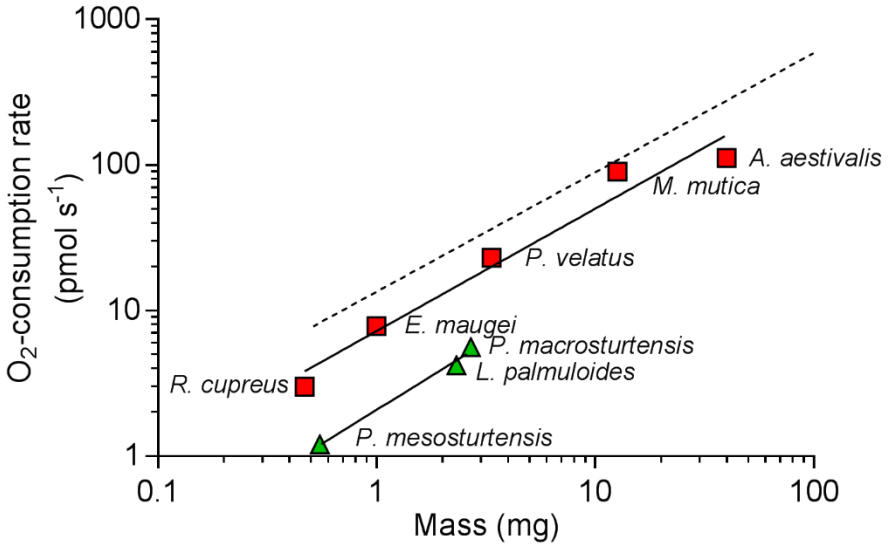

Figure 8. Comparison of O_2-consumption rate and body mass in insects. The allometric analysis includes the three subterranean dytiscids from this study (triangles, $\dot{M}O_2 = 2.0744M_b^{0.93}$), plastron breathing insects (Seymour and Matthews, 2013) (squares, $\dot{M}O_2 = 7.221M_b^{0.84}$, adjusted to 25°C assuming a Q_{10} of 2 (Chown et al., 2007)), and 391 insect species (resting O_2-consumption rate, dashed line, $\dot{M}O_2 = 13.452M_b^{0.82}$) (Chown et al., 2007). The slope of the regression for plastron breathing insects is not significantly different from the subterranean dytiscids, however, the elevation is significantly higher (ANCOVA, $P<0.05$). O_2-consumption rate data for subterranean dytiscids are from the water-only chambers using calculated wet mass.

The cuticle thicknesses of the three subterranean species in this study are between 6.3 – 8.4 µm, and are similar between the species despite the size differences (Table 1). These measurements give an indication of the thickness of two major surfaces of the beetles, the elytra and ventral sternites. However, cuticle thickness varies across the body including overlap of sternites, and the edges of the elytra over the edge of the abdomen, which could influence O_2 diffusion. The similarity in cuticle thickness between the subterranean species may indicate a trade-off between being thin enough to facilitate cutaneous respiration and thick enough to provide sufficient strength and integrity to allow the beetles to function within their environment without physical damage (Lane et al., 2017). Surface dytiscids may require thicker cuticles to resist damage from high energy environments and to protect them from predators. This hypothesis is supported by surface species *S. clavatus* and *N. dispar* having thicker than expected cuticles given their mass (Fig. 3), and potentially why the surface dytiscid *Deronectes aubei*, which has a relatively thick cuticle given its size (~50 µm, Kehl and Dettner, 2009), uses setal tracheal gills. The tracheal gills reduce resistance to O_2 diffusion, which would be much greater through the unelaborated cuticle, while still maintaining its strength.

Cuticle thicknesses of the subterranean beetles are within the range of other cutaneously-respiring insects. Fifth instar *Aphelocheirus aestivalis* (20 mg) respires through a 45 µm thick cuticle (Thorpe and Crisp, 1947b), and the diffusion distance of the tracheal gills of lestid damselfly larvae is estimated at 10 – 20 µm (Eriksen, 1986). In *D. aubei*, diffusion distance through the respiratory setae is <1 µm, like in the tracheal gills of Trichopteran larvae (Kehl and Dettner, 2009).

As dytiscids become larger the internal structure of the elytra changes (Fig. 2). In the subterranean and small surface dytiscids the elytra consists of a layer of cuticular laminae with a layer of soft tissue on the ventral surface containing the tracheae (Fig. 2D). However, in the larger dytiscids haemolymph spaces occur within the cuticular laminae separated by pillar-like trabeculae (Fig. 2A–C). The spaces may help lighten the elytra, assisting with flight, and the trabeculae provide additional mechanical strength (Ni et al., 2001; Van de Kamp and Greven, 2010). The tracheae, which appear to be within the haemolymph spaces (Iwamoto et al., 2002), would allow diffusion of respiratory gases throughout the elytra. This may also allow O_2 diffusion into the tracheal system through the cuticle from the water, or from the sub-elytral cavity, the latter being more likely due to the ventral cuticular laminae being thinner than the dorsal. Some beetles have air sacs within the elytra (Chen and Wu, 2013; Gokan, 1966), however, it is unclear if they are present in the larger dytiscids.

The subterranean beetles in this study differ from surface dytiscids that use air stores and gas gills and return to the surface regularly. However, they also differ from submergence-tolerant surface dytiscids because they lack structures like respiratory setae or pores (Fig. 1). The submergence-tolerant dytiscid *D. aubei* has ~20 µm long, spoon-shaped setae on their body, which have tracheoles running to the base and likely into the setae themselves (Kehl and Dettner, 2009). These setae, which are found at 5,900 per mm^2 on the elytra, allow O_2 diffusion from the water into the tracheal system through the thin cuticle of the setae (< 1 µm) traversing the ~50 µm thick elytral cuticle (Kehl and Dettner, 2009). In other submergence-tolerant surface dytiscids, punctures, small openings in the cuticle surface from which structures emerge (Wolfe and Zimmerman, 1984), and other small openings have been identified as potentially having respiratory roles. Individual punctures or openings/pores are 7 – 43 μm^2 at densities of 3,400 to 14,000 per mm^2. Similar structures of these sizes and densities are absent on the subterranean dytiscid species (Fig. 1).

Ecology and evolution

Observations with the borescope in boreholes show there were more occurrences of beetles near the water's surface. This may be associated with a higher PO_2 near the water's surface due to O_2 diffusion from the atmosphere, a general trend shown in boreholes known to have beetles (Fig. S1). However, O_2 levels can be inverted within a borehole with higher O_2 levels being deeper down (Watts and Humphreys, 2006). Beetles may also be congregating near the water's surface because insects and detritus fall into the water providing a food source. On two occasions in the laboratory, *P. macrosturtensis* was observed to crawl out of the water completely, associated with a strong odour above the water before they returned. This behaviour is likely to be secretion grooming, which surface dytiscids undertake to reduce bacterial growth with antimicrobial chemicals and to increase wettability of the cuticle (Dettner, 1985). This behaviour may also result in the beetles being closer to the surface. It is unclear whether smaller species like *P. mesosturtensis* undertake this behaviour as they easily become stuck to the water's surface due to surface tension and are unable to dive. However, having a clean cuticle would be important for ensuring optimal cutaneous respiration by reducing O_2-consumption caused by microbial growth, and encouraging convection of the boundary layer.

Most subterranean dytiscids are from the subfamily Hydroporinae in which members are generally <5 mm long and weigh <5 mg (Miller and Bergsten, 2016). Small size is useful for both evolving cutaneous respiration and occupying intermediate habitats between terrestrial and subterranean environments where beetles occupy small interstitial spaces. These include water-filled gravels where surface water interfaces with ground water or where surface waters dry up and ground waters are used as a refuge (Kato et al., 2010; Leys et al., 2010; Leys and Watts, 2008). Other groups of dytiscids are likely to have been removed from the transition to the subterranean habitats due to difficulties of fitting into small spaces, limited resource availability for larger species, and propensity to disperse under adverse conditions (Leys and Watts, 2008). Many aquatic insects, and in particular small species, are likely to benefit to some degree from cutaneous respiration (Vlasblom, 1970). The ability of these subterranean dytiscids to rely solely on this mode of respiration, and at relatively high temperature, has enabled this group to adapt to and survive in the aquifer environment. Given the considerable number of independent incursions into the subterranean environment (Cooper et al., 2002; Leys et al., 2003), cutaneous respiration in these dytiscids has contributed to the largest radiation of subterranean diving beetles in the world (Balke et al., 2004).

6. Acknowledgements

We thank Flora, Peter and Paul Axford for providing access and accommodation at the Sturt Meadows pastoral property, Chris Watts from the South Australian Museum for assisting with species identification, Lyn Waterhouse and Lisa O'Donovan from Adelaide Microscopy, William Humphreys from the Western Australian Museum for water quality data, Sally Maxwell and Silvia Clarke from DEWNR and Thomas Nelson and Qiaohui Hu from Adelaide University for assisting with collecting beetles and maintaining them, and two anonymous reviewers whose comments and suggestions helped improve this manuscript. KKJ was supported by the University of Adelaide for award of an Australian Government Research Training Program Scholarship. Funding was also provided by a South Australian Royal Society Small Research grant to KKJ and an ARC Discovery grant (#120102132) to SJBC.

7. Supplementary material

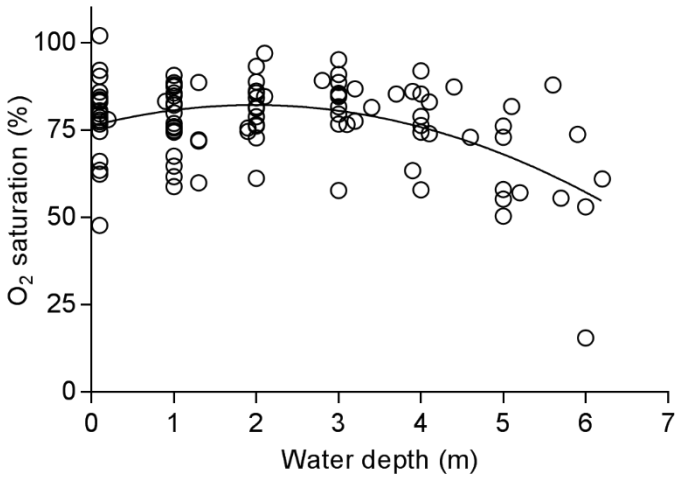

Figure S1. Change in the percentage of atmospheric O_2 saturation with depth in boreholes known to have subterranean beetles at the Sturt Meadows aquifer (*N*=22 boreholes, *N*=107 samples). Second order polynomial regression, $y = 76.11+6.079x+-1.539x^2$. Data collected April 2015, courtesy William (Bill) Humphreys, Western Australian Museum.

Table S1. A mathematical model based on Fick's general diffusion equation to calculate P_{O_2} at different points within the O_2 cascade of subterranean diving beetles to determine where limitations to cutaneous respiration may exist. The model calculates the P_{O_2} at the surface of the beetle and on the inside of the cuticle representing O_2 diffusion through the boundary layer and cuticle, respectively. The model has the following assumptions: (1) surface area for gas exchange (A) is defined as the surface area of a lozenge (ellipsoid and elliptical cylinder, Fig. S2), (2) conductance of O_2 is constant through the water or cuticle and is the product of the Krogh's coefficient of O_2 in each medium and the quotient of A and boundary layer (X_w) or cuticle thickness (X_c), (3) water is well-mixed and in equilibrium with atmospheric P_{O_2} (20.6 kPa) at 25°C, and (4) diffusion to and into the surface of the beetle is linear. Variables and constants used in the model are shown in Table S2, and O_2-consumption rate values are those measured experimentally in the water-only chambers (Table 2).

	Equation	*Description*
(1)	$\dot{M}_{O_2} = K_{O_2} \times A/X \times \Delta P_{O_2}$	Fick's diffusion equation used to describe O_2 diffusion through water to a respiratory surface (Rahn and Paganelli, 1968). Where $\dot{M}_{O_2}$ (pmol s^{-1}) is the rate of O_2-consumption, K_{O_2} (pmol s^{-1} kPa^{-1} cm^{-1}) is the Krogh's coefficient of diffusion, the product of capacitance and diffusivity, A (cm^2) is the surface area for gas exchange, X (cm) is the boundary layer thickness, a fluid layer above a respiratory surface deficient in O_2 that provides resistance to O_2 diffusion, and ΔP_{O_2} (kPa) is the P_{O_2} difference between the surrounding water and respiratory surface.
(2)	$P_{O_{2,s}} = P_{O_{2,w}} - ((\dot{M}_{O_2} \times X_w)/(K_{O_{2,w}} \times A))$	Rearrangements of Eq. 1 allow the calculation of P_{O_2} at the surface of the beetle (Eq. 2, $P_{O_{2,s}}$, kPa) and on the inside of the cuticle (Eq. 3, $P_{O_{2,in}}$, kPa), representing diffusion through the boundary layer and cuticle respectively. Where $P_{O_{2,w}}$, is the P_{O_2} of the bulk surrounding water, $\dot{M}_{O_2}$ is the experimentally determined O_2-consumption rate, X_w is the O_2 boundary layer surrounding the surface of the beetle, X_c is the cuticle thickness, $K_{O_{2,w}}$
(3)	$P_{O_{2,in}} = P_{O_{2,s}} - ((\dot{M}_{O_2} \times X_c)/(K_{O_{2,c}} \times A))$	

		is the Krogh's coefficient for water, $K_{O_{2,C}}$ is the Krogh's coefficient for the cuticle, and A is the surface area for gas exchange.
(4)	$A = 4\pi((ab)^{1.6}+(ac)^{1.6}+(bc)^{1.6}) \div 3)^{1/1.6} + (2\pi\sqrt{(1/2(a^2 + b^2))} \times h)$	Surface area of the beetle (A) can be calculated assuming the beetles are a lozenge shape, the sum of an ellipsoid (Knud-Thomsen approximation, the two ends) and an elliptical cylinder (the middle) (Michon, 2015; Spiegel et al., 2013), according to Eq. 4. Semi-axes a, b and c, and length (h) of the elliptical cylinder are shown in Fig. S2. Axis b (half of beetle width) is determined for each species from the diagrams given in Watts and Humphreys (2006), with the total length to width ratio (L:2b) being 1:2.5 for *P. macrosturtensis*, 1:2.97 for *L. palmulaoides*, and 1:2.45 for *P. mesosturtensis*. Axis c equals axis b. Axis a is determined for each species in the model by producing a linear regression of the mass of the lozenge, where mass (mg) $M_b = V \times 1078.4$ mg cm^{-3} (Density value determined for backswimmers, (Matthews and Seymour, 2008)) with an increasing value for a. Volume (V, cm^3) is determined with Eq. 5, the sum of the volume of an ellipsoid and elliptical cylinder (Spiegel et al., 2013). The linear mass regression is then rearranged to calculate a from the predicted wet mass of each species. The model can be adjusted to calculate P_{O_2} with increasing size by taking the average ratios between L and axes a, b and c (a = 1:10.3, b,c = 1:5.3) in the three beetle species and maintaining the ratios of axes with increasing length. The size range used was 0.04 – 4.82 mg (L = 0.1 – 5 mm).
(5)	$V = 4/3\pi abc + \pi abh$	Calculation for the volume of the lozenge shape.

Table S2. Variables and constants used in the mathematical model to calculate the P_{O_2} at the surface of the beetle and on the inside of the cuticle (Table S1).

Variable	Value	Units	Reference
$P_{O_{2,w}}$	20.6	kPa	1
X_w	0.010 (circulated water, all species), 0.075 (*P. macrosturtensis* in stagnant water), 0.070 (*L. palmulaoides* in stagnant water), 0.045 (*P. mesosturtensis* in stagnant water)	cm	2, 3
X_c	0.00076 *P. macrosturtensis*, 0.00078 *P. mesosturtensis*, 0.000645 *L. palmulaoides*	cm	3
$K_{O_{2,w}}$	0.290	pmol s^{-1} kPa^{-1} cm^{-1}	4
$K_{O_{2,C}}$	0.010	pmol s^{-1} kPa^{-1} cm^{-1}	5, 6
a	0.042 *P. macrosturtensis*, 0.027 *P. mesosturtensis*, 0.032 *L. palmulaoides*	cm	3
b, *c*	0.08 *P. macrosturtensis*, 0.039 *P. mesosturtensis*, 0.086 *L. palmulaoides*	cm	3, 7
L	0.4 *P. macrosturtensis*, 0.23 *P. mesosturtensis*, 0.42 *L. palmulaoides*	cm	7
Mb	2.72 *P. macrosturtensis*, 0.55 *P. mesosturtensis*, 2.32 *L. palmulaoides*	mg	3

References: 1, Dejours (1981); 2, Seymour et al. (2015); 3, present study; 4, Seymour (1994); 5, Krogh (1919); 6, Bartels (1971); 7, Watts and Humphreys (2006); Symbols: X_w = O_2 boundary layer thickness, X_c = cuticle thickness, $K_{O_{2,w}}$ = Krogh's coefficient of diffusion for O_2 in water at 25°C, $K_{O_{2,C}}$ = Krogh's coefficient for chitin used for the cuticle, adjusted to 25°C with a Q_{10} of 1.1 according to Bartels (1971) , *a* = semi-axis *a* of the lozenge shape used to estimate surface area of the beetles, *b* = semi-axis *b* of lozenge, *c* = semi-axis *c* of lozenge shape, *L* = total length of lozenge shape, and total length of each beetle species (See Fig. S2), Mb = beetle body mass.

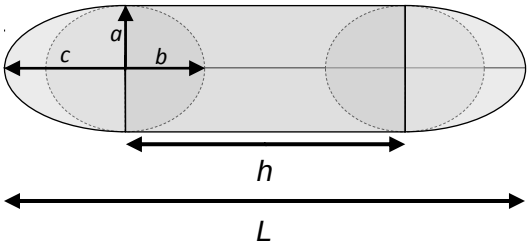

Figure S2. 3D geometric lozenge shape model that approximates the shape of subterranean diving beetles and allows estimation of surface area of the beetle. Axis a<*b, b*=*c*, *L* = total length, and h = elliptical cylinder length (*L* – 2*c*). Axis b is perpendicular to the plane of the page.

Chapter Four: Respiration, gas exchange and dive characteristics in the diving beetle *Platynectes decempunctatus* (Coleoptera: Dytiscidae)

Statement of Authorship

Title of Paper	Respiration, gas exchange and dive characteristics in the diving beetle *Platynectes decempunctatus* (Coleoptera: Dytiscidae)
Publication Status	☐ Published ☐ Accepted for Publication ☐ Submitted for Publication ☑ Unpublished and Unsubmitted work written in manuscript style
Publication Details	

Principal Author

Name of Principal Author (Candidate)	Karl K. Jones		
Contribution to the Paper	Undertook collection of study species, experiments, data and statistical analysis, writing of the initial manuscript, and reviewed and edited manuscript drafts.		
Overall percentage (%)	85%		
Certification:	This paper reports on original research I conducted during the period of my Higher Degree by Research candidature and is not subject to any obligations or contractual agreements with a third party that would constrain its inclusion in this thesis. I am the primary author of this paper.		
Signature		Date	21/1/19

Co-Author Contributions

By signing the Statement of Authorship, each author certifies that:

i. the candidate's stated contribution to the publication is accurate (as detailed above);

ii. permission is granted for the candidate in include the publication in the thesis; and

iii. the sum of all co-author contributions is equal to 100% less the candidate's stated contribution.

Name of Co-Author	Roger S. Seymour		
Contribution to the Paper 15%	Provided guidance on experiments, and reviewed and edited manuscript drafts.		
Signature		Date	1/2/2019

1. Abstract

Aquatic insects contend with the challenge of having a gas-filled respiratory system while living in water. To overcome this challenge many use bubbles on the surfaces of the body to store and supply O_2 for their dives. There are two types of bubbles: air stores, which are simple stores for O_2 gained at the surface, and gas gills that allow the passive extraction of O_2 from the water. Many insects using air stores and gas gills need to return to the surface to replenish their bubbles and, therefore, their requirement for O_2 influences their dive behaviour and interactions with their surrounding environment. In this study, we investigate gas exchange and dive behaviour in the diving beetle *Platynectes decempunctatus* that uses a sub-elytral air store and a small compressible gas gill. We directly link O_2-consumption rate at three temperatures (10, 15 and 20°C) with dive duration, surfacing frequency and movement activity. We also measure the PO_2 within the air store during tethered dives, as well as the amount of O_2 exchanged during surfacing events. Buoyancy experiments show how the volume of gas held by the beetles' changes during dives, and the size of the gas gill. These data are incorporated into a gas exchange model, which shows that the small gas gill of *P. decempunctatus* contributes only a small amount of O_2 during a dive relative to other aquatic insects, generally <10%. In addition, cutaneous O_2 uptake from the water may contribute up to 10% of total respiration.

2. Introduction

Insects evolved in a terrestrial environment, as indicated by their gas filled tracheal system (Pritchard et al., 1993). This provides a challenge for insects that have become aquatic secondarily. Several insect groups have overcome this challenge by utilising an air bubble on the surface of their bodies in communication with the tracheal system to supply O_2 for their dives underwater (Ege, 1915; Seymour and Matthews, 2013; Thorpe and Crisp, 1947a). There are two types of bubbles: air stores and gas gills (Ege, 1915; Rahn and Paganelli, 1968). Air stores are simple bubbles from which O_2 can be consumed, whereas gas gills allow passive O_2 extraction from the water. Gas gills can be either compressible or incompressible, the latter having structures to prevent collapse of the bubble due to O_2-consumption and N_2 and CO_2 loss to the water (Rahn and Paganelli, 1968; Thorpe and Crisp, 1947a; Thorpe and Crisp, 1947b).

In aquatic insects that use air stores and gas gills, there is a relationship between gas exchange (O_2-consumption, CO_2 loss) and dive characteristics (Calosi et al., 2007; Ege, 1915; Jones et al., 2015). Dive characteristics are measurable parts of the dive cycle and include dive duration, surfacing duration and surfacing frequency. The dive cycle begins with the insects exchanging gas with the atmosphere. Once the gas gill or air store is replenished, the insect dives and begins consuming O_2, which may also diffuse into the gas gill from the water. Once the O_2 level becomes too low or the gas volume too small, the insect needs to return to the surface. These dive variables are important because they affect an insect's allocation of time and energy to foraging and mating, and their exposure to predators and parasites (Aiken, 1985; Calosi et al., 2007; Miller and Bergsten, 2016). Dive duration is expected to decrease with greater activity or higher temperature, due to increased O_2 demand, and would be expected to increase with more gas volume stored or increased O_2 diffusion from the water. Assuming surfacing duration remains constant, surfacing frequency would therefore be the inverse of dive duration. The surfacing duration is thought to be constant in aquatic insects due the need to balance replenishment of the air store with the need to minimise exposure to predators at the surface (Calosi et al., 2007; Jones et al., 2015).

Diving beetles (Dytiscidae) are a diverse and widespread group of predatory aquatic beetles that use a sub-elytral air store and a small compressible gas gill to survive underwater (Calosi et al., 2007; Ege, 1915; Gilbert, 1986; Kehl and Dettner, 2009). Despite the prevalence of dytiscid species, few studies have investigated the relationships between gas exchange and dive characteristics in this group. Ege (1915) noted that an increase in temperature increases surfacing frequency in dytiscids as well as other aquatic insects, related to higher O_2-

consumption rates. Calosi *et al.* (2007) showed in *Ilybius montanus* that increased temperature increases surfacing frequency, decreased dive duration, and surfacing duration remained constant. Combined data for two genera and 25 species of dytiscids also show these relationships, although there is variation in the response to temperature between genera and species (Calosi et al., 2012). The dive responses of some species may be complicated by additional respiratory structures on the surfaces of some small diving beetles as well as cutaneous respiration (Jones et al., 2018a; Kehl and Dettner, 2009; Madsen, 2012). None of the studies to date have measured O_2-consumption rate and gas exchange in dytiscids and related this to dive characteristics under various conditions. This is partly due to the difficulty in measuring gas exchange in insects that utilise both aquatic and atmospheric O_2 (Calosi et al., 2007).

In this study, we investigate the relationships between O_2-consumption rate, gas exchange, and dive characteristics in the diving beetle *Platynectes decempunctatus* (Fabricius 1775). Using fibre-optic O_2-sensing probes (optodes), we measure O_2-consumption rate in closed-chamber respirometers and the P_{O_2} within the air store of the beetles. Dive duration, surfacing frequency, surfacing duration and a metric for activity are measured in beetles in the respirometry chambers and larger control dive chambers at three temperatures (10, 15 and 20°C) to make comparisons between temperatures and experimental results. We measure the respiratory gas volume, which includes the gas within air store and tracheal system, the rate of volume change during dives in free diving beetles, as well as the size of the gas gill used by this species. This study directly links O_2-consumption rate with the dive characteristics and explores their interactions under different experimental conditions. It also provides direct measurements of air store P_{O_2} decline during a dive, and quantifies the importance of the gas gill and cutaneous respiration to respiratory gas exchange in this species with experiments and mathematical modelling.

3. Methods and materials

Animals

Platynectes decempunctatus, identified according to Watts and Hamon (2014) were collected from a pond in Balhannah and creeks near Strathalbyn, South Australia between January and April 2016 and 2018, and May 2017, respectively. Water temperatures were between 9-22°C at collection sites. Individual beetles were placed in 800 ml plastic containers two-thirds filled with a mixture reverse osmosis (RO) and pond water and lightly aerated with an air pump. Dead leaves and living plant material provided cover within the containers. Beetles were placed into a CT

(constant temperature) cabinet set to the treatment temperature (10, 15 or 20°C), and were fed 8-15 live black worms twice a week. Beetles were maintained at the treatment temperatures for at least 7 days on a 12 h day-night cycle prior to experiments (Calosi et al., 2007; Calosi et al., 2012; Terblanche et al., 2005). After experiments beetles were dried with paper towel and weighed with an analytical balance (0.01 mg precision, AE 163, Mettler, Greifensee, Switzerland).

Respirometry

Respirometry chambers were glass jars 41 mm tall and 18 mm in diameter with a 7 mm diameter opening. Individual beetles were placed into a dry chamber that contained a small piece of rubber approximately 2 mm^3 that the insects could cling to. Chambers were completely filled with air-equilibrated RO water at the treatment temperature and sealed with a stopper that had a 1.5 mm diameter hole through the centre. The chamber was then dried on the outside and weighed, followed by the injection of *ca.* 0.2 ml air into the chamber that was then dried and reweighed. These measurements along with the known chamber and stopper masses allowed precise calculation of water and air volumes within the chamber.

A water-filled Pasteur pipette was then inserted through the hole in the stopper, and the chamber was placed into a water bath in a CT cabinet. Water within the pipette provided a barrier to O_2 diffusion into the chamber and allowed pressure within the chamber to remain in equilibrium with the atmosphere. The water in the bath was circulated with a small 5W aquarium pump with the top of the chamber 1 – 2 cm below the water's surface.

A fast response, tapered tip, fibre-optic oxygen sensing optode (PreSense GmbH, Regensburg, Germany) was then placed into the water within the chamber through the pipette and the initial P_{O_2} of the water was recorded for 2 min once the O_2 trace became stable. The optode was then moved into the air space for 40 min, producing a record of P_{O_2} decline within the air. Afterward, the optode was removed and the water within the chamber was gently mixed. The optode was returned to the water for the final P_{O_2} measurement which was recorded for 2 min once the trace became stable. Beetles were then removed from the chambers, their body surface dried, and weighed.

Background respiration was measured by returning the experimental water to the chamber and topping up with RO water to completely fill the chamber. 1 h elapsed between initial and final background P_{O_2} measurements with the chamber water being gently mixed prior to final P_{O_2} measurement.

Oxygen consumption rate was calculated according to the following equation;

$$\dot{M}O_2 = \beta \times V \times \dot{P}O_2 \quad (1)$$

where oxygen consumption rate ($\dot{M}O_2$; μM h^{-1}) in either air or water is the product of water or air's capacitance for O_2 (β; μmol ml^{-1} kPa^{-1}) at the experimental temperature in pure water or air, the volume (V; ml) of either air or water, and the rate of PO_2 change ($\dot{P}O_2$; kPa h^{-1}) in either media over the duration of the experiment. The capacitance values used at 10, 15 and 20°C are as follows, for air 0.425, 0.417 and 0.410 μmol ml^{-1} kPa^{-1}, and for water 0.0168, 0.0151, 0.0137 μmol ml^{-1} kPa^{-1}, respectively (calculated from Dejours (1981)).

O_2-consumption rate of the beetles was calculated by subtracting the O_2-consumption rate measured in the water filled chamber without the beetle from that measured with the beetle in the chamber (the sum of both air and water $\dot{M}O_2$). Background respiration measurements contributed 1.1±1.7% of total respiration. Some experiments experienced a small increase in PO_2 over the duration of the background experiment which is likely due to a small amount of O_2 diffusion into the chamber or sensor drift.

While measuring PO_2 in the respirometry chambers the beetles were recorded with a video camera at 25 frames per second (XA-20, Canon Inc., Tokyo, Japan). This allowed calculation of (1) surfacing frequency, the number of surfacing events per h, (2) dive duration, the time between surfacing events minus the surfacing duration (s), (3) surfacing duration, the time (s) spent at the surface where the tip of the abdomen had broken the water's surface signifying gas exchange, and (4) activity, which was determined by removing 1 video frame every 5 s over the duration of the experiment with a media player (VLC media player, Version 2.2.3, USA) and determining whether the beetle moved position between frames. Activity was calculated as the number of times beetles moved between frames divided by the number of frames used minus 1. This produced a value between 0 and 1 of the proportion of the experiment the beetle was active. Surfacing events were identifiable from the angle at which the beetles ascended to the surface and remained there with the tip of the abdomen touching the water's surface, which is distinct from the beetle simply floating at the surface (Fig. S1) (Gilbert, 1986).

Median surfacing duration was determined, in addition to mean surfacing duration, because many beetles had a small number of surfacing durations that were considerably longer than the

others undertaken by the beetle. Maximum dive durations were determined from the single longest dive recorded for each individual.

Points at which the beetles surfaced and exchanged gases could be identified from some of the P_{O_2} traces in air, indicated by a rapid drop in P_{O_2} within the air space above the water. The amount of O_2 exchanged at each surfacing event was calculated from P_{O_2} traces where all surfacing events clearly matched those identified in video recordings. To do this, 20-60 s of stable P_{O_2} trace just prior and just after the steep P_{O_2} decline were selected and averaged. The amount of O_2 exchanged was then calculated using Eq. 1 with these two P_{O_2} averages and the known air volume in the chamber. The gas volume held by the beetle was only ~2% of that in the chamber. O_2-consumption rate for the proceeding dive was then calculated, assuming no gas exchange with the water, by dividing the amount of O_2 exchanged at the surface by the dive duration. To make a comparison between the total O_2-consumption rate and that calculated from all surface exchanges throughout an experiment, the O_2-consumption rate determined for each dive was multiplied by the proportion of time during the experiment that that dive occupied. These results were then summed to produce an O_2-consumption rate from surfacing exchange that represents the entire experimental period.

During many experiments clear surfacing events were not observable in P_{O_2} traces. This was due to short dive durations and high levels of activity near the surface that result in inadvertent surfacing and therefore small amounts of O_2 being exchanged that were difficult to detect.

The integrity of the respirometry chambers was checked at 25°C by filling the chambers with pure gaseous N_2 and leaving them for approximately 3.5 h. P_{O_2} increased on average at 0.0163 kPa h^{-1} with a P_{O_2} gradient >20 kPa equivalent to 0.04 μmol h^{-1} (Min 0.00262 kPa h^{-1}, Max. 0.0783 kPa h^{-1}, N=12). Beetles used in this study produced average rates of O_2 decline of 3.103 kPa h^{-1} in air and 0.749 kPa h^{-1} in water, but the lowest P_{O_2} experienced by the beetle in the chambers was ~ 15 kPa in air, so O_2 diffusion would have been less than recorded in the N_2-filled chambers.

Two cohorts (N=11, N=8) of beetles were exposed to the temperature treatment sequence in opposite orders to counter adjustment of the beetles to the experiments and order of treatments. Data were excluded if experiments were deemed unsuitable due to excessive time spent at the surface (e.g. in 4 of 57 cases).

Determination of air store P_{O_2}

Similar methods were used to measure air store P_{O_2} in the beetles as plastron P_{O_2} in the aquatic bug *Aphelocheirus* (Jones et al., 2018b). Beetles were attached to a piece of wire with warm melted depilatory wax (Klorane, Boulogne, France) on the pronotum. A small hole was drilled with a dental drill (bit 0.63 mm dia.) through an elytron into the subelytral cavity approximately 1/3 the way along the elytron from the anterior end, being careful not to damage the soft tissue. A ~5 mm long polyethylene tube (ID 0.28, OD 0.61mm) was placed through the hole into the subelytral cavity. The hole in the elytron was sealed around the tube with cyanomethacrylate adhesive, ensuring the end of the tube was not blocked. The beetle, in swimming orientation with the wire attached, was held in place with a small magnet above a glass container (11 cm L x 10.5 cm H x 3.5 cm W). The container, which was filled with air-equilibrated water, was on a platform that could be raised and lowered. A fast-response, taper-tipped optode attached to a micromanipulator was inserted into the air store tube until the optode's protective sheath made contact with the tube. The top of the tube, with the optode inserted, was then sealed with vacuum grease (D1400 high vacuum grease, Dow Corning Corporation, MI, USA). The suspended beetle was viewed from the side along the frontal plane with a horizontal dissecting microscope (Fig. 1). The water container was then raised so that the beetle was ~ 1 cm below the water's surface. Once submerged, air store P_{O_2} would begin to decline. After air store P_{O_2} had plateaued for a period, the water container was lowered and the beetle was exposed to the air again replenishing the air store. This occurred six times per individual in a CT room set to 20°C. The optode temperature sensor was placed in the water container.

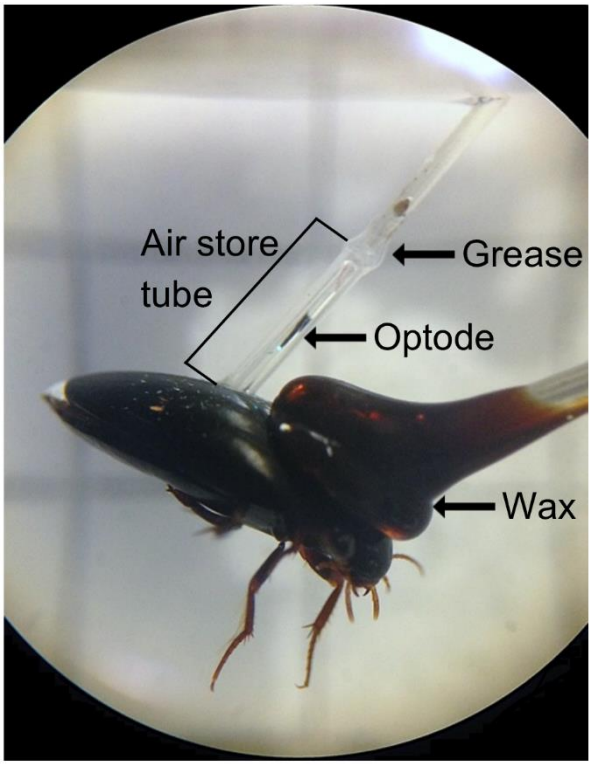

Figure 1. Microscope image showing measurement of air store P_{O_2}. The beetle was attached to a piece of wire with depilatory wax, with the air store tube inserted through the elytron on the far side of the beetle. The cyanomethacrylate adhesive around the tube and elytron hole cannot be seen. The optode is inserted into the top of the air store tube which was sealed with vacuum grease.

Control dive chambers

As a control to compare dive responses of beetles within the respirometry chambers, beetles' dive characteristics were recorded in 1 L Schott bottles. Each bottle contained gravel (2 mm dia.) to cover the bottom, a piece of black plastic with weighted ends (2 × 7.5 cm) to provide cover for the beetles, and air-equilibrated RO water to 8 cm deep. Four bottles were placed next to each other in a water-filled aquarium to reduce optical distortion. The aquarium, which was in a CT cabinet at the treatment temperature, was lit from above with a florescent light and had a white background. White dividers visually isolated the beetles in each jar. Individual beetles were placed into each jar and left to adjust for 1 h before commencing recording for 12 h with the video camera (Canon XA-20). Videos were then inspected for surfacing frequency, dive duration, surfacing duration and activity. The number of hours of footage analysed for each beetle varied so that at least eight surfacing events were recorded. This ranged from 1 – 4 h at 20°C, 4 h at 15°C and 1 – 11 h at 10°C. Three separate cohorts of beetles were used, and temperatures were maintained within ±1°C of the treatment temperatures.

Determination of beetle density and gas volume during dives

Density of beetles was determined according to Archimedes' principle (Matthews and Seymour, 2008). Beetles were euthanized with chloroform fumes, gently blotted dry with paper towel and weighed with the analytical balance. Beetles were then placed underwater into a 10 ml glass syringe. A finger was placed over the end of the syringe and the plunger drawn out to remove air from the surface and tracheal system of the beetle. While under negative pressure the finger was released and the gas within the syringe was expelled before undertaking the process an additional 4 – 5 times. The beetle was then placed in a small tube underwater that was flicked to remove any bubbles on the outside of the beetle. The negatively buoyant beetle was then transferred to a custom made weighing pan hanging in a 4 cm deep Petri dish of water below the AE 163 balance. The submerged weight was then determined, and body volume was calculated according to the formula;

$$V = (W_{air} - W_{H_2O}) \div \rho H_2O \quad (2)$$

where V is volume (cm^3), W_{air} is the insect's weight in air and W_{H_2O} is its weight underwater (g), and ρH_2O is the density of pure water at the temperature used in the measurement (g cm^{-3}). The density of the beetles (ρ_b, g cm^{-3}) was then calculated with the following equation;

$$\rho_b = W_{air} \div V \quad (3)$$

To determine volume of respiratory gas carried by free-diving beetles, a glass vial (dia. 25 mm, height 50 mm) containing 20 ml of air-equilibrated RO water was placed below the AE 163 balance in a water-filled glass container (11 cm L x 10.5 cm H x 3.5 cm W). A wire rod, weighted (~45g) to compensate for removal of the weighing pan and reduce lateral movement, was hung from the weighing hook on the bottom of the balance (Matthews and Seymour, 2008). The wire extended into the water in the vial with a small D-loop at the end perpendicular to the wire. This provided a platform for the beetles to hold onto. The apparatus was placed in a CT room pre-adjusted to the experimental temperature (20°C). Before an individual beetle was placed into the vial the fan was turned off to allow air movement to settle, which otherwise affected force measurements. Once the beetle was in the vial and not touching the wire, the balance was tared to account for mass of the wire and buoyant force on the wire. Beetles could then voluntarily hold onto the wire platform when diving. The CT room was then closed with the lights turned off and the beetle allowed to adjust to conditions for 1 h. Buoyant force was then recorded at 1 Hz with the balance through a Mettler 012 data interface connected to a computer. The beetle was filmed

simultaneously in infrared with the video camera (Canon XA-20) to accurately determine dive duration and when the beetle was holding onto the platform.

The gas volume of the beetle (V_{air}) was then calculated according to the formula (Matthews and Seymour, 2008):

$$V_{air} = -1(W_{tot} - W_i) \quad (4)$$

where W_{tot} (g) is the total submerged weight of the insect and gas held by the beetle, and W_i is the submerged weight of the beetle which was calculated with the formula;

$$W_i = W_{air} - (W_{air}/\rho_b)\rho H_2O \quad (5)$$

To calculate the respiratory gas volume of the beetle, which includes gas within the air store and tracheal system at the beginning and end of a dive and the rate of decline, gas volume was calculated from the force trace when the beetle was on the platform (Eq. 4 and 5). A linear regression was then applied to the calculated gas volume trace, corrected for the time from the beginning of the dive and delay of the balance once force was applied, generally 6 – 12 s (Fig. 2). The initial bubble volume was the y-intercept of the regression, final bubble volume was calculated from the dive duration time, and the rate of bubble volume decline was the slope. Drift was corrected in the force traces with linear regressions using two periods when the beetle was not on the platform before and after analysable dives using the platform.

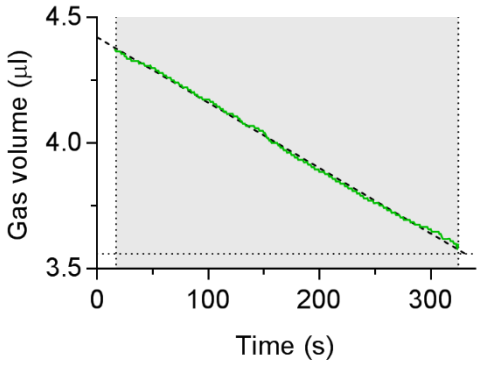

Figure 2. Example of the decline in respiratory gas volume of *P. decempunctatus* using the buoyancy platform. Shaded area shows when the beetle was on the platform, with the green solid line showing the change in gas volume recorded. Dashed black line indicates the linear regression corrected to the beginning of the dive and projected to the end of the dive at 332 s. The y-intercept is the initial bubble volume, and final bubble volume is the volume at dive termination (332 s, horizontal dotted line), with the slope of the regression being the rate of bubble volume decline.

Gas gill volume

Gas gill volume was calculated from video frames recorded during buoyancy experiments by measuring the size of the gas gill bubbles in the images (Fig. 3). In dives where gas gills were identified, one frame every 5 s was removed from the video using a media player (VLC media player). From the first frame identified with a gas gill, where beetles were stationary, frames were analysed every 30 s from then on. Square grids (5 mm graduations) allowed calculation of the number of pixels per mm at the front and back of the glass container. The distance in pixels between the two grids could be measured from an image of the side of the glass container in a mirror placed next to it. A linear regression was used to determine how the number of pixels mm^{-1} changed from the front to the back of the chamber. This varied by only 4.5 – 6.5%. The distance of the gas gill bubble from the front of the chamber and the size of the bubble, using a circle or an ellipse, was measured with ImageJ (Version 1.5i, Wayne Rasband, NIH, USA). The linear regression was used to correct the pixels mm^{-1} to the distance of the gas gill from the front of the chamber. Volume (V, µl) was calculated as the volume of an ellipsoid (Eq. 6; Spiegel et al., 2013), and area (A, mm^2) was calculated from the approximate equation for an ellipsoid (Eq. 7, Knud-Thomsen approximation, (Michon, 2015)). It was assumed in both equations that the minor semi-axis (half of the diameter) of the ellipse was equal to two perpendicular ellipsoid semi-axes and that the major semi-axis was equal to the third ellipsoid semi-axis, perpendicular to the two other semi-axes. Additionally, the bubble formed a full ellipsoid, or a sphere if semi-axes were equal, with the equivalent volume and surface area. At larger bubble sizes the gas gill did form an almost perfect sphere on the tip of the abdomen. a = the major semi-axis, b = minor semi-axis and c = b (mm).

$$V = 4/3\pi abc \quad (6)$$

$$A = 4\pi((ab)^{1.6}+(ac)^{1.6}+(bc)^{1.6}) \div 3)^{1/1.6} \quad (7)$$

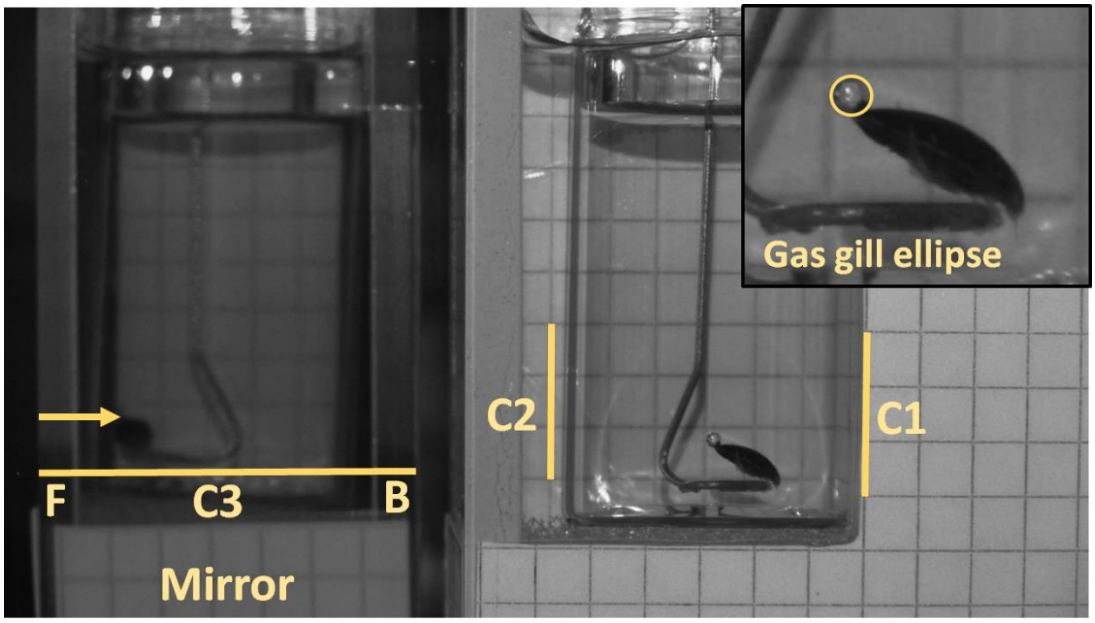

Figure 3. Frame image from buoyancy experiments showing features used in determining gas gill volume and surface area with a beetle on the wire platform attached to the analytical balance above (not shown). C1, determination of pixels mm^{-1} at the front of the chamber; C2, determination of pixels mm^{-1} at back of the chamber; C3 distance between the grids at the front and back of the chamber in pixels. The side of container shown in the mirror on the left. The arrow indicates the distance from the front of the chamber to the gas gill. Inset shows the overlay of the ellipse to measure the major and minor axes of the bubble. Grid squares 5 mm.

Statistics

Linear and power regressions, and ANOVA and Tukey's Post-hoc tests were performed with Excel and GraphPad Prism 7.02 (GraphPad Software Inc., La Jolla, CA, USA). Means, and where noted, medians, are reported with 95% confidence intervals (CI).

4. Results

Respirometry

Both whole-animal and mass-specific O_2-consumption rates were significantly higher at 20°C than at 10°C and 15°C in the respirometry chambers (Table 1). The Q_{10}, the factor by which metabolic rate increases with a 10°C rise in temperature, was 1.6 between 10°C and 15°C, 2.7 between 15°C and 20°C, and 2.1 between 10°C and 20°C. Beetle mass between treatments was not significantly different from each other (Table 1). Mean temperatures for the treatments were 10.0±0.0°C, 15.0±0.0°C and 20.0±0.0°C.

Table 1. Mass and O_2-consumption rate of *P. decempunctatus* at the three treatment temperatures. * indicates significantly lower O_2-consumption rate than 20°C treatment (Pair-wise ANOVA $P<0.0001$, Tukey's post-hoc $P<0.001$). Mean values shown with 95% CIs ($N=13$ individuals).

Treatment	Mass (mg)	O_2-consumption rate (µmol h^{-1})	Mass-specific O_2-consumption rate (µmol h^{-1} g^{-1})
10°C	24.63±1.85	0.23±0.05*	9.24±1.97*
15°C	24.65±1.81	0.29±0.04*	11.68±1.49*
20°C	24.52±1.78	0.47±0.08	19.40±3.08

In nine of the respirometry experiments all surface exchanges with the air space in the chamber could be measured with the O_2 probe and verified with video footage (Table 2). Beetles could exchange gases with air in a second or less causing a rapid decline in PO_2 in the air space (Fig. 4A). However, if they remained at the surface the beetles could continuously exchange O_2 with the air space after the initial O_2 exchange (Fig. 4B). The O_2-consumption rate calculated from the amount of O_2 exchanged with the air space during surfacing events, assuming no gas exchange with the water, was 71– 82% of the O_2-consumption rate determined from the total O_2 consumed from both the air and water during each experiment (Table 2). The O_2-consumption rate from surfacing exchanges was determined from the initial amount of O_2 exchanged during a surfacing event, e.g. only the rapid decline in PO_2 (Fig. 4), divided by the duration of the proceeding dive. This value was then multiplied by the proportion of time the dive occupied during the experiment, and these values were summed for all dives to produce an average O_2-consumption rate from surface exchanges during each experiment. The difference between the whole-animal O_2-consumption rate and that calculated from surfacing exchanges indicates the amount of O_2 gained from the water. The mean amount of O_2 exchanged at the surface for each event was between ~18 – 23 nmol.

Table 2. O_2-consumption rate and exchanges in respirometry chambers where all O_2 exchanges with the air space could be measured. Data includes whole-animal O_2-consumption rate determined from O_2-consumption from both air and water, mass-specific O_2-consumption rate, average amount of O_2 exchanged with the air space during each surfacing event, surfacing frequency, the O_2-consumption rate calculated from surfacing exchanges, and O_2-consumption rate calculated from surfacing exchanges as a percentage of whole-animal O_2-consumption rate. O_2-consumption rate calculated from surfacing exchanges was determined from the initial rapid decline in P_{O_2} when the beetle surfaces, divided by the duration of the dive proceeding that surfacing event. The O_2-consumption rate for each dive in an experiment was then multiplied by the proportion of time that dive occupied during the entire experiment. These values were then summed for all dives producing an average O_2-consumption rate determined from surfacing, which assumes no O_2 exchange with the water. Means shown with 95% CIs. *N* = number of experiments.

Temp. (°C)	Mass (mg)	Whole-animal O_2-consumption rate (μmol h^{-1})	Mass-specific O_2-consumption rate (μmol h^{-1} g^{-1})	Mean amount of O_2 exchanged at the surface per surfacing event (nmol)	Surfacing frequency (N h^{-1})	O_2-consumption rate calculated from surfacing (μmol h^{-1})	O_2-consumption rate calculated from surfacing exchanges as a % of whole-animal O_2-consumption rate	*N*
10	25.02±2.82	0.18±0.04	7.25±1.22	18.7±5.4	8.8±1.7	0.14±0.03	82±11	4
15	25.27±0.22	0.28±0.09	11.24±3.60	23.2±4.9	9.4±3.5	0.21±0.10	71±17	3
20	22.38±6.82	0.30±0.07	14.07±7.23	23.1±3.4	10.7±0.2	0.23±0.04	78±4	2

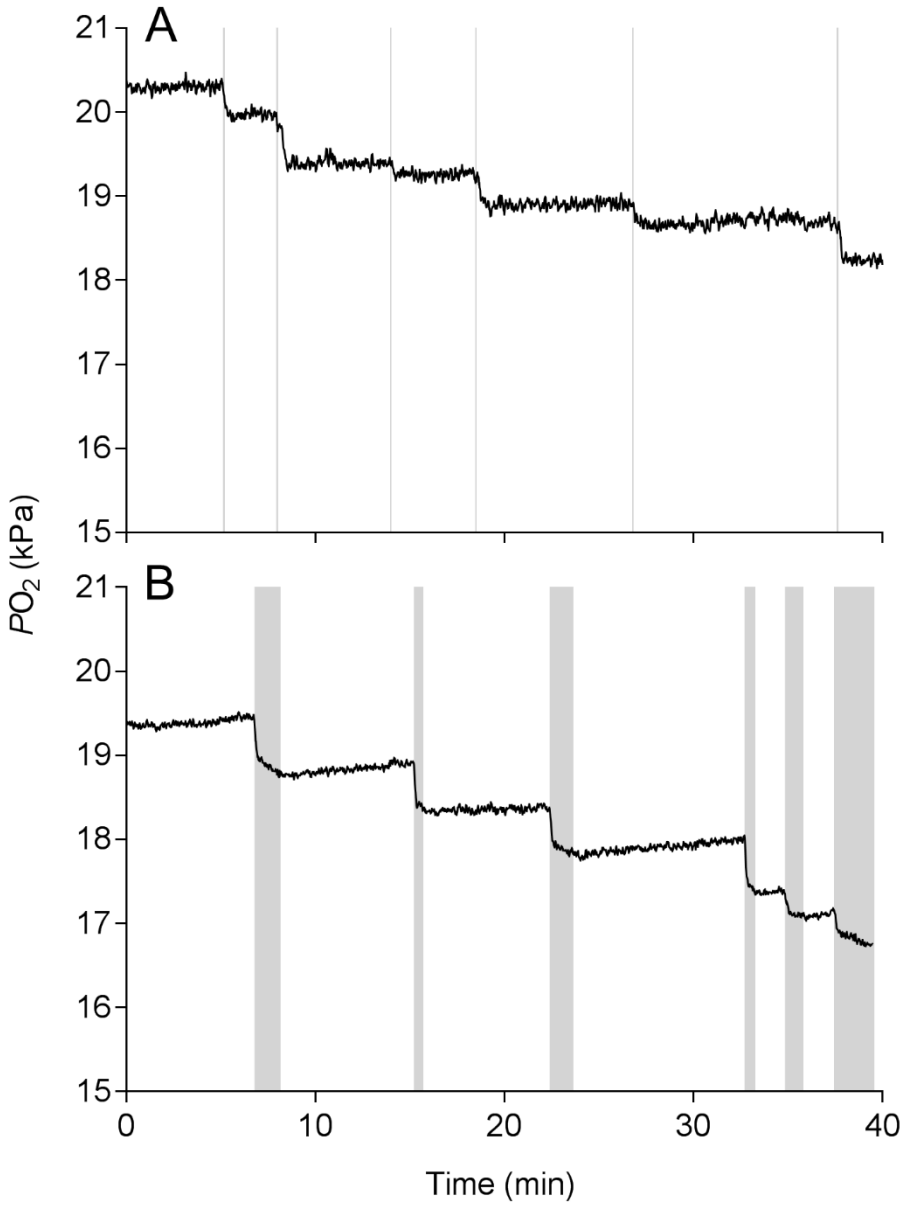

Figure 4. P_{O_2} decline in the *ca.* 0.2 ml air space within a respirometry chamber containing a *P. decempunctatus* at (A) 15°C and (B) 10°C. Steep drops in P_{O_2} indicate a surfacing event, shaded grey areas/bars indicate when the beetle was at the water's surface determined from video analysis. The slow increase in P_{O_2} following a surfacing event is due to O_2 diffusion from the water within the respirometry chamber. (A) Illustrates O_2 can be exchanged within 1 s when surfacing. In A, all surfacing events were about 1 s in duration, apart from the second and last surfacing events, each 6 s in duration (the first surfacing event being at ~5 min, and surfacing duration was measured in 1 s increments). (B) Shows that after the initial exchange of gas with the air space the beetle can continue exchanging O_2 while at the surface.

Air store P_{O_2}

When beetles were forced to submerge, the air store P_{O_2} began to decline, with figure 5 illustrating examples of variation in this decline. The rate of decline was slower when beetles were quiescent, but increased during generally short periods of activity (Fig. 5, traces 1–3). Air store P_{O_2} stabilised when the P_{O_2} became very low (Fig. 5, traces 1 and 2), or when the beetle had a large gas gill (trace 3). Sometimes after beetles were removed from the water the air store P_{O_2} would not return to atmospheric levels indicating the air store was sealed from the atmosphere. Paper towel was then gently used to dry any water that may have entered the air store and encourage the beetle to open the air store by adjusting the elytra or abdomen. In quiescent beetles the rate of P_{O_2} decline in the air store was 1.85±0.48 kPa min^{-1} and in active beetles 6.85±0.78 kPa min^{-1} (*N*=7 beetles, 3-6 measurements per beetle). These measurements were calculated from the P_{O_2} difference 10 s apart where P_{O_2} was above 10 kPa to avoid potential O_2 limitation affecting results at low P_{O_2} levels. Data were excluded if the minimum rate of P_{O_2} decline corresponded with an observation of activity, or if the maximum rate of P_{O_2} decline corresponded with an observation of inactivity. This was to ensure the maximum and minimum rates of P_{O_2} decline were associated with activity and inactivity, respectively. Additionally, data were excluded if the beetles had large gas gills because O_2 diffusion from the water would reduce the rate of P_{O_2} decline caused by O_2 consumption of the beetles.

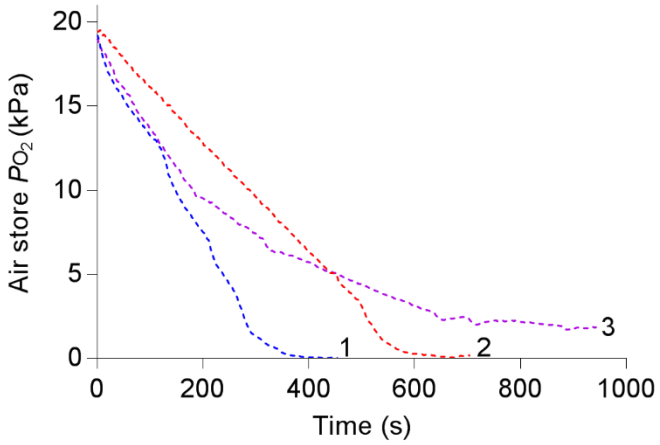

Figure 5. Air store P_{O_2} decline in submerged tethered *P. decempunctatus*. Trace 1 shows a intermittently active beetle, indicated by rapid declines in P_{O_2}, before P_{O_2} becomes stable at almost zero. Trace 2 shows a beetle that is inactive up to ~500 s, after which P_{O_2} declines rapidly due to activity and then becomes stable at almost zero. This beetle only had a very small amount of gas gill bubble exposed to the water. Trace 3 shows a periodically active beetle using a large gas gill from ~120 s resulting in stabilisation of P_{O_2} at ~2 kPa.

Dive characteristics

Mean and maximum dive duration were significantly shorter, and surfacing frequency significantly higher, at 20°C than 10°C or 15°C in the respirometry chambers when comparing 12 sets of paired data within the full dataset (Pair-wise ANOVA, Tukey's post-hoc, $P \leq 0.05$, Table S1 and S2, Full dataset Fig. 6). Activity was significantly lower at 15°C than 20°C (Pair-wise ANOVA, Tukey's post-hoc, $P \leq 0.01$). There were no significant differences in either the mean or the median surfacing duration between the different temperatures (Pair-wise ANOVA, $P>0.05$).

In the control dive chambers mean and maximum dive durations were significantly shorter at 20°C compared to the 10°C and 15°C treatments (ANOVA, Tukey's post-hoc $P \leq 0.05$, Fig. 6A and B, See Table S1 for means and 95% CIs, and S2 for statistical results). However, there were no significant differences between temperatures for surfacing frequency, mean and median surfacing duration, and activity (ANOVA $P>0.05$, Fig. 6C, D, E and F). In the respirometry chambers mean surfacing frequency was significantly higher at 20°C than 10°C and 15°C (ANOVA, Tukey's post-hoc $P \leq 0.01$), and median surfacing duration was significantly higher at 10°C than 15°C (ANOVA, Tukey's post-hoc $P \leq 0.05$). There were no significant differences in dive duration, mean surfacing duration and activity between the temperature treatments (ANOVA, $P>0.05$).

Comparing the dive characteristics of the beetles in the respirometry chambers and control dive chambers showed that mean and maximum dive durations were significantly shorter (ANOVA, Tukey's post-hoc $P \leq 0.01$) at 10°C and 15°C in the respirometry chambers than the respective treatments in the controls (Table S1 and S2). Activity was significantly higher (ANOVA, Tukey's post-hoc $P \leq 0.05$) at 15°C in the respirometry chambers, and mean surfacing duration significantly longer at all temperatures in the respirometry chambers than the respective treatments in the controls (ANOVA, Tukey's post-hoc $P \leq 0.05$). Median surfacing duration was significantly longer at 10°C in the respirometry chambers than the controls (ANOVA, Tukey's post-hoc $P \leq 0.05$).

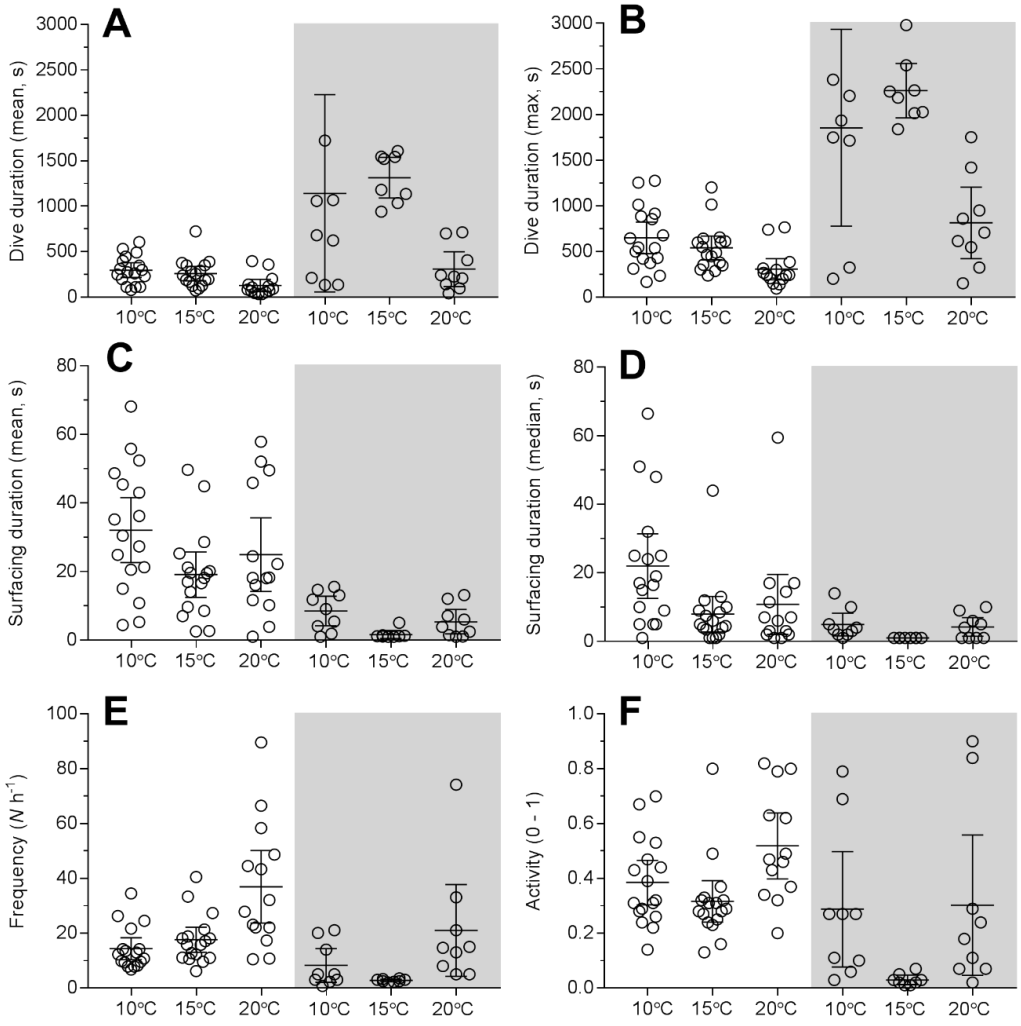

Figure 6. Dive characteristics recorded during respirometry (left of each plate) and control dive experiment (right, shaded) at the different treatment temperatures. A, mean dive duration; B, max. dive duration; C, mean surfacing duration; D, median surfacing duration; E; mean surfacing frequency; F, mean activity. Grand means are shown with 95% CIs. Two outliers were removed from the control dive data at 10°C for mean dive duration at 4,643 s and max. dive duration at 24,274 s.

Relationships between dive characteristics and O_2-consumption rate

Comparisons were made between dive duration, activity and surfacing frequency with O_2-consumption rate. O_2-consumption rate ($\dot{M}O_2$; µmol h^{-1}) is inversely related to dive duration (t; s) across the three temperature treatments and forms a linear relationship when log transformed, where $\log \dot{M}O_2 = -0.3796 \times \log t + 0.3176$ (R^2=0.48, Fig. 7A and B). Activity (A; proportion of 1) and surfacing frequency (f; N h^{-1}) are both positively and linearly correlated with O_2-consumption rate. O_2-consumption rate increases with activity where $\dot{M}O_2 = 0.013 \times A + 0.11$ (R^2=0.45, Fig.

7C), and increases with surfacing frequency following $\dot{M}O_2 = 0.006567 \times f + 0.1736$ (R^2=0.59, Fig. 7D).

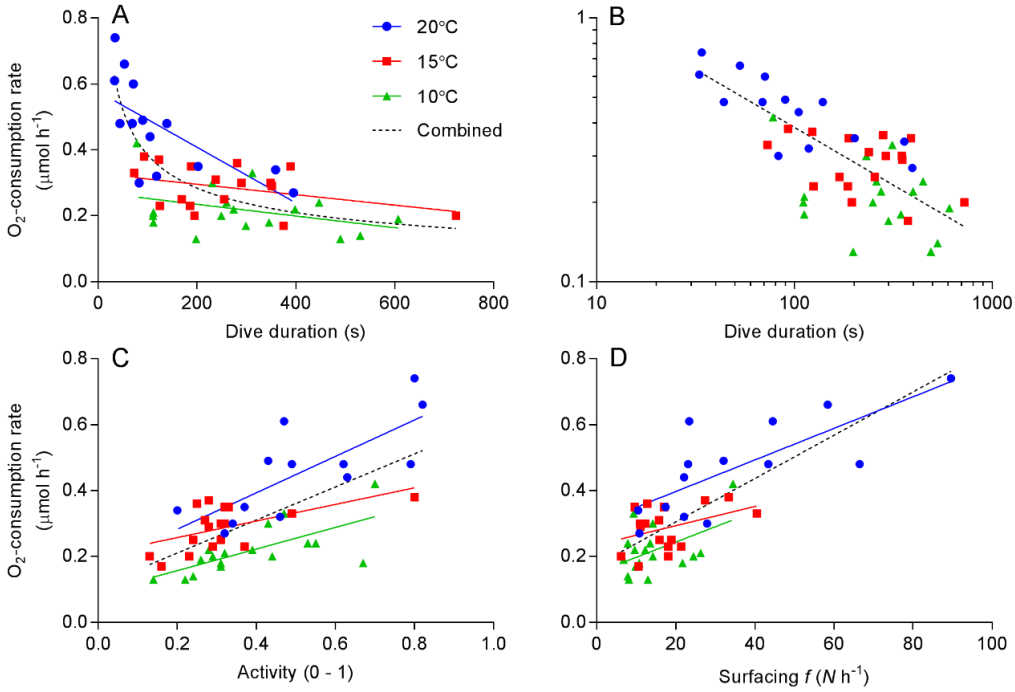

Figure 7. Correlations between dive duration, activity and surfacing duration with O_2-consumption rate. A, dive duration; B, dive duration on log axes; C, activity; D surfacing frequency. Each temperature treatment shown with linear regressions applied except B, where only the combined temperature treatment regression is shown. Regressions where temperature treatment data are combined are shown with dashed line, A and B show a power regression, C and D linear regressions.

Buoyancy and density

The mean initial respiratory gas volume held by the beetles during dives was 3.95±0.40 µL, which declined at a mean rate of 0.12±0.03 µL min^{-1} to the final gas volume of 3.26±0.29 µL. Mean dive duration was 367±120 s. Water temperature in these experiments ranged from 19-22°C but varied by 2°C within each experiment with middle temperature being used to calculate water density where mean values were 20.2±0.3°C. Six beetles were used with six dives per beetle, except one where only four suitable dives occurred. Beetle mass was 26.07±1.50 mg and mean gas-free density 1.0871±0.0068 g cm^{-3}.

Gas gill volume and surface area

The external bubble seen at the tip of the abdomen is the gas gill. The volume of the gas gill is variable, being taken in or pushed out of the air store, and its volume appears to be independent of the volume of gas within the air store. Gas gill sizes were measured in 17 dives of six beetles during buoyancy experiments (1 – 5 dives per beetle, Fig. 8). Mean gas gill volume was 0.73±0.16 µL and surface area was 3.77±0.54 mm^2. Gas gill size changed throughout a dive from zero to ~2 µL. When the gas gill was not present these zero values were not included in reported means.

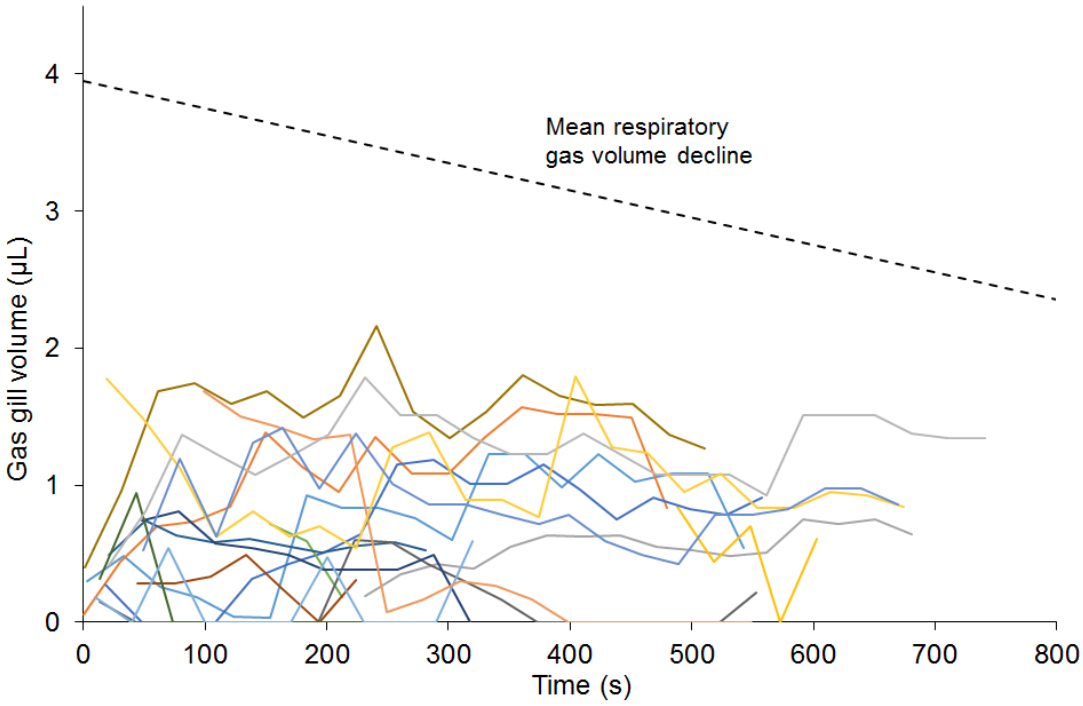

Figure 8. Change in gas gill volume, the external bubble at the tip of the abdomen, during dives in free-diving *P. decempunctatus* (solid lines). Dashed line shows mean rate of decline in respiratory gas volume which includes gas within the air store, tracheal system, and gas gill, if present, determined from the buoyancy measurements. The different colours indicate the 17 individual dives measured from the six beetles used to measure change gas gill volume.

5. Discussion

The effect of temperature and experimental setup up on metabolic rate and dive characteristics.

Temperature increases metabolic demand in ectotherms, which we show here for *P. decempunctatus* (Table 1). The increased O_2 demand causes O_2 in the air store to be exhausted more quickly, resulting in the shorter dive duration and increased surfacing frequency (Fig. 6, Table S1 and S2). Levels of activity did not change consistently with temperature, indicating temperature was the main driver for increased O_2 demand. Surfacing durations showed few significant differences between temperatures, however, the factors regulating surfacing duration are expected to be predation and parasitism risk (e.g. mites) at the surface, and rate of gas exchange with the atmosphere (Aiken, 1985; Calosi et al., 2007; Calosi et al., 2012). These responses of dive characteristics to increased temperature are generally consistent with those reported previously for dytiscids, although there is some variation between taxa (Calosi et al., 2007; Calosi et al., 2012).

Some dive characteristics have been suggested as being useful indicators of metabolism in aquatic insects (Calosi et al., 2007), and this was shown by correlations between dive duration, surfacing frequency, activity, and O_2-consumption rate (Fig. 7). Dive duration is likely to be the most useful metric because the data are more regularly distributed and have a non-linear relationship more consistent with the relationships between measured O_2-consumption rates (Fig. 7). Surfacing frequency has the strongest relationship, however, it is weakly supported by a few points at high values and there is more overlap between temperatures compared to dive duration. There is considerable overlap between temperatures for activity, because resting metabolic rate increases at higher temperature, but beetles may move around the same amount, resulting in the same activity level corresponding to different O_2-consumption rates.

There were significant differences in dive behaviour between the respirometry chambers and the control dive chambers. Dive duration tended to be shorter in the respirometry chambers, with longer mean surfacing duration, and more activity at lower temperatures than the controls, although at high temperatures dive behaviour tended to converge (Fig. 6). O_2-consumption rate estimated from dive duration in the control dive chambers indicated overall metabolic rate was lower than in the respirometry chambers (Fig. S2). In respirometry chambers beetles were in a confined space with nothing to hide underneath, unlike the controls, although light was reduced in the CT cabinet. Beetles in the respirometry chambers were not given additional time to settle before measurements began due to the fast rate of P_{O_2} decline in the chamber. This contrasts

with the 1 h of settling time in control experiments. Given the differences between the experimental setups and the beetle's natural habitat, the beetles' behaviour is likely to be different to what would occur under natural conditions. However, behaviour observed in the control dive chambers is probably closer to what would be expected under natural conditions. The variability observed in the dive characteristics is likely related to variation between individual beetles and cohorts of beetles, which make it difficult to detect relationships between variables. This is highlighted by comparing the paired and unpaired respirometry data, where more consistent relationships were found in the paired data (Table S1 and S2). The large amount of variability between control dive experiments is likely associated with the three separate cohorts of beetles used, which were collected at either different times during the year or location. To help reduce variation in future studies of physiological and dive traits in dytiscids, dytiscid should be collected from the same location at the same time, and paired data used for comparisons.

Gas exchange and the dive

Although *P. decempunctatus* exchanges some gas with the water, the majority of the gas exchanged is with the atmosphere when replenishing the air store. The beetles can continuously take-up O_2 from the atmosphere while remaining on the surface, or the air store can be renewed in a second before diving (Fig. 4). When beetles dive, the volume of gas taken underwater includes that within the air store, tracheal system and gas gill (if present). This comprises the insect's total respiratory gas volume. The volume of respiratory gas is sufficient to keep the beetles positively buoyant throughout the duration of a dive. Using a phylogenetically-adjusted regression for tracheal volume in tenebrionid beetles (Kaiser et al., 2007), the estimated tracheal volume of *P. decempunctatus* (24.5 mg) is 0.32 µL, 8% of the total respiratory gas volume at the beginning of a dive (3.95 µL). At dive termination, the average respiratory gas volume is 3.26 µL, therefore, 2.94 µL in the air store. A previous study, based on internal anatomy and sectioning of the dytiscid *Hydroporus palustris,* suggested that 1/3rd of the gas in the air store remains after exhaling the respiratory gas at the surface (Gilbert, 1986). If this is the case in *P. decempunctatus*, then 1.3 µL of respiratory gas remains when exchanged at the surface and 2.65 µL of fresh air is brought in. Using the relationship, $P_{O_2}=\dot{M}_{O_2}/(\beta \times V)$ at 20°C, and assuming that the atmospheric air P_{O_2} is 21 kPa and the dive is terminated with a respiratory gas P_{O_2} of 3 kPa (the approximate P_{O_2} at which metabolism becomes limited in some aquatic insects; Matthews and Seymour, 2010; Seymour et al., 2015), it is possible to calculate that the respiratory gas P_{O_2} at the beginning of the dive is 15.1 kPa, having exchanged 22.8 nmol of O_2 with the atmosphere. This amount of O_2 is comparable to experiments (Table 2), but assumes

momentary exchange at the surface. However, if the beetles remained at the surface longer the P_{O_2} within respiratory gas would rise further, extending the following dive, or the beetles terminate their dive at a higher P_{O_2} (~6 kPa) and begin their next dive with a P_{O_2} closer to 21 kPa. The higher P_{O_2} at dive termination is supported by calculating the P_{O_2} within the respiratory gas at the end of the dive. This is done by calculating the moles of O_2 in the respiratory gas at the beginning of the dive (20°C, 3.95 µL, 21 kPa P_{O_2}) with $M_{O_2} = \beta \times V \times P_{O_2}$, then subtracting the mean amount of O_2 exchanged at the surface (23.1 nmol, Table 2) and calculating the P_{O_2} in the respiratory gas (3.26 µL) at dive termination with the amount of O_2 remaining, using $P_{O_2}=M_{O_2}/(\beta \times V)$, which indicates a P_{O_2} of 8.2 kPa at the end of the dive.

Dive duration and O_2-consumption rates can be estimated from the rate of air store P_{O_2} decline. Assuming a respiratory gas P_{O_2} of 21 kPa at the beginning of the dive and dive termination at 3 kPa, the dive duration for inactive beetles would be 584 s ((21-3 kPa)/1.85 kPa min^{-1}×60 s), and active beetles 158 s ((20-3 kPa)/6.85 kPa min^{-1}×60 s), and reducing the P_{O_2} difference to 21-6 kPa, 486 s and 131 s, respectively. O_2-consumption rates (20°C) are 0.19 µmol h^{-1} for inactive beetles and 0.71 µmol h^{-1} for active ones, as calculated using Eq. 1, assuming the initial respiratory gas volume of 3.95 µL, plus 0.28 µL of gas within the air store tube (0.28 mm dia. × 5 mm long minus the optode volume 0.14 mm dia. × 2 mm long). Both these calculations are comparable to the experimental results (Fig. 6, Table 1 and 2).

P. decempunctatus sometimes uses a small compressible gas gill of adjustable size to exchange gases with the water (Fig. 8). The gill is held by hydrophobic hairs on the tergites at end of the abdomen (Kehl, 2014), and its ultimate size is likely limited by the volume of gas within the air store, the size of the hydrophobic portion of the tergites, and how far the end of the abdomen extends beyond the elytra. A range of variables influence the maximum size of bubbles that form from orifices, including orifice diameter, gas pressures, gas flow rates, and hydrostatic pressure, as well as the properties of the surface surrounding the orifice (Simmons et al., 2015; Tsuge and Hibino, 1978). Due to the complexities of where the gill forms in these beetles, in terms of tergite shape, location and surface properties, and the many other factors that influence bubble formation, estimating the maximum size of the gas gill is challenging. Nevertheless, due to the small surface area dedicated to the gas gill, and the gill having a low surface area to volume ratio due to its spherical shape, the compressible gas gill of *P. decempunctatus* is not as effective for gas exchange as those carried by other aquatic insects. Fig. 9 shows the surface area of the gas gill relative to mass in several species of aquatic insects. *P. decempunctatus* has a considerably smaller gas gill area than the similar sized water boatman *Agraptocorixa eurynome* that uses the

gas gill to greater benefit. The proportion of O_2 gained from the water during a dive was calculated in *P. decempunctatus* by comparing the whole-animal O_2-consumption rate determined from both the air and water with the O_2-consumption rate determined from O_2 exchanges with the gas space in the respirometry chamber (Table 2). This indicates between 18 – 29% of the total O_2 consumed comes from the water, less than the ~92% estimated for the dytiscid *H. palustris* (Gilbert, 1986) and the water boatman (theoretical maximum 88%) (Matthews and Seymour, 2010), but similar to the backswimmer *Anisops deanei* at ~20% which dedicates a similar gas gill area relative to mass as *P. decempunctatus* ((Jones et al., 2015) Fig. 9). *H. palustris* is smaller (3.5 mm) than *P. decempunctatus* (7.4 mm) and is likely to have a larger gas gill surface area to size ratio, and, therefore, derives greater benefit from the gas gill (Gittelman, 1975). This higher relative gas gill area in smaller dytiscids is supported by estimates of gas gill areas in several dytiscid species (Fig. 9). However, values of O_2 gain from the water may include a contribution of O_2 *via* cutaneous exchange, particularly in smaller insects (Jones et al., 2018a; Vlasblom, 1970).

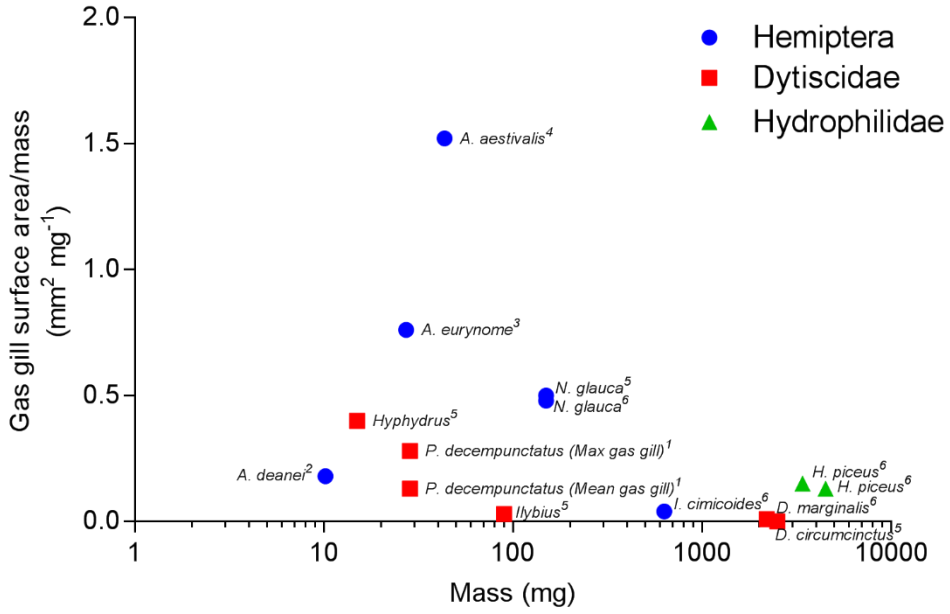

Figure 9. Estimated gas gill surface area relative to body mass in aquatic bugs (Hemiptera, blue circles) and beetles (Coleoptera; Dytiscidae, red squares; Hydrophilidae, green triangles). [1] *P. decempunctatus* from this study with a mean sized gas gill and the maximum size recorded during experiments, [2] backswimmer *A. deanei* (Jones et al., 2015), [3] water boatmen *A. eurynome* (Matthews and Seymour, 2010), [4] *Aphelocheirus aestivalis*, a plastron breather that can remain underwater indefinitely (Seymour et al., 2015), [5] *Hyphydrus*, *Ilbius*, *Dytiscus circumcinctus* and *Notonecta glauca* (Ege, 1915), [6] *Hydrophilus piceus*, *Ilyocoris cimicoides*, *N. glauca*, *Dytiscus marginalis* (De Ruiter et al., 1951).

A model of respiration in P. decempunctatus

A model based on Fick's general diffusion equation was developed to understand the importance of the gas gill, and potentially cutaneous respiration to the dive duration of *P. decempunctatus* at 20°C (Jones et al., 2018a; Rahn and Paganelli, 1968). A recent study has shown that small subterranean dytiscids use cutaneous respiration through the unelaborated body surface (Jones et al., 2018a), and therefore this mode of respiration may contribute to extending the dive duration of *P. decempunctatus* despite its larger size.

The model includes both O_2-consumption and CO_2 production by the beetle, calculating the rate of O_2 diffusion into the insect, and the rate of N_2 and CO_2 loss into the water, across both the gas gill and cuticle.. The total respiratory gas volume, defined as the gas within air store and tracheal system, and the P_{O_2}, P_{N_2} and P_{CO_2} within the respiratory gas, are calculated throughout the duration of the dive which ends when the P_{O_2} reaches 3 kPa in the respiratory tracheal gas.

In the model, O_2 is consumed (µmol s^{-1}) from the respiratory gas at the rate measured in the respirometry chambers at 20°C (Table 1 and 3) and CO_2 is produced (µmol s^{-1}) with a respiratory quotient of 0.8 given the beetles are predatory and are likely to consume large amounts of protein. The initial conditions (partial pressures, initial respiratory gas volume) of the respiratory gas are outlined in Table 3, from which the initial quantities (µmol) of each gas are determined (See Eq. 15)). O_2, N_2 and CO_2 are exchanged with the water ($\dot{M}_g$; µmol s^{-1}) according to Fick's general diffusion equation, Eq. 8 (Rahn and Paganelli, 1968; Seymour and Matthews, 2013).

$$\dot{M}_g = G_g \times \Delta P_g \quad (8)$$

where G_g (µmol s^{-1} kPa^{-1}) is the conductance of O_2, N_2 or CO_2 into or from the respiratory gas to the water, and ΔP_g is the gas partial pressure difference between the respiratory gas and water. Conductance is equal to $K_g \times A/X$ where K_g (µmol mm^{-1} s^{-1} kPa^{-1}) is the Krogh's coefficient of diffusion in water or the cuticle (the product of diffusivity and capacitance), A (mm^2) is the surface area for gas exchange and X (mm) is either the boundary layer thickness (a fluid layer that provides resistance to diffusion or the thickness of the cuticle through which diffusion takes place).

The model has three conductances: diffusion through the boundary layer of the gas gill (G_{Ggil}), diffusion through the boundary layer above the beetles' surface (G_{BL}) and diffusion through the cuticle of the beetle ($G_{Cut.}$) which are calculated as follows:

$$G_{Ggill} = K_{g,H_2O} \times A_{Ggill}/X_{BL} \quad (9)$$

$$G_{BL} = K_{g,H2O} \times A_{Beetle} / X_{BL} \quad (10)$$

$$G_{Cut.} = K_{g,Cut.} \times A_{Beetle} / X_{Cut.} \quad (11)$$

where $K_{g,H2O}$ and $K_{g,Cut.}$ are the Krogh's coefficients of O_2, N_2 or CO_2 in water and cuticle respectively, A_{Ggill} and A_{Beetle} are the surface areas of the gas gill and beetle respectively, X_{BL} is the boundary layer thickness, and $X_{Cut.}$ is the cuticle thickness (Table 3).

As conductance through the boundary layer above the beetle's surface and of the cuticle are in series, but parallel with conductance through the gas gill boundary layer, the total conductance for each gas is calculated as follows;

$$G_g = (1/G_{BL} + 1/G_{Cut.})^{-1} + G_{Ggill} \quad (12)$$

To determine the ΔP_{O2} *and* ΔP_{CO2} in Eq. 8, the P_{O2} and P_{CO2} (kPa) within the respiratory gas (P_{rg}) are calculated according to Eq. 13.

$$P_{rg} = M_g / (\beta_g \times V_{rg}) \quad (13)$$

where M_g (µmol) is the moles of O_2 or CO_2 in the respiratory gas, β_g (µmol gas µL^{-1} kPa^{-1}) is the capacitance of O_2 and CO_2 (and N_2) in air, and V_{rg} (µL) is the respiratory gas volume calculated with Eq. (14).

$$V_{rg} = M_{tot} / (\beta_g \times (P_b - P_{H2O})) \quad (14)$$

Where M_{tot} (µmol) is the total moles of gas (O_2, N_2 and CO_2) within the respiratory gas, P_b is barometric pressure and P_{H2O} is water vapour pressure. P_b is equal to total gas pressure assuming the beetle is just below the water's surface, and hydrostatic pressure and surface tension are negligible (Seymour and Matthews, 2013).

The moles of each gas (M_g) are calculated with Eq. 15 where P_g (kPa) are the relevant gas partial pressures (Table 3).

$$M_g = \beta \times V_{rg} \times P_{rg} \quad (15)$$

P_{N2} (kPa) in the respiratory gas is determined according to Dalton's law where the sum of partial pressures in the gas is equal to the total gas pressure (Eq. 16 (Seymour and Matthews, 2013)). The nitrogen fraction includes trace gases with the exception of CO_2.

$$P_{N2} = P_b - P_{H2O} - P_{O2} - P_{CO2}. \quad (16)$$

Table 3. Constants and variables used to calculate the dive duration of *P. decempunctatus* with different gas gill sizes and water convection conditions at 20°C.

Symbol	Value	units	Description	Source
β_g	0.0004101	µmol µl^{-1} kPa^{-1}	O_2, N_2 and CO_2 capacitance in air, values are the same as they are ideal gases	(Dejours, 1981)
$\dot{M}_{O_2}$	0.47	µmol h^{-1}	O_2-consumption rate at 20°C	This study
$\dot{M}_{CO_2}$	0.38	µmol h^{-1}	Estimated CO_2 production rate at 20°C assuming a respiratory quotient of 0.8^	This study
P_b	101.3	kPa	Barometric pressure	(Seymour and Matthews, 2013)
P_{H_2O}	2.34	kPa	Water vapour pressure	(Dejours, 1981)
Initial/Water P_{O_2}	20.73	kPa	P_{O_2} in the water, and initial respiratory gas P_{O_2}	(Dejours, 1981)
Initial/Water P_{N_2}	78.23	kPa	P_{N_2} in the water, and initial respiratory gas P_{N_2}	(Dejours, 1981)
Water P_{CO_2}	0.31	kPa	P_{CO_2} in the water	(Hasler et al., 2016)
Initial P_{CO_2}	0.04	kPa	Initial respiratory gas P_{CO_2}, atmospheric P_{CO_2}	(Hasler et al., 2016)
K_{O_2,H_2O}	3.11×10^{-8}	µmol mm^{-1} s^{-1} kPa^{-1}	Krogh's coefficient of diffusion for O_2 in water	(Rahn and Paganelli, 1968)
K_{N_2,H_2O}	1.42×10^{-8}	µmol mm^{-1} s^{-1} kPa^{-1}	Krogh's coefficient of diffusion for N_2 in water	(Rahn and Paganelli, 1968)
K_{CO_2,H_2O}	1.37×10^{-5}	µmol mm^{-1} s^{-1} kPa^{-1}	Krogh's coefficient of diffusion for CO_2 in water	(Rahn and Paganelli, 1968)
$K_{O_2,Cut.}$	9.5×10^{-10}	µmol mm^{-1} s^{-1} kPa^{-1}	Krogh's coefficient of diffusion for O_2 in chitin/cuticle	(Krogh, 1919)
$K_{N_2,Cut.}$	5.7×10^{-10}	µmol mm^{-1} s^{-1} kPa^{-1}	Krogh's coefficient of diffusion for N_2 in chitin/cuticle	(Krogh, 1919)
$K_{CO_2,Cut.}$	9.5×10^{-10}	µmol mm^{-1} s^{-1} kPa^{-1}	Estimated Krogh's coefficient of diffusion for CO_2 in chitin/cuticle#	This study
V_{rg} (Initial)	3.95	µl	Initial respiratory gas volume	This study
A_{Ggill}	3.77	mm^2	Mean gas gill surface area	This study
A_{Beetle}	62.59	mm^2	Beetle surface area*	This study
X_{BL}	0.1, 0.5	mm	Boundary layer thickness in circulated and stagnant water, respectively	(Jones et al., 2018a; Seymour et al., 2015)
$X_{Cut.}$	0.034	mm	Cuticle thickness†	(Jones et al., 2018a)

^ respiratory quotient assuming the beetles are consuming mostly protein (Schmidt-Nielsen, 1997), # estimated the Krogh's coefficient for CO_2 in the cuticle, calculated by dividing the molecular mass of CO_2 by that of O_2 and multiplying this value by the Krogh's coefficient for O_2 in cuticle. * beetle surface area determined from the mean length (7.4 mm), width (4.0 mm) and mass (28.54 mg) of eight *P. decempunctatus* assuming the beetles were a lozenge shape using the methodology described in (Jones et al., 2018a), † mean cuticle thickness of the elytra and ventral cuticle.

The model suggests that the dive duration of *P. decempunctatus* with an average sized gas gill (0.73 µl, 3.77 mm^2) in convected water (100 µm boundary layer) would be 279 s assuming the dive is terminated when the respiratory gas PO_2 is 3 kPa (Fig. 10.1). If the boundary layer thickness increases to 500 µm, equivalent to stagnant water (Seymour et al., 2015), the dive duration decreases to 246 s (Fig. 10.2). The cumulative O_2 diffusion from the water with a 100 µm boundary layer is 19% of the total O_2 consumed during the dive, however, with a 500 µm boundary layer this decreases to 9%, which corresponds well to the 12% decline in dive duration in stagnant conditions. Without the gas gill in convected water (gas gill surface area = 0), cutaneous respiration is still able to contribute 10% of the O_2 consumed during the dive from the water, and 8% in stagnant water, indicating the contribution of O_2 from the gas gill is 9% in circulated water and 1% in stagnant water. With the largest gas gill recorded (2.17 µl, 8.09 mm^2, Fig. 8), in circulated water, the dive duration is 324 s with a total of 30% of the O_2 consumed being contributed from the water. These dive durations and percentages of O_2 gain from the water are comparable to those recorded in experiments (Fig. 6, Table 2). If the beetles terminate their dives at 6 kPa PO_2, dive durations and proportion of O_2 uptake from the water decrease to 228 s and 16% in circulated water with an average sized gas gill, 202 s and 8% without a gas gill, and 203 s and 8% with an average gas gill in stagnant water and 197 s and 6% without a gas gill.

PCO_2 values predicted by the model range from 4.5 to 15.3 kPa in the respiratory gas at dive termination (Fig. 10). These values are higher than those measured in the air store gas of three species of dytiscid, the highest being ~3.7 kPa (Ege, 1915). Under natural circumstances these values would likely be lower than calculated by the model due to the buffering capacity of the haemolymph (Harrison et al., 1990; Lee et al., 2018), and vary depending on the value of the Krogh's coefficient for CO_2 in cuticle. CO_2 may build up in the respiratory gas if the gas gill is small, or absent, and the beetles are in stagnant water (Fig. 10). However, aquatic insects show little response to hypercapnia (Ubhi and Matthews, 2018), and therefore dytiscids may not actively manage high PCO_2 if they are exposed to it. Damselfly larvae *Calopteryx splendens* do increase movement when exposed to 5-10% aquatic CO_2 (Miller, 1994), which, although increasing CO_2 production, would also aid CO_2 diffusion into the water. Further measurements of air store CO_2, the Krogh's coefficient of CO_2 in cuticle and the responses of dytiscids to hypercapnia are needed to fully understand CO_2 exchange in dytiscids.

Despite including CO_2 within the model in this study, these data should be considered with caution. CO_2 exchange through the cuticle cannot currently be modelled accurately because there are no robust values for the Krogh's coefficient of CO_2 in cuticle/chitin. Values used in

previous studies are likely too high because the Krogh's coefficient of CO_2 is assumed to be ~35 times greater than the Krogh's coefficient of O_2 in the same tissue (Schmitz, 2015; Schmitz and Perry, 2001; Schmitz and Perry, 2002). Here, we estimate the Krogh's coefficient for CO_2 in the cuticle by dividing the molecular mass of CO_2 by that of O_2 and multiplying this value by the Krogh's coefficient for O_2 in cuticle. The inclusion of CO_2 exchange in the model has little effect on when the dive is terminated because the CO_2 exchange does not influence the rate of O_2 decline. However, CO_2 build-up in the respiratory gas reduces the rate of respiratory gas volume decline (Fig. 10). The 95% CI for the final respiratory gas volume in experiments is 2.97 – 3.55 µL. Only in circulated water with an average sized gas gill, do the model results fall within this range (Fig. 10.1), further indicating that there is less build-up of CO_2 and that the conductance of CO_2 into the water is higher than the conditions shown in Fig. 10.2, 10.3 and 10.4.

These model results show that the gas gill used by *P. decempunctatus* can significantly increase the beetle's dive duration, although not to the extent of some other aquatic insects. The results also suggest cutaneous respiration contributes significantly to extending dive duration despite the cuticle's thickness. This indicates that cutaneous respiration is likely to benefit other dytiscid species, as well as other aquatic insects that have previously been thought of as using only one of the more obvious forms of respiration, like a gas gill.

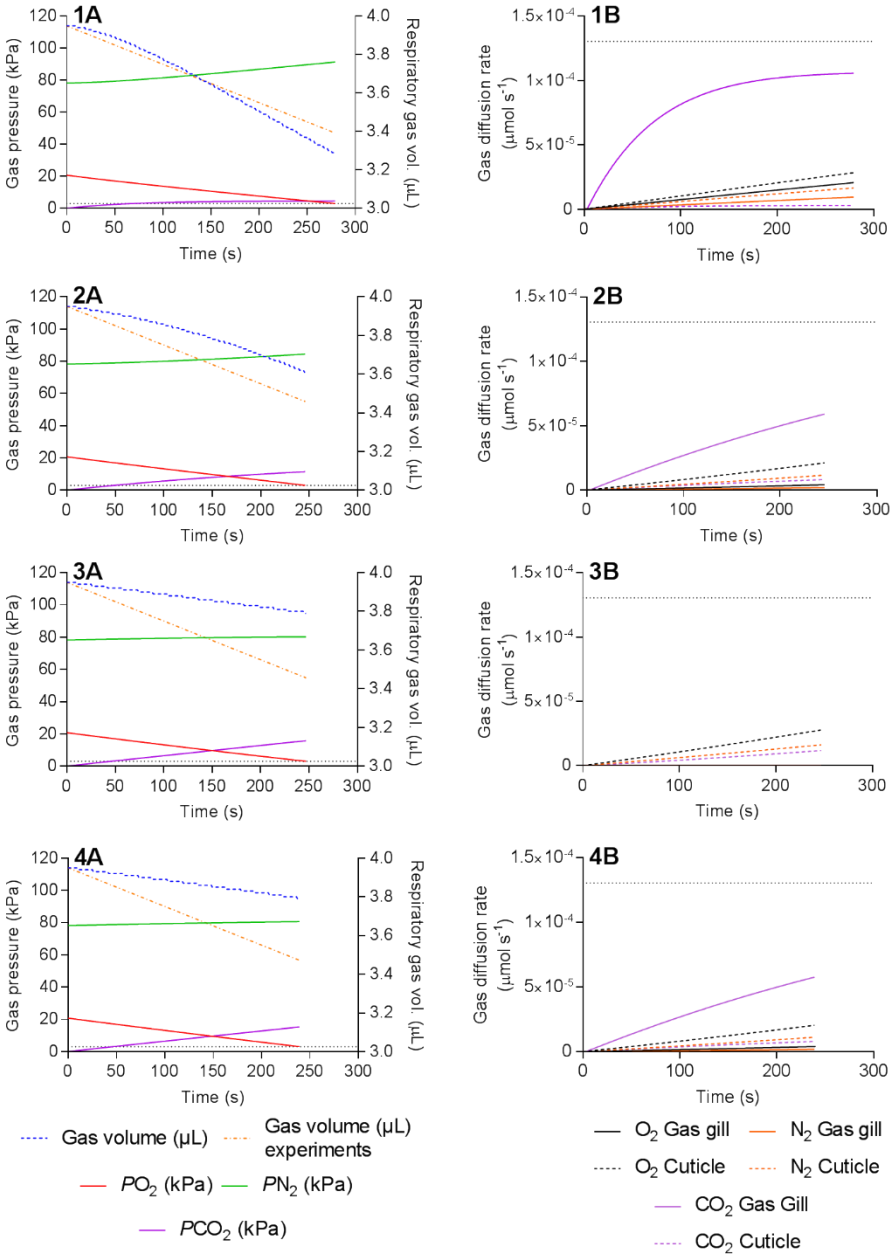

Figure 10. Modelling of gas exchange with the water in *P. decempunctatus* during a dive. A, change in PO_2, PN_2 PCO_2 and respiratory gas volume. Horizontal dotted line shows the 3 kPa PO_2 at which the dive is terminated and approximately the PO_2 where metabolism becomes limited in other aquatic insects. "Gas volume experiments" shows the average rate of respiratory gas volume decline from experimental data. B, rate of O_2, N_2 or CO_2 diffusion through the gas gill boundary layer, and the cuticle and associated boundary layer. Dotted horizontal line shows the beetle's O_2-consumption rate. (1), average sized gas gill (0.73 µL, 3.77 mm^2) in convected water (100 µm boundary layer); (2), average sized gas gill in stagnant water (500 µm boundary layer); (3), no gas gill in convected water; (4), no gas gill in stagnant water.

6. Acknowledgements

We thank Edward Snelling for providing some initial guidance on experimental design. Sally Maxwell and Silvia Clarke from DEWNR, and Thomas Nelson and Qiaohui Hu from Adelaide University for assisting with collecting beetles and/or maintaining them. KKJ was supported by the University of Adelaide for award of an Australian Government Research Training Program Scholarship.

7. Supplementary material

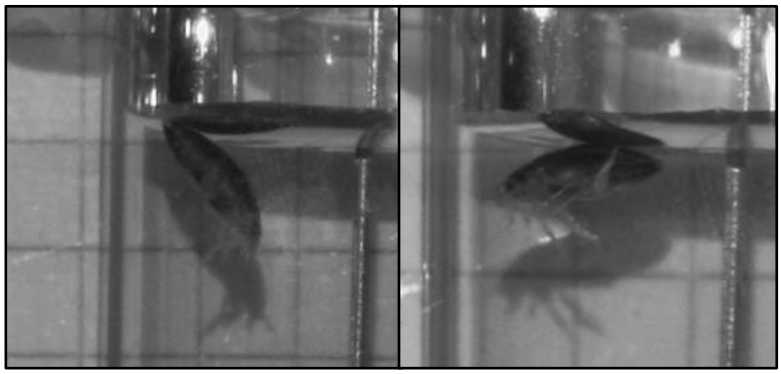

Figure S1. When exchanging gases with the atmosphere, *P. decempunctatus* floats with the tip of the abdomen at the water's surface and the body at ~45° from the surface (left). This allows a gas connection between the air and air store. If simply floating at the surface the beetle's body remains more horizontal and the tip of the abdomen does not touch the surface (right). Images from buoyancy experiments.

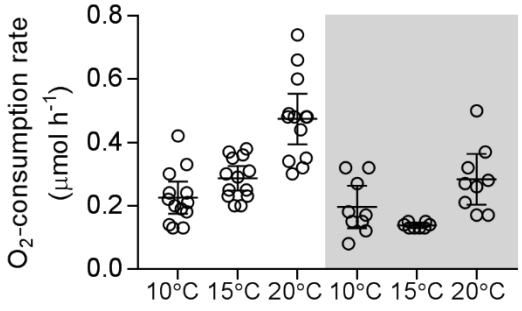

Figure S2. O_2-consumption rate in the respirometry chambers (left) compared to O_2-consumption rate estimated from dive duration in the controls (right, shaded) using the correlation between dive duration and O_2-consumption rate in Fig. 7. 20°C in the respirometry chamber is significantly higher than calculated O_2-consumption rate at all temperatures in the control chambers (ANOVA, P<0.0001, Tukey's post-hoc, P<0.001). Within the control chambers the 15°C treatment is significantly lower than the 20°C treatment (Tukey's post-hoc, P<0.05).

Table S1. Dive characteristics recorded during respirometry and control dive experiments at different temperatures. Values are means±95%CI with *N* in parentheses. †Outlier removed mean dive duration 4,643 s, max. dive duration 24,274 s.

	Respirometry			Respirometry (Paired)			Control		
	10°C	15°C	20°C	10°C	15°C	20°C	10°C	15°C	20°C
Dive duration (Mean, s)	297±74 (17)	259±74 (17)	128±60 (14)	314±101 (12)	265±92 (12)	114±51 (12)	705±388 (8) †	1315±185 (8)	308±162 (9)
Dive duration (Max, s)	651±159 (17)	541±120 (17)	308±106 (14)	669±217 (12)	539±106 (12)	289±93 (12)	1856±892 (8) †	2264±247 (8)	815±332 (9)
Surfacing Duration (Mean, s)	32±9 (17)	19±6 (17)	25±10 (14)	31±11 (12)	22 ±8 (12)	25±10 (12)	9±4 (9)	2±1 (8)	5±3 (9)
Surfacing Duration (Median, s)	22±9 (17)	8±5 (17)	11±8 (14)	25±12 (12)	9±7 (12)	12±9 (12)	5±3 (9)	1±0 (8)	4±2 (9)
Surfacing Frequency (N h^{-1})	14.4±3.7 (17)	17.7±4.2 (17)	36.9±12.0 (14)	14±5 (12)	16±3 (12)	38±13 (12)	8.3±5.2 (9)	2.8±0.4 (8)	21.0±14.2 (9)
Activity (0-1)	0.39±0.08 (17)	0.32±0.07 (17)	0.54±0.11 (13)	0.36±0.09 (11)	0.28±0.04 (11)	0.54±0.12 (11)	0.29±0.18 (9)	0.03±0.01 (8)	0.30±0.22 (9)

Table S2. ANOVA and Tukey's post-hoc tests results for dive duration, surfacing duration, surfacing frequency and activity of beetles in the respirometry chambers (R) and control dive chambers (C), and paired data from the respirometry chambers. * $P \leq 0.05$, ** $P \leq 0.01$, *** $P \leq 0.001$, **** $P \leq 0.0001$.

Mean dive duration (ANOVA, $P<0.0001$)

Tukey's multiple comparisons test	Mean Diff.	95.00% CI of diff.	Significant?	Summary	Adjusted P Value
10°C R vs. 15°C R	38.24	-478.2 to 554.7	No	ns	>0.9999
10°C R vs. 20°C R	169.1	-374.3 to 712.5	No	ns	0.9420
10°C R vs. 10°C C	-845.2	-1466 to -224.4	Yes	**	0.0022
10°C R vs. 15°C C	-1017	-1663 to -371.6	Yes	***	0.0002
10°C R vs. 20°C C	-10.71	-631.4 to 610	No	ns	>0.9999
15°C R vs. 20°C R	130.8	-412.6 to 674.3	No	ns	0.9806
15°C R vs. 10°C C	-883.4	-1504 to -262.7	Yes	**	0.0012
15°C R vs. 15°C C	-1055	-1701 to -409.9	Yes	***	0.0001
15°C R vs. 20°C C	-48.94	-669.6 to 571.8	No	ns	>0.9999
20°C R vs. 10°C C	-1014	-1658 to -370.9	Yes	***	0.0002
20°C R vs. 15°C C	-1186	-1854 to -518.9	Yes	****	<0.0001
20°C R vs. 20°C C	-179.8	-823.1 to 463.5	No	ns	0.9629
10°C C vs. 15°C C	-172.1	-903.7 to 559.6	No	ns	0.9825
10°C C vs. 20°C C	834.4	124.6 to 1544	Yes	*	0.0120
15°C C vs. 20°C C	1007	274.9 to 1738	Yes	**	0.0019

Max. dive duration (ANOVA, $P<0.0001$)

Tukey's multiple comparisons test	Mean Diff.	95.00% CI of diff.	Significant?	Summary	Adjusted P Value
10°C R vs. 15°C R	109.5	-411 to 629.9	No	ns	0.9894
10°C R vs. 20°C R	343.3	-204.4 to 890.9	No	ns	0.4485
10°C R vs. 10°C C	-1206	-1856 to -555	Yes	****	<0.0001
10°C R vs. 15°C C	-1613	-2264 to -962.6	Yes	****	<0.0001
10°C R vs. 20°C C	-164.2	-789.7 to 461.4	No	ns	0.9716
15°C R vs. 20°C R	233.8	-313.9 to 781.4	No	ns	0.8092
15°C R vs. 10°C C	-1315	-1966 to -664.4	Yes	****	<0.0001
15°C R vs. 15°C C	-1723	-2373 to -1072	Yes	****	<0.0001

15°C R vs. 20°C C	-273.6	-899.2 to 351.9	No	ns	0.7929
20°C R vs. 10°C C	-1549	-2221 to -876.3	Yes	****	<0.0001
20°C R vs. 15°C C	-1956	-2629 to -1284	Yes	****	<0.0001
20°C R vs. 20°C C	-507.4	-1156 to 140.9	No	ns	0.2101
10°C C vs. 15°C C	-407.6	-1166 to 351.1	No	ns	0.6168
10°C C vs. 20°C C	1041	304 to 1779	Yes	**	0.0013
15°C C vs. 20°C C	1449	711.7 to 2186	Yes	****	<0.0001

Surfacing frequency (ANOVA, *P*<0.0001)

Tukey's multiple comparisons test	Mean Diff.	95.00% CI of diff.	Significant?	Summary	Adjusted P Value
10°C R vs. 15°C R	-3.274	-17.39 to 10.84	No	ns	0.9836
10°C R vs. 20°C R	-22.55	-37.41 to -7.696	Yes	***	0.0005
10°C R vs. 10°C C	6.129	-10.84 to 23.1	No	ns	0.8955
10°C R vs. 15°C C	11.62	-6.024 to 29.27	No	ns	0.3924
10°C R vs. 20°C C	-6.626	-23.59 to 10.34	No	ns	0.8606
15°C R vs. 20°C R	-19.28	-34.13 to -4.422	Yes	**	0.0040
15°C R vs. 10°C C	9.403	-7.564 to 26.37	No	ns	0.5851
15°C R vs. 15°C C	14.9	-2.751 to 32.54	No	ns	0.1460
15°C R vs. 20°C C	-3.352	-20.32 to 13.61	No	ns	0.9921
20°C R vs. 10°C C	28.68	11.09 to 46.27	Yes	***	0.0001
20°C R vs. 15°C C	34.17	15.93 to 52.42	Yes	****	<0.0001
20°C R vs. 20°C C	15.92	-1.661 to 33.51	No	ns	0.0980
10°C C vs. 15°C C	5.493	-14.51 to 25.49	No	ns	0.9656
10°C C vs. 20°C C	-12.76	-32.16 to 6.647	No	ns	0.3945
15°C C vs. 20°C C	-18.25	-38.25 to 1.751	No	ns	0.0936

Surfacing duration (Mean) (ANOVA, *P*<0.0001)

Tukey's multiple comparisons test	Mean Diff.	95.00% CI of diff.	Significant?	Summary	Adjusted P Value
10°C R vs. 15°C R	12.92	-1.001 to 26.84	No	ns	0.0841
10°C R vs. 20°C R	7.094	-7.555 to 21.74	No	ns	0.7148
10°C R vs. 10°C C	23.55	6.819 to 40.28	Yes	**	0.0014
10°C R vs. 15°C C	30.42	13.02 to 47.82	Yes	****	<0.0001
10°C R vs. 20°C C	26.69	9.959 to 43.43	Yes	***	0.0002

15°C R vs. 20°C R	-5.827	-20.48 to 8.823	No	ns	0.8511
15°C R vs. 10°C C	10.63	-6.103 to 27.36	No	ns	0.4335
15°C R vs. 15°C C	17.5	0.09541 to 34.9	Yes	*	0.0480
15°C R vs. 20°C C	13.77	-2.962 to 30.5	No	ns	0.1662
20°C R vs. 10°C C	16.46	-0.8853 to 33.8	No	ns	0.0726
20°C R vs. 15°C C	23.33	5.335 to 41.32	Yes	**	0.0040
20°C R vs. 20°C C	19.6	2.255 to 36.94	Yes	*	0.0177
10°C C vs. 15°C C	6.868	-12.86 to 26.59	No	ns	0.9093
10°C C vs. 20°C C	3.141	-15.99 to 22.28	No	ns	0.9967
15°C C vs. 20°C C	-3.728	-23.45 to 16	No	ns	0.9935

Surfacing frequency (Median) (ANOVA, *P*<0.001)

Tukey's multiple comparisons test	Mean Diff.	95.00% CI of diff.	Significant?	Summary	Adjusted P Value
10°C R vs. 15°C R	14	1.688 to 26.31	Yes	*	0.0167
10°C R vs. 20°C R	11.18	-1.776 to 24.13	No	ns	0.1298
10°C R vs. 10°C C	17.06	2.258 to 31.85	Yes	*	0.0147
10°C R vs. 15°C C	21	5.61 to 36.39	Yes	**	0.0021
10°C R vs. 20°C C	17.78	2.98 to 32.58	Yes	**	0.0096
15°C R vs. 20°C R	-2.821	-15.78 to 10.13	No	ns	0.9876
15°C R vs. 10°C C	3.056	-11.74 to 17.85	No	ns	0.9903
15°C R vs. 15°C C	7	-8.39 to 22.39	No	ns	0.7653
15°C R vs. 20°C C	3.778	-11.02 to 18.58	No	ns	0.9749
20°C R vs. 10°C C	5.877	-9.459 to 21.21	No	ns	0.8698
20°C R vs. 15°C C	9.821	-6.088 to 25.73	No	ns	0.4661
20°C R vs. 20°C C	6.599	-8.737 to 21.94	No	ns	0.8044
10°C C vs. 15°C C	3.944	-13.5 to 21.39	No	ns	0.9853
10°C C vs. 20°C C	0.7222	-16.2 to 17.64	No	ns	>0.9999
15°C C vs. 20°C C	-3.222	-20.66 to 14.22	No	ns	0.9942

Activity (ANOVA, *P*<0.0001)

Tukey's multiple comparisons test	Mean Diff.	95.00% CI of diff.	Significant?	Summary	Adjusted P Value
10°C R vs. 15°C R	0.06882	-0.1339 to 0.2715	No	ns	0.9176
10°C R vs. 20°C R	-0.1332	-0.3509 to 0.08458	No	ns	0.4764

10°C R vs. 10°C C	0.09752	-0.1461 to 0.3411	No	ns	0.8474
10°C R vs. 15°C C	0.3553	0.1019 to 0.6087	Yes	**	0.0015
10°C R vs. 20°C C	0.08307	-0.1606 to 0.3267	No	ns	0.9162
15°C R vs. 20°C R	-0.202	-0.4197 to 0.01576	No	ns	0.0843
15°C R vs. 10°C C	0.02869	-0.2149 to 0.2723	No	ns	0.9993
15°C R vs. 15°C C	0.2865	0.03308 to 0.5399	Yes	*	0.0177
15°C R vs. 20°C C	0.01425	-0.2294 to 0.2579	No	ns	>0.9999
20°C R vs. 10°C C	0.2307	-0.02559 to 0.487	No	ns	0.1016
20°C R vs. 15°C C	0.4885	0.2229 to 0.754	Yes	****	<0.0001
20°C R vs. 20°C C	0.2162	-0.04004 to 0.4725	No	ns	0.1462
10°C C vs. 15°C C	0.2578	-0.0294 to 0.545	No	ns	0.1034
10°C C vs. 20°C C	-0.01444	-0.293 to 0.2642	No	ns	>0.9999
15°C C vs. 20°C C	-0.2722	-0.5594 to 0.01495	No	ns	0.0731

Respirometry chambers (paired, mean) dive duration (ANOVA, *P*<0.01)

Tukey's multiple comparisons test	Mean Diff.	95.00% CI of diff.	Significant?	Summary	Adjusted P Value
10°C R vs. 15°C R	48.33	-96.9 to 193.6	No	ns	0.6521
10°C R vs. 20°C R	199.8	26.47 to 373	Yes	*	0.0246
15°C R vs. 20°C R	151.4	25.12 to 277.7	Yes	*	0.0199

Respirometry chambers (paired, max) dive duration (ANOVA, *P*<0.05)

Tukey's multiple comparisons test	Mean Diff.	95.00% CI of diff.	Significant?	Summary	Adjusted P Value
10°C R vs. 15°C R	130.8	-159.8 to 421.3	No	ns	0.4689
10°C R vs. 20°C R	380	20.79 to 739.2	Yes	*	0.0383
15°C R vs. 20°C R	249.3	74.14 to 424.4	Yes	**	0.0071

Respirometry chambers (paired) surfacing frequency (ANOVA, *P*<0.01)

Tukey's multiple comparisons test	Mean Diff.	95.00% CI of diff.	Significant?	Summary	Adjusted P Value
10°C R vs. 15°C R	-1.683	-9.413 to 6.047	No	ns	0.8293
10°C R vs. 20°C R	-24.02	-44.73 to -3.3	Yes	*	0.0239
15°C R vs. 20°C R	-22.33	-39.69 to -4.973	Yes	*	0.0132

Respirometry chambers (paired, mean) surfacing duration (ANOVA, *P*<0.01)

Tukey's multiple comparisons test	Mean Diff.	95.00% CI of diff.	Significant?	Summary	Adjusted P Value
10°C R vs. 15°C R	9.433	-6.582 to 25.45	No	ns	0.2900
10°C R vs. 20°C R	6.761	-14.11 to 27.63	No	ns	0.6663
15°C R vs. 20°C R	-2.672	-18.75 to 13.4	No	ns	0.8959

Respirometry chambers (paired, median) surfacing duration (ANOVA, $P>0.05$, ns)

Tukey's multiple comparisons test	Mean Diff.	95.00% CI of diff.	Significant?	Summary	Adjusted P Value
10°C R vs. 15°C R	16.29	0.6633 to 31.92	Yes	*	0.0411
10°C R vs. 20°C R	13.08	-9.12 to 35.29	No	ns	0.2897
15°C R vs. 20°C R	-3.208	-18.91 to 12.49	No	ns	0.8476

Respirometry chambers (paired) activity (ANOVA, $P<0.01$)

Tukey's multiple comparisons test	Mean Diff.	95.00% CI of diff.	Significant?	Summary	Adjusted P Value
10°C R vs. 15°C R	0.08273	-0.02774 to 0.1932	No	ns	0.1500
10°C R vs. 20°C R	-0.1809	-0.3848 to 0.02294	No	ns	0.0825
15°C R vs. 20°C R	-0.2636	-0.4506 to -0.07668	Yes	**	0.0080

Chapter Five: Allometric analysis of respiration in diving beetles (Coleoptera; Dytiscidae)

Statement of Authorship

Title of Paper	Allometric analysis of respiration in diving beetles (Coleoptera; Dytiscidae)
Publication Status	☐ Published ☐ Accepted for Publication ☐ Submitted for Publication ☑ Unpublished and Unsubmitted work written in manuscript style
Publication Details	

Principal Author

Name of Principal Author (Candidate)	Karl K. Jones		
Contribution to the Paper	Undertook field work to collect study species, experiments, data and statistical analysis and wrote the initial draft of the manuscript, and edited and reviewed subsequent manuscript drafts.		
Overall percentage (%)	90%		
Certification:	This paper reports on original research I conducted during the period of my Higher Degree by Research candidature and is not subject to any obligations or contractual agreements with a third party that would constrain its inclusion in this thesis. I am the primary author of this paper.		
Signature		Date	21/1/19

Co-Author Contributions

By signing the Statement of Authorship, each author certifies that:

i. the candidate's stated contribution to the publication is accurate (as detailed above);

ii. permission is granted for the candidate in include the publication in the thesis; and

iii. the sum of all co-author contributions is equal to 100% less the candidate's stated contribution.

Name of Co-Author	Roger S. Seymour		
Contribution to the Paper 10%	Provided direction on the study during development and undertaking, and edited and reviewed the manuscript drafts.		
Signature		Date	1/2/2019

1. Abstract

Aquatic insects use a range of mechanisms to help them utilise underwater environments with their gas filled respiratory systems. The ability of an aquatic insect to effectively use a particular mechanism for O_2-uptake during dives underwater is related to body size which affects O_2 demand, surface area for gas exchange, cuticle thickness and O_2 store volume. Diving beetles (Dytiscidae) use several forms of aquatic gas exchange as adults, but some types are only found in small species. In this study, we investigate the relationships between O_2-consumption rate, volume of gas held by the beetles during dives, and dive characteristics in several species of dytiscids across a >300-fold mass range. We show dive duration and surfacing frequency do not change significantly with body size, associated with O_2 store volume scaling with the same allometric exponent as O_2-consumption rate. We then use these data with information from previous studies to assess how body size affects the capacity for diving beetles to gain O_2 from the water using different forms of respiration. Mathematically modelling the gas exchange process in the beetles' shows that only small dytiscids are able to remain underwater indefinitely using cutaneous respiration, setal tracheal gills and respiratory pores, and small beetles benefit the most from small gas gill bubbles that passively gain O_2 from the water and extend dive duration. These forms of respiration are more effective in cool conditions with high water convection, however, at higher temperatures and in still water the beetles can use their air stores to collect air from the water's surface if necessary.

2. Introduction

Aquatic insects utilise several different mechanisms to allow them to survive under water with their gas filled respiratory system, the tracheal system (Seymour and Matthews, 2013). Some of these include air stores, gas gills and cutaneous respiration. Air stores are bubbles collected from above the water's surface that supply O_2 for the insects' dive, but the insect needs to return to the surface once the O_2 becomes depleted. Gas gills are bubbles that allow the passive extraction of O_2 from the water through the bubble-water interface (Ege, 1915; Rahn and Paganelli, 1968). There are two types of gas gill, compressible and incompressible or plastrons (Seymour and Matthews, 2013; Thorpe and Crisp, 1947a). Compressible gas gills require periodic replenishment at the surface due to O_2-consumption and CO_2 and N_2 loss to the water. However, plastrons can be maintained indefinitely due to hydrophobic structures that retain a thin air layer over the body and prevent water ingress (Jones et al., 2018b; Marx and Messner, 2012; Seymour et al., 2015; Seymour and Matthews, 2013; Thorpe and Crisp, 1947a). Cutaneous respiration is the exchange of respiratory gases directly across the body surface, which may be associated with elaboration of the surface like the tracheal gills of damselfly and mayfly larvae or setal tracheal gills in some diving beetles (Bäumer et al., 2000; Eriksen, 1986; Kehl and Dettner, 2009; Thorpe and Crisp, 1947b; Verberk et al., 2018).

Different life stages of aquatic insects may use different respiratory modes or the same life stage may use several. For example, the fifth instar aquatic bug *Aphelocheirus* uses cutaneous respiration, but the adult uses a plastron (Thorpe and Crisp, 1947b), and adult diving beetles use both an air store and a gas gill (Kehl, 2014). There may also be variation in the mode of respiration across a family due to differences in body size, as many factors involved in respiration are strongly related to size. These include metabolic rate, surface area available for gas exchange, thickness of the cuticle and air store volume (Calosi et al., 2012; Jones et al., 2018a; Seymour and Matthews, 2013; Vlasblom, 1970). These variables influence the effectiveness of a particular mode of respiration for different sized insects. Metabolic rate in resting insects scales allometrically with body mass (M_b) to the exponent 0.82 (Chown et al., 2007; phylogenetically-adjusted exponent is 0.75). However, surface area (A) is expected to scale $M_b^{0.66}$, so a discrepancy develops between surface area available for gas exchange and O_2-demand as an insect becomes larger (Seymour and Matthews, 2013). This is applicable to insects using gas gills. The discrepancy between O_2-demand and supply is magnified in insects that use cutaneous respiration, where cutaneous exchange is expected to be proportional to surface area for gas exchange divided by cuticle thickness (X, $M_b^{A/X}$). Cuticle thickness in diving beetles scales $M_b^{0.34}$

(Jones et al., 2018a), therefore cutaneous exchange is expected to scale $M_b^{0.32}$ ($M_b^{0.66-0.34}$), making satisfying O_2 demand even more difficult than in gas gill breathers, particularly as the cutaneously respiring insects become larger. Conversely, it may be beneficial for insects using air stores to become larger, because O_2-store volumes potentially scale isometrically with mass (M_b^1), therefore, resulting in longer dive durations in larger insects that scales $M_b^{0.18}$ ($M_b^{1-0.82}$; Calosi et al., 2012). Our study aims to increase understanding of these relationships in aquatic insects by measuring O_2-consumption rate, surface area for gas exchange, and using cuticle thickness measurements from a previous study in a mathematical model to determine the size constraints for different modes of aquatic gas exchange.

Diving beetles (Dytiscidae) are a diverse and widespread group of predatory aquatic insects that use aerial and aquatic forms of respiration (Jones et al., 2018a; Kehl, 2014; Kehl and Dettner, 2009; Miller and Bergsten, 2016). The general dytiscid dive cycle begins with the beetles collecting air in the sub-elytral air store at the water's surface. The beetle dives and then begins consuming O_2 from the air store. A small bubble can be pushed from the tip of the abdomen which acts as a compressible gas gill, and once the O_2 is exhausted, the beetle returns to the surface to replenish the air store (Jones and Seymour, 2018). The dive cycle can be divided into readily quantifiable features that include dive duration, surfacing duration, and surfacing frequency.

Recently, other aquatic respiratory modes have been identified in dytiscids (Jones et al., 2018a; Kehl and Dettner, 2009; Madsen, 2008; Madsen, 2012). These include cutaneous respiration through the unelaborated body surface of subterranean dytiscids and setal tracheal gills in some surface species. Setal tracheal gills are small structures at high densities on the cuticle through which tracheoles run (Kehl and Dettner, 2009). They greatly reduce the diffusion distance through the cuticle and bring the surrounding water into close proximity to the gas within the tracheal system. Pores that may have respiratory function have been found on the surfaces of other submergence-tolerant surface dytiscids (Madsen, 2008; Madsen, 2012). However, it is not clear how they function in respiration. They may function like a plastron or they may be similar to the setal tracheal gills (Madsen, 2012). Nevertheless, all species that use these forms of respiration are small, indicating factors relating to size limit the use of these modes of respiration in larger beetles.

This study investigates the allometric relationships of dytiscid metabolism, dive behaviour and gas exchange. Using several dytiscid species across a >300-fold mass range, we undertook

experiments in closed respirometry chambers to determine the O_2-consumption rate and activity of the beetles. Beetles were placed in control dive chambers to measure dive characteristics (dive duration, surfacing duration and surfacing frequency), and the gas volume held by the insects at the beginning and end of dives, while the rates of gas volume decline were determined in free-diving beetles. These data show how metabolism and gas store volume scale with mass in dytiscids and how these variables relate to dive characteristics. The experimental data were then combined with information from previous studies to develop a mathematical model, based on Fick's general diffusion equation, to assess cutaneous, setal tracheal gill, pore and gas gill respiration in dytiscids, to understand how beetle size influences the effectiveness of each mode of respiration.

3. Methods and materials

Collection and maintenance of beetles

Onychohydrus scutellaris (Germar 1848) and *Hyderodes shuckardi* (Hope 1838) were collected in February 2017 from swamps near Nangwarry in South Australia (SA), and *Cybister tripunctatus* (Olivier 1795) in October 2017 from a dam and spring on Willow Springs Station in the Flinders Ranges, SA. *Chostonectes nebulosus* (Macleay 1871) and *Necterosoma dispar* (Germar 1848) were collected from ponds near Forreston (SA) in January and February 2018, respectively. *Hyphydrus elegans* (Montrouzier 1860) was caught from a dam in Mt Torrens (SA) in February 2018, and *Sternopriscus clavatus* (Sharp 1882) from a dam in Verdun (SA) in April 2018. Beetles were identified according to Watts and Hamon (2014), with assistance from C. H. S. Watts (SA Museum).

Beetles were placed individually in 800 mL containers approximately three quarters filled with water, with some vegetation, leaf litter and bark to hide in. The containers were in a constant temperature (CT) cabinet set to 25±1°C with a 12:12 hour light dark cycle. Each container was lightly aerated and beetles were fed every two to three days with suitably sized pieces of whitebait fish. Beetles were kept at 25°C for at least seven days prior to experiments (Calosi et al., 2007; Calosi et al., 2012; Terblanche et al., 2005), and were not provided with food less than 16 h before experiments. All experiments were conducted in a CT room at 25°C in air-equilibrated, reverse osmosis (RO) water, and they took place during the day, when beetles are less active (Aiken, 1986; Dolmen and Solem, 2002; Hilsenhoff, 1987). After each experiment beetles were dried with paper towel and weighed with an analytical balance (0.01 mg precision, AE 163, Mettler, Greifensee, Switzerland).

Respirometry

Three different sized glass respirometry chambers were used to measure O_2-consumption rate. All chambers consisted of glass jars with a magnetic flea in the bottom separated from the main chamber by nylon mesh. The largest chamber was 67 mm dia. x 106.5 mm tall for *O. scutellaris*, *C. tripunctatus* and *H. shuckardi* containing approximately 227 mL water and 12 mL air, the medium sized was 15.5 mm dia. x 51 mm tall for *C. nebulosus*, *H. elegans* and *N. dispar* containing 18.5 mL water and 0.77 mL air, and the smallest was 18 mm dia. with a 7 mm opening and 41 mm tall for *S. clavatus* containing 6 mL of water and 0.2 mL air.

To measure O_2 uptake, the respirometry chamber was filled with water at the treatment temperature. Any air bubbles were removed and an individual beetle was placed into the chamber. The chamber was sealed with a stopper that had two 14G hypodermic needles containing water inserted through it. The chamber was then dried on the outside and weighed with a balance (Mettler AE 163, 0.01 mg precision, or Sartorius 1265 MP, 1 mg precision). Air saturated with water vapour at 25°C was injected into the chamber with a syringe through the needles, pushing excess water out, and the chamber was again dried and weighed. The chamber was then placed into a water-filled aquarium to reduce diffraction for filming, with a small pump circulating water to maintain a stable temperature. Beetles in the chambers were filmed in the dark in infrared using a video camera (XA-20, Canon Inc., Tokyo, Japan). This was necessary because beetles could not hide in the chambers and bright conditions may have increased activity and disturbance.

A magnetic stirring plate was placed underneath the aquarium. The stirrer rotated the magnetic flea in the chamber sufficiently to allow complete mixing of the water in < 5 min. Mixing was specific to each chamber and determined using dye. Having the stirring rate too high would modify the beetles' behaviour causing them to cling to the bottom of the chamber due to the high water velocity. A fibre-optic O_2-sensing probe (optode; taper-tip fast response, probe model B2, PreSense GmbH, Regensburg, Germany) was inserted into the air and another (blunt tip) into the water through the water-filled needles, effectively sealing the inside of the chamber from the atmosphere. Needles inserted into the large and medium chambers had a small opening ~5 mm long halfway through the diameter of the needle a few mm from the end so the optodes could have exposure to the water without being damaged by the beetles. P_{O_2} within the chamber was recorded every second for 1.5 h with the optodes. The optodes were connected to a TX-3 data

acquisition unit (PreSense GmbH, Regensburg, Germany), with the temperature sensors placed in the aquarium, and a laptop computer. After this period, the optodes were removed and the chamber opened to remove the beetle. The water within the chamber was then topped up with fresh RO water and sealed, before being dried on the outside and weighed. The chamber was replaced into the aquarium, and the optodes were inserted to measure background respiration for 60 min. Water volumes and air volumes in the respirometry chamber were calculated from masses of the chambers, with and without air and accounting for the mass of the beetles.

O_2-consumption rate ($\dot{M}O_2$, μmol h^{-1}) was calculated with the following equation (Eq. 1);

$$\dot{M}O_2 = \beta \times V \times \dot{P}O_2 \quad (1)$$

where β is the O_2 capacitance (μmol ml^{-1} kPa^{-1}) of air or water, at the experimental temperature (Dejours, 1981), V is the volume of water or air in the chambers and $\dot{P}O_2$ (kPa h^{-1}) is the rate of PO_2 decline within the chamber. Total $\dot{M}O_2$ was calculated as the sum of the $\dot{M}O_2$ in water and air, with beetle $\dot{M}O_2$ calculated as total $\dot{M}O_2$ minus the background $\dot{M}O_2$, which was determined from the average $\dot{M}O_2$ of the two probes in the water-filled chamber. $\dot{P}O_2$ was measured from 40 min after the beetles had been in the chambers to allow the beetles to settle and for the PO_2 trace to stabilise due to small initial temperature differences between the aquarium and chamber. The initial 10 – 20 min was also excluded from the background respiration trace to allow stabilisation.

Activity of the beetles in the chambers was quantified by removing one video frame every 5 s from recordings over the period that was used for O_2-consumption rate measurements using VLC media player (VLC media player, Version 2.2.3). Frames were then viewed sequentially, and the number of times beetles moved between frames was scored. This value was divided by the total number of frames minus one, producing a value between 0 and 1, where 0 is no movement and 1 is movement between every frame.

Dive characteristics

To determine dive characteristics, individual beetles were placed in 1 L Schott bottles with 800 mL air-equilibrated RO water at the treatment temperature (Jones and Seymour, 2018). Each bottle contained a ~ 5 mm layer of gravel on the bottom, a piece of black rubber for beetles to hide under and flywire mesh for large beetles to hold onto because they could not hold onto the gravel. Four bottles were placed in a water-filled aquarium to reduce diffraction and illuminated with florescent lights in the CT room. Behind the aquarium was a white background and each bottle was visually separated with a white divider so the beetles could not see each other. The

video camera was placed so the beetles could be viewed throughout the chamber, other than when hiding under the rubber. After being left undisturbed for 1 h, the video camera was remotely set to record for 6 – 8 h.

Dive characteristics were determined by watching the videos and recoding when beetles returned to the water's surface to exchange gas and when they left the surface after exchanging gas. The first ten dives for each individual beetle were analysed unless they did not complete ten full dives over the duration of video recording. This occurred three times: twice in *S. clavatus* (7 and 8 dives) and once in *H. shuckardi* (8 dives). The dive duration (s) was calculated as the time between when a beetle left the surface after collecting air to when it returned to the surface. Surfacing frequency (N h^{-1}) was calculated as the number of surfacing events over time from the beginning of the video until the time of the end of the final analysed dive. Surfacing duration (s) was the duration of time between when the beetles surfaced to exchange gas to when they left the surface after exchanging gas.

Respiratory gas volume and density

The respiratory gas volume held by the beetles was determined according to Archimedes' principle using the density of the beetles and the buoyant force exerted by the beetles on a submerged platform that they voluntarily clung to (Jones and Seymour, 2018; Matthews and Seymour, 2008). To measure beetle density, beetles were euthanized with chloroform fumes, gently blotted dry with paper towel and weighed with an analytical balance (AE 163). Individual beetles were then placed underwater into a 10 or 20 ml glass syringe. A finger was placed over the end of the syringe and the plunger drawn out to remove air from the surface and tracheal system of the beetle. After being under negative pressure for 30 – 60 s the finger was released and the gas within the syringe expelled before undertaking the process an additional 5 – 10 times. The beetle was then placed in a small tube underwater that was flicked to remove any bubbles on the outside of the beetle. The negatively buoyant beetle was transferred to a custom made weighing pan hanging in a 4 cm deep Petri dish of water below the AE 163 balance. The submerged weight was then measured, and body volume (V, cm^3) calculated according to the Eq. 2;

$$V = (W_{air} - W_{H_2O}) \div \rho_{H_2O} \quad (2)$$

Where W_{air} is the insect's weight in air (g) and W_{H_2O} is its weight underwater, and ρ_{H_2O} is the density of pure water at the temperature used during the measurement (g cm^{-3}). The density of the beetles (ρ_b, g cm^{-3}) was calculated with Eq. 3:

$$\rho_b = W_{air} \div V \quad (3)$$

The density measurements were used with the buoyant force exerted by the free-diving beetles on a submerged platform to calculate the initial and final respiratory gas volumes and the rate of gas volume decline (Jones and Seymour, 2018). The gas volume includes that within the air store and tracheal system. The platform was attached to the bottom of the AE 163 balance *via* a rigid, weighted wire. When the beetles dove, they could cling to the platform and buoyant force measured with the balance each second and recoded with a laptop computer through a Mettler 012 data interface. Platforms were placed so that the beetles could not get underneath them, or if they could, not push off the bottom of the container up onto the platform increasing force beyond the buoyant force. The three largest species were in a 130 × 90 × 90 mm clear plastic container with 60 mm deep water and a 60 × 75 mm mesh platform. A 20 x 20 mm piece of mesh was placed on the bottom of the container so the beetles could cling to that sometimes instead of the platform, to allow baselining and drift correction of the force trace. The remaining small species were placed in a glass vial 23 dia. × 100 mm tall with 45 mm deep water. The platform (16 × 10 mm) was made of two pieces of rubber separated so that the beetles could climb in between. The glass vial was positioned in a small water filled glass aquarium to reduce diffraction. The apparatus was placed in a CT room at 25-26°C. The fan was switched off and the door closed prior to beginning experiments, because air movement would disrupt the force measurements. Each beetle was filmed in the dark in infrared with the video camera (XA-20) to accurately determine dive duration and when the beetle was holding onto the platform. *C. nebulosus* was filmed in the light because this species would rarely use the platform in the dark. Video and force recording were started simultaneously from outside the CT room. After recording began, the beetles remained in the container for 5 – 6 h. Beetles were not disturbed during this time, except *N. dispar* that would spend long periods at the surface and would require encouragement to dive and use the platform. No dives were analysed prior to 40 min from the beginning of the experiment to allow the beetles to adjust to the conditions. Six dives where beetles were using the platform without placing pressure on the bottom or sides of the chamber were analysed from each individual, and six individuals of each of the six species. *S. clavatus* did not perform a sufficient number of dives for analysis because they either did not spend enough time off the platform to allow baselining and drift correction, or they held onto the glass, or remained at the surface.

The respiratory gas volume of the beetle (V_g) was then calculated according Eq. 4 (Matthews and Seymour, 2008);

$$V_g = -1(W_{tot} - W_i) \quad (4)$$

Where W_{tot} (g) is the total submerged weight of the insect and gas held by the beetle, and W_i is the submerged weight of the beetle which was calculated with Eq. 5;

$$W_i = W_{air} - (W_{air} \div \rho b)\rho H_2O \quad (5)$$

To calculate the volume of gas carried by the beetle at the beginning and end of a dive, as well as the rate of volume decline, gas volume was calculated from the force trace when the beetle was on the platform (Eq. 4 and 5). A linear regression was then applied to the calculated gas volume trace, corrected for the time from the beginning of the dive and delay of the balance once force was applied, generally 6 – 12 s (Fig. 1B). The initial bubble volume was the y-intercept of the regression, final bubble volume was calculated from the dive duration time, and the rate of bubble volume decline was the slope of the regression. Drift was corrected in the force traces with linear regressions using two periods, when the beetle was not on the platform before and after analysable dives using the platform (Fig. 1A).

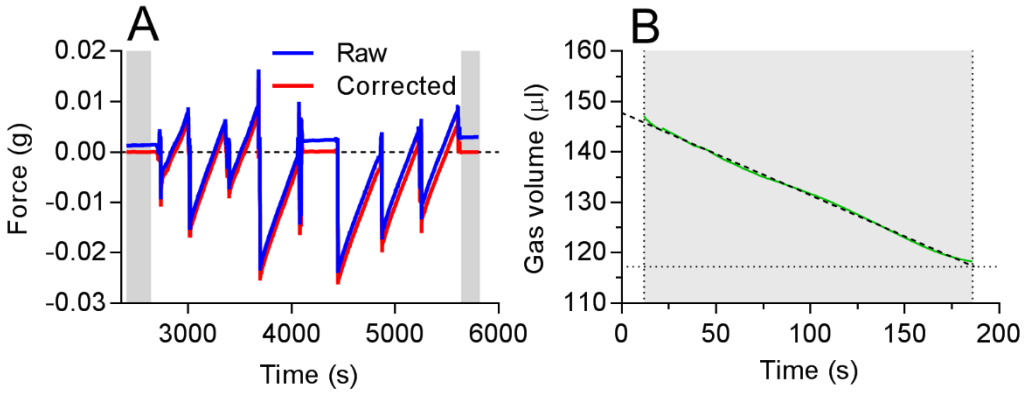

Figure 1. Examples of a force trace and respiratory gas volume decline. (A) Raw force trace (blue), and baselined and drift corrected trace (red) from buoyancy experiments with *C. tripunctatus*. Grey bars show segments used for correcting the data when the beetle was not on the platform. Sudden decreases in force followed by a slow increase are when the beetle was on the platform with the increase in force resulting from the decline in respiratory gas volume. (B) Example showing the decline in respiratory gas volume of *O. scutellaris* using the buoyancy platform. Shaded area shows when the beetle was on the platform, with the green solid line showing the change in gas volume recorded. Dashed black line indicates the linear regression corrected to the beginning of the dive and projected to the end of the dive at 187 s, only 1 s after the beetle left the platform. The y-intercept is the initial bubble volume, and final bubble volume is the volume at dive termination (187 s, shown by horizontal dotted line), with the slope of the regression being the rate of bubble volume decline.

Total beetle length

Beetle length was measured to produce a regression with mass, and enable calculation of beetle surface area. Euthanized beetles were photographed next to a millimetre incremented scale with a digital microscope (ViTiny Pro10 Plus). Length from the head to the tip of the abdomen was then measured with ImageJ (Version 1.5i, Wayne Rasband, NIH, USA).

Statistics

Power and linear regressions, ANOVA and Tukey's post-hoc tests were performed in Graphad Prism 7.02 (GraphPad Software Inc., La Jolla, CA, USA). Means, exponents and intercepts are shown with 95% CIs.

4. Results

Whole animal O_2-consumption rate increased with mass while mass-specific metabolic rate declined (Table 1 and 5, Fig. 2A). Activity levels of the beetles in chambers, although trending towards more activity at smaller size, were not significantly different from one another except *S. clavatus* where activity was significantly greater than all other species (ANOVA, $P<0.0001$, Tukey's post-hoc, $P<0.001$, Table 1). Activity-transformed O_2-consumption rates were calculated as O_2-consumption rate/(activity×9+1), which assumes a metabolic scope of 10 between rest and activity, comparable to that recorded in the aquatic bug *Aphelocheirus* and the difference between rest and terrestrial activity in other beetle species (Table 1; Bartholomew and Casey, 1977; Rogowitz and Chappell, 2000; Seymour et al., 2015). These activity-transformed data were combined with data from previous studies to produce an overall regression for dytiscids, including three subterranean dytiscids (Jones et al., 2018a), *P. decempunctatus* (activity corrected, (Jones and Seymour, 2018)) and *Dytiscus marginalis* (Di Giovanni et al., 1999). The activity-transformed data, in addition to the data from previous studies, increased the exponent for metabolic rate (Fig. 3).

Table 1. Mass, activity, O_2-consumption rate, mass-specific O_2-consumption rate, background respiration and drift, temperature and number of samples (*N*) measured in the respirometry chambers. Means with 95% CIs. Data for *Paroster nigroadumbratus* (Clark 1862) were measured during a pilot study in the smallest sized respirometry chambers, but without a magnetic stirrer, only a single optode, which was moved between the chamber water (mixed prior to measurements) and air, and beetles were not filmed, so activity could not be determined.

Species	Mass (mg)	Activity (0-1)	O_2-consumption rate (pmol s^{-1})	Activity corrected O_2-consumption rate (pmol s^{-1})	Mass-specific O_2-consumption rate (pmol s^{-1} g^{-1})	Background and drift (% of O_2-consumption rate)	Mean Temp. (°C)	*N*
O. scutellaris	1183.05±70.90	0.06±0.02	3833±979	2599±858	3275±833	1.6±1.5	25.4±0.1	11
C. tripunctatus	1013.76±84.78	0.01±0.01	2147±307	2032±240	2113±216	1.5±1.7	25.3±0.1	8
H. shuckardi	627.56±41.63	0.14±0.07	1019±270	527±194	1641±474	5.4±4.1	25.5±0.2	10
H. elegans	12.38±0.51	0.24±0.21	77±19	34±13	6345±1782	2.5±1.4	25.3±0.1	8
N. dispar	7.07±0.45	0.26±0.18	31±8	12±5	4376±1232	3.8±2.2	25.5±0.1	8
C. nebulosus	4.08±0.38	0.26±0.15	23±3	10±4	5832±859	10.8±2.9	25.5±0.3	10
S. calvatus	3.90±0.12	0.75±0.25	18±3	3±1	4519±876	1.8±10.9	24.8±0.3	8
P. nigroadumbratus	2.77±0.20	-	14±2	-	5015±824	0.6±1.3	24.9±0.0	10

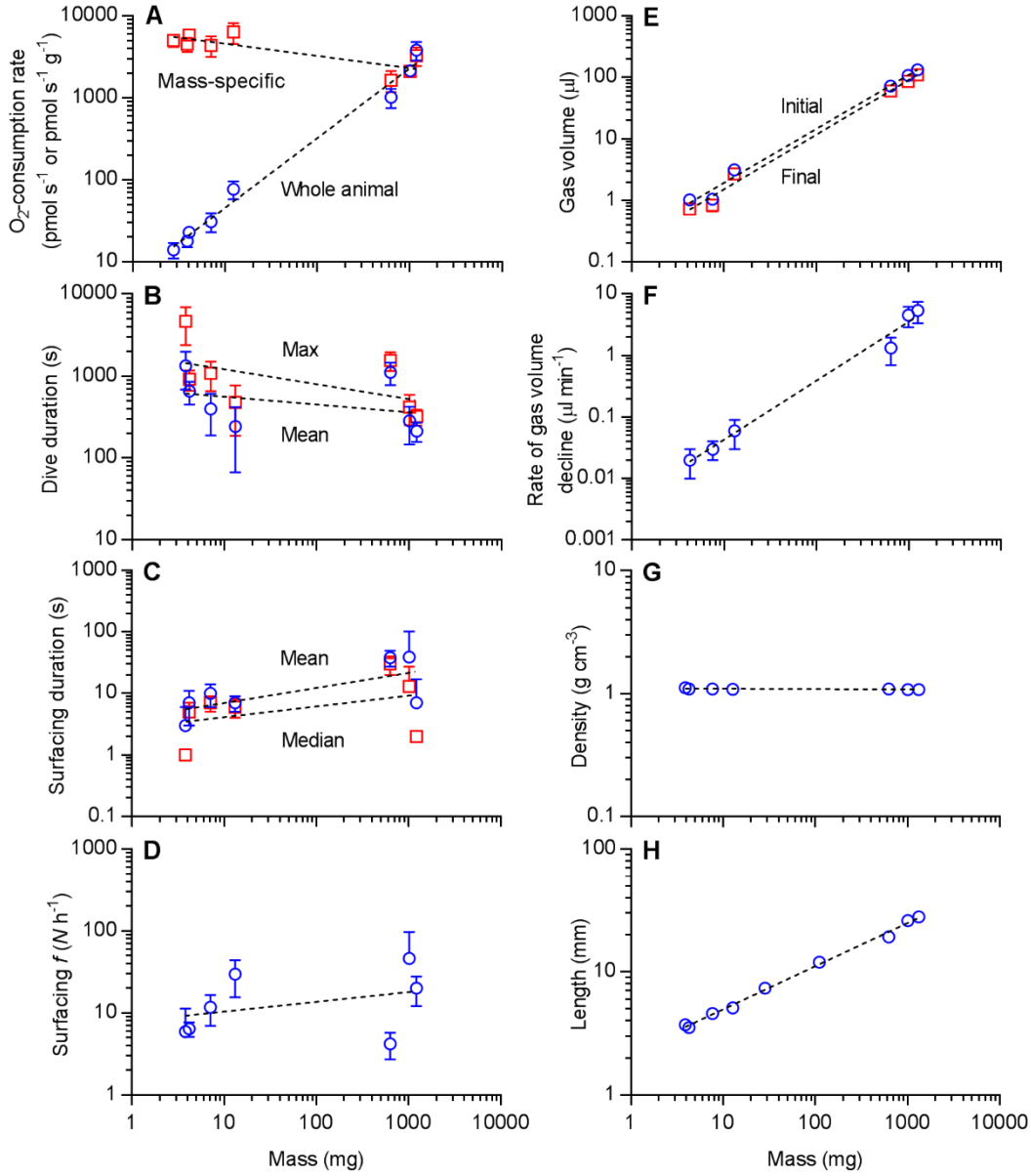

Figure 2. Allometric relationships of variables measured in diving beetles in this study. A, O_2-consumption rate, whole animal (blue circles), mass-specific (red squares); B, dive duration, mean (blue circles), max. (red squares); C, surfacing duration, mean (blue circles), median (red squares); D, mean surfacing frequency; E, respiratory gas volume, initial (blue circles), final (red squares); F, rate of respiratory gas volume decline; G, beetle density; H, total body length. Dashed lines show allometric relationships (Table 5). Means are shown with 95% CIs unless intervals are narrower than the symbols and can't be seen, or clip the x-axis.

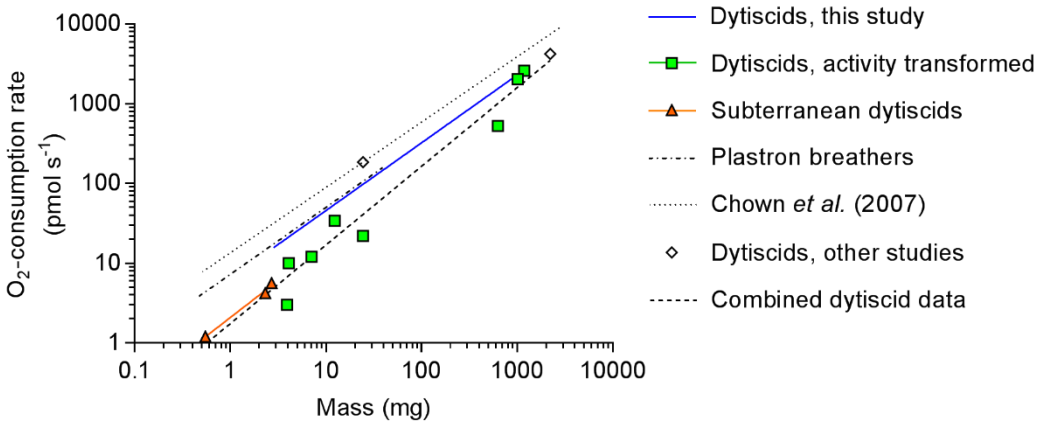

Figure 3. Metabolic rate comparisons between resting insects in general (dotted line, $\dot{M}O_2 = 13.46\ M_b^{0.82}$) (Chown et al., 2007), plastron breathers (dash-dot line, $\dot{M}O_2 = 7.22\ M_b^{0.84}$ (Seymour and Matthews, 2013), and dytiscids. Blue solid line, O_2-consumption rate of dytiscids from this study $\dot{M}O_2 = 6.43\ M_b^{0.85}$; green squares, activity transformed O_2-consumption rate of dytiscids; orange solid line and triangles, subterranean dytiscids $\dot{M}O_2 = 2.07\ M_b^{0.93}$; diamonds, dytiscids from other studies (*P. decempunctatus* 28.3 mg (Jones and Seymour, 2018), *D. marginalis* 2219 mg (Di Giovanni et al., 1999)); dashed line, combined data for subterranean, activity-corrected dytiscids, and *D. marginalis* ($\dot{M}O_2 = 1.74\ M_b^{0.99}$).

In the control dive chambers, the allometric exponents for mean and max. dive duration, mean and median surfacing duration, and mean surfacing frequency, did not differ significantly from zero (Table 2 and 5, Fig. 2B to D). Initial and final respiratory gas volume, as well as the rate of gas volume decline, increased significantly with mass (Table 3 and 5, Fig. 2E and F). Total beetle length increased with mass, but beetle density was independent across the mass range (Table 4 and 5, Fig. 2H and G).

Allometric data were not phylogenetically-adjusted due to the small number of taxa used in this study. The ability to detect phylogenetic signal in a trait is much lower where analyses have less than 20 taxa (Blomberg et al., 2003). Additionally, if phylogenetically-adjusted regressions differ from the observed regressions, and if they are used in models of gas exchange, the models become less representative of the actual system.

Table 2. Mass, mean and max. dive durations, mean and median surfacing duration, surfacing frequency and number of measurements (*N*) collected during control dive experiments. Temperature was measured with a thermocouple placed into the water-filled aquarium and was between 23.9 – 25.7°C.

Species	Mass (mg)	Dive duration (s, Mean)	Dive duration (s, Max)	Surfacing duration (s, Mean)	Surfacing duration (s, Median)	Surfacing *f* (*N* h^{-1})	*N*
O. scutellaris	1213.30±87.74	213±56	321±71	7±10	2±0	20.0±7.8	10
C. tripunctatus	1015.69±82.57	284±138	420±168	39±63	13±14	46.2±50.1	8
H. shuckardi	628.67±37.88	1114±337	1545±397	38±11	30±10	4.2±1.5	10
H. elegans	13.15±0.32	243±176	478±292	7±2	6±2	29.7±14.2	8
N. dispar	7.09±0.51	399±210	1077±419	10±4	7±2	11.7±4.8	8
C. nebulosus	4.18±0.39	653±203	916±257	7±4	5±2	6.4±1.3	10
S. calvatus	3.81±0.13	1334±651	4644±2256	3±3	1±0	5.9±5.4	8

Table 3. Mass, mean dive duration, initial and final respiratory gas volume, proportion of initial gas volume remaining at dive termination, rate of gas volume decline and number of measurements (*N*) collected during buoyancy experiments. Water temperatures used for calculating gas volume ranged from 22.8 – 27.3°C (mean of 24.9°C).

Species	Mass (mg)	Dive duration (s, Mean)	Initial gas vol. (µL)	Final gas vol. (µL)	Proportion of initial bubble vol. remaining at dive termination	Rate of bubble vol. decline (µL min^{-1})	*N*
O. scutellaris	1249.21±99.04	283±89	133.14±18.81	110.65±15.25	0.83±0.02	5.43±2.07	6
C. tripunctatus	989.13±94.27	333±118	107.74±14.89	86.60±13.20	0.80±0.02	4.55±1.66	6
H. shuckardi	640.34±60.43	604 ±128	72.51±3.93	59.85±4.42	0.82±0.03	1.33±0.36	6
H. elegans	12.99±0.51	612±225	3.15±0.19	2.69±0.18	0.86±0.02	0.06±0.03	6
N. dispar	7.53±0.74	477±202	1.05±0.19	0.84±0.18	0.80±0.05	0.03±0.01	6
C. nebulosus	4.25±0.41	739±173	1.02±0.19	0.73±0.12	0.73±0.06	0.02±0.01	6

Table 4. Dytiscid mass, length, density and number of sample for each species (*N*). *Rhantus suturalis* (W. S. Macleay 1825) and *Platynectes decempunctatus* (Fabricius 1775) were collected in the Adelaide Hills as incidentals, or for other studies.

Species	Mass (mg)	Length (mm)	Density (g cm^3)	*N*
O. scutellaris	1319.42±119.77	28.08±1.29	1.07710±0.00577	8*
C. tripunctatus	1009.29±85.89	26.12±0.82	1.08184±0.00897	8
H. shuckardi	627.45±37.79	19.30±0.62	1.09457±0.01025	8
R. suturalis	110.88±6.75	11.97±0.21	-	11
P. decempunctatus	28.54±2.24	7.36±0.19	-	8
H. elegans	12.75±0.71	5.09±0.08	1.08696±0.01101	6
N. dispar	7.66±0.67	4.59±0.10	1.09058±0.01066	6
C. nebulosus	4.29±0.40	3.53±0.12	1.09356±0.01254	6
S. clavatus	3.89±0.15	3.73±0.06	1.11701±0.01833	6

* *N*=7 for density

Table 5. Allometric regressions of variables measured during this study. Regressions are described by Y = aM_b^b, where M_b is body mass in mg.

Variable (Y)	Scaling factor (a)	Exponent (b)	R^2	*N* of species	Source data
O_2-consumption rate (pmol s^{-1})	6.43±1.52	0.85±0.10	0.988	8	Table 1
Mass-specific O_2-consumption rate (pmol s^{-1} g^{-1})	6456.54±1.54	-0.15±0.10	0.697	8	Table 1
Dive duration (mean, s)	695.02±3.98	-0.09±0.29	0.120*	7	Table 2
Dive duration (max, s)	1836.54±4.69	-0.18±0.33	0.286*	7	Table 2
Surfacing duration (mean, s)	4.02±3.90	0.24±0.29	0.485*	7	Table 2
Surfacing duration (median, s)	2.78±7.67	0.17±0.43	0.176*	7	Table 2
Surfacing *f* (N h^{-1})	7.87±5.36	0.12±0.36	0.128*	7	Table 2
Dive duration (mean, s)†	748.17±2.00	-0.10±0.14	0.507*	6	Table 3
Initial gas vol. (µL)	0.26±1.71	0.88±0.11	0.992	6	Table 3
Final gas vol. (µL)	0.20±1.76	0.89±0.11	0.992	6	Table 3
Rate of gas vol. decline (µL min^{-1})	0.00±2.17	0.96±0.15	0.987	6	Table 3
Length (mm)	2.21±1.09	0.35±0.02	0.996	9	Table 4

* regression exponent not significantly different from zero. † mean dive duration from buoyancy experiments.

5. Discussion

Respiration and dive characteristics in dytiscids

Beetles in this study primarily use air stores and sometimes gas gills for respiration underwater. This is associated with a reduced metabolic rate that scales with nearly the same exponent as insects in general, but with a lower elevation, and comparable to that of plastron breathers (Chown et al., 2007; Seymour and Matthews, 2013; Fig. 3, Table 5). This lower O_2-consumption rate provides the benefit of extending dive duration and allowing more time and energy to be allocated to foraging and mating, and minimising exposure to predators and parasites at the surface (Aiken, 1985; Calosi et al., 2007; Miller and Bergsten, 2016). In contrast, plastron breathing insects and subterranean diving beetles that generally don't surface, have lower metabolism, which is associated with low O_2 conductance through the boundary layer and cuticle (Jones et al., 2018a; Seymour et al., 2015; Seymour and Matthews, 2013). Combining activity-transformed O_2-consumption rate data from this study with data from previous studies, increases the O_2-consumption rate exponent to 0.99 (Fig. 3). Two factors could contribute to this. Firstly, diffusion-limited, unimodal cutaneous respiration in the smallest subterranean dytiscids severely limits metabolic rate. In contrast, the largest species rely heavily on air stores and are less restricted by O_2 diffusion from the water, allowing a higher relative metabolic rate. Secondly, insects that undertake highly energetic activities such as flying, have higher resting metabolic rates than those that do low-energy activities, such as terrestrial locomotion (Reinhold, 1999). The larger species of dytiscids can fly but the subterranean dytiscids have lost this ability (Watts and Humphreys, 2006).

The O_2-store volume of dytiscids has been assumed to scale isometrically (Calosi et al., 2012), however, we show that respiratory gas volume held by the beetles, which includes gas in the air store and tracheal system, scales with the exponent 0.88±0.11. This exponent does not differ significantly from metabolic rate at either 0.85±0.10 or 0.99±0.21. The O_2-storage-use hypothesis in diving birds and mammals suggests dive duration should increase with body mass to the exponent of 0.33 or 0.25 if O_2 store volume scales isometrically and metabolic rate scales with the exponent 0.67 or 0.75 (Halsey et al., 2006). The dive duration in dytiscids would then be expected to be independent of size or decrease slightly at larger size with exponents of 0.03 to -0.11. The measured exponents were -0.09 and -0.18 for mean and max. dive duration, respectively, indicating that larger beetles do not benefit from relatively larger O_2 stores than smaller beetles (Table 5). Why the respiratory gas volume does not scale isometrically is unclear. A previous study investigating two genera (*Deronectes* and *Ilybius*) of dytiscids determined an

exponent of 0.20 for dive duration (Calosi et al., 2012). This could indicate differences in relative respiratory gas volumes between those two genera when compared with species used in this study. *Deronectes* also have setal tracheal gills which would be expected to extend dive duration, however, the stagnant water conditions the beetles were measured in, are likely to reduce tracheal gill effectiveness, reducing O_2 conductance through the fluid layer around the body, and the beetles would rely more heavily on the air store (Calosi et al., 2012; Kehl and Dettner, 2009; Madsen, 2008; Verberk et al., 2018).

The allometric regressions for surfacing frequency and duration are not significantly different from zero, as with dive duration (Table 5, Fig. 2). Surfacing frequency is inversely related to dive duration when surfacing duration is constant. However, mean surfacing duration scales with the exponent 0.24 and median with 0.17, which is similar to the exponent reported previously ($M_b^{0.26}$) (Calosi et al., 2012). Surfacing duration is thought to remain relatively constant due to a trade-off between the rate of exchange gas with the atmosphere and risk of predation and parasitism while at the water's surface (Aiken, 1985; Calosi et al., 2007; Miller and Bergsten, 2016). If surfacing duration was limited by diffusion through the tracheal system, the expected exponent would be 0.33, due to the linear diffusion distance. However, there is evidence that exchange at the surface occurs not only by diffusion, but the beetles can actively ventilate their air stores (Gilbert, 1986). In the medium sized dytiscid *P. decempunctatus*, gas can be exchanged at the surface within a second (Jones and Seymour, 2018). This suggests the diffusion rate may be too fast to affect the surfacing duration in a significant way, and other factors influence the longer surfacing durations recorded in this, and previous studies (Calosi et al., 2007; Calosi et al., 2012; Jones and Seymour, 2018). There are likely to be differences between the behaviour of beetles under natural conditions compared with the experimental conditions. Factors such as water clarity, activity of other animals and movement of the water's surface may influence their behaviour. Under natural conditions surfacing durations may be shorter and better reflect the trade-off between gas exchange and risk at the surface. There is more variation in the measurement of dive characteristics in this study, compared to physiological and morphological measurements, due to variation in the beetles' behaviour both within species and between species. This variation contributes to difficulties in detecting relationships between physiological variables and dive characteristics.

Models of dytiscid respiration

A mathematical model based on Fick's general diffusion equation was developed to calculate the P_{O_2} difference (ΔP_{O_2}, kPa) required to sustain metabolism under different respiratory modes with increasing beetle size. These four modes include cutaneous respiration only (Jones et al., 2018a), setal tracheal gills (Kehl and Dettner, 2009), diffusion through plastron-like respiratory pores (Madsen, 2012), and diffusion through the gas gill. Diffusion of O_2 though water to a respiratory surface like the gas gill or cuticle, and diffusion though the cuticle itself can be represented by the following equation (Jones et al., 2018a; Jones et al., 2015; Rahn and Paganelli, 1968):

$$\dot{M}_{O_2} = K_{O_2} \times A/X \times \Delta P_{O_2} \quad (6)$$

where $\dot{M}_{O_2}$ (pmol s^{-1}) is the O_2-consumption rate of the beetle, K_{O_2} (pmol s^{-1} kPa^{-1} cm^{-1}) is the Krogh's coefficient of diffusion of O_2 through either water or the cuticle, which is the product of diffusivity and capacitance, A (cm^2) is the surface area through which diffusion can take place, X (cm) is the boundary layer thickness, the fluid layer above a respiratory surface deficient in O_2 which provides resistance to diffusion, or the thickness of the cuticle, and ΔP_{O_2} (kPa) is the O_2 partial pressure difference between the respiratory surface and the surrounding bulk fluid, or the outside and inside of the cuticle. The conductance (G_{O_2}, pmol s^{-1} kPa^{-1}) of O_2 through the water or cuticle is equal to $K_{O_2} \times A/X$. Eq. 6 is rearranged to calculate ΔP_{O_2} as follows;

$$\Delta P_{O_2} = \dot{M}_{O_2}/G_{O_2} \quad (7)$$

Total O_2 conductance ($G_{O_2\,tot}$) is calculated differently for each mode of respiration depending on the relationships, parallel or in series, between conductances within the O_2 cascade (Fig. 4). In model 1, diffusion is through the boundary layer and cuticle and the conductances are in series. In model 2, diffusion is through the cuticle boundary layer and cuticle in series, but parallel with the setal tracheal gill boundary layer and tracheal gills which are in series. In model 3, diffusion is though the cuticle boundary layer and cuticle in series, but parallel with the respiratory pore boundary layer. In model 4, diffusion through the cuticle boundary layer and cuticle are in series, and are parallel with diffusion through the gas gill boundary layer. The total conductance for each model is calculated as follows;

$$\text{Model 1 } G_{O_2\,tot} = (1/G_{O_2,cut} + 1/G_{O_2,BL})^{-1} \quad (8)$$

Model 2 $GO_{2\,tot} = (1/GO_{2,cut^*} + 1/ GO_{2,BL^*})^{-1} + (1/GO_{2,TGills} + 1/GO_{2,BLTGill})^{-1}$ (9)

Model 3 $GO_{2\,tot} = (1/GO_{2,cut^*} + 1/GO_{2,BL^*})^{-1} + GO_{2,BLPores}$ (10)

Model 4 $GO_{2\,tot} = (1/GO_{2,cut} + 1/GO_{2,BL})^{-1} + GO_{2,BLGGill}$ (11)

Where $GO_{2,cut}$ is the O_2 conductance through the cuticle, $GO_{2,BL}$ is conductance through the boundary layer, GO_{2,cut^*} is conductance through the cuticle of the area not occupied by setal tracheal gills or respiratory pores, GO_{2,BL^*} is conductance through the boundary layer excluding the area associated with the tracheal gills or respiratory pores, $GO_{2,TGills}$ is the conductance through the setal tracheal gills, $GO_{2,BLTGill}$ is the conductance through the boundary layer relating to the tracheal gills, $GO_{2,BLPores}$ is the conductance of the boundary layer of the respiratory pores, and $GO_{2,BLGGill}$ is the conductance of the boundary layer surrounding the gas gill.

The following allometric regressions (mass in mg) and constants were used in the model. O_2-consumption rate $\dot{M}O_2$ (pmol s^{-1}) = 6.43 $M_b^{0.85}$ at 25°C (Table 5), which was also adjusted to 10°C with a Q_{10} of 2 (Chown et al., 2007) because submergence-tolerant species often occupy cool waters (the Q_{10} is the factor by which a rate process, i.e. metabolism, or diffusion, increases with a 10°C raise in temperature), body surface area (mm^2, equal to cuticle surface area) = 5.95 $M_b^{0.69}$ (Supplementary table 1), cuticle thickness (µm) = 10.162 $M_b^{0.31}$ (Jones et al., 2018a) and gas gill surface area (mm^2) = 0.64 $M_b^{0.59}$ (Supplementary table 2). In model 1, diffusion occurs through the whole body surface (Jones et al., 2018a). In model 2, 30% of the body surface area is taken up by the tracheal gills, and the remainder to cutaneous respiration (Kehl and Dettner, 2009). Cuticle thickness of the tracheal gills is 1 µm (Kehl and Dettner, 2009). In model 3, 10% of the body surface area is taken up by the respiratory pores and the remainder to cutaneous respiration (Madsen, 2012). In model 4, the whole body surface area is allocated to cutaneous respiration, with the surface area of the gas gill being allocated for diffusion into the gas gill. Krogh's coefficients for O_2 in water are 0.240 (10°C) and 0.290 (25°C) pmol s^{-1} kPa^{-1} cm^{-1} (Seymour, 1994), and for cuticle 0.009 (10°C) and 0.010 (25°C) pmol s^{-1} kPa^{-1} cm^{-1} (Krogh, 1919) which are adjusted for temperature with a Q_{10} of 1.1 (Bartels, 1971). Two boundary layer thicknesses, representing stagnant (500 µm boundary layer) and convected water (100 µm boundary layer), were used (Seymour et al., 2015). The two water temperatures and convective conditions represent the range of conditions dytiscids experience. Subterranean species and some surface species live in water at 25°C (Jones et al., 2018a; Watts and Humphreys, 2006), Jones pers. obs.), while some submergence-tolerant species live in cool fast flowing streams and rivers (Kehl and Dettner, 2009; Miller and Bergsten, 2016; Verberk et al., 2018).

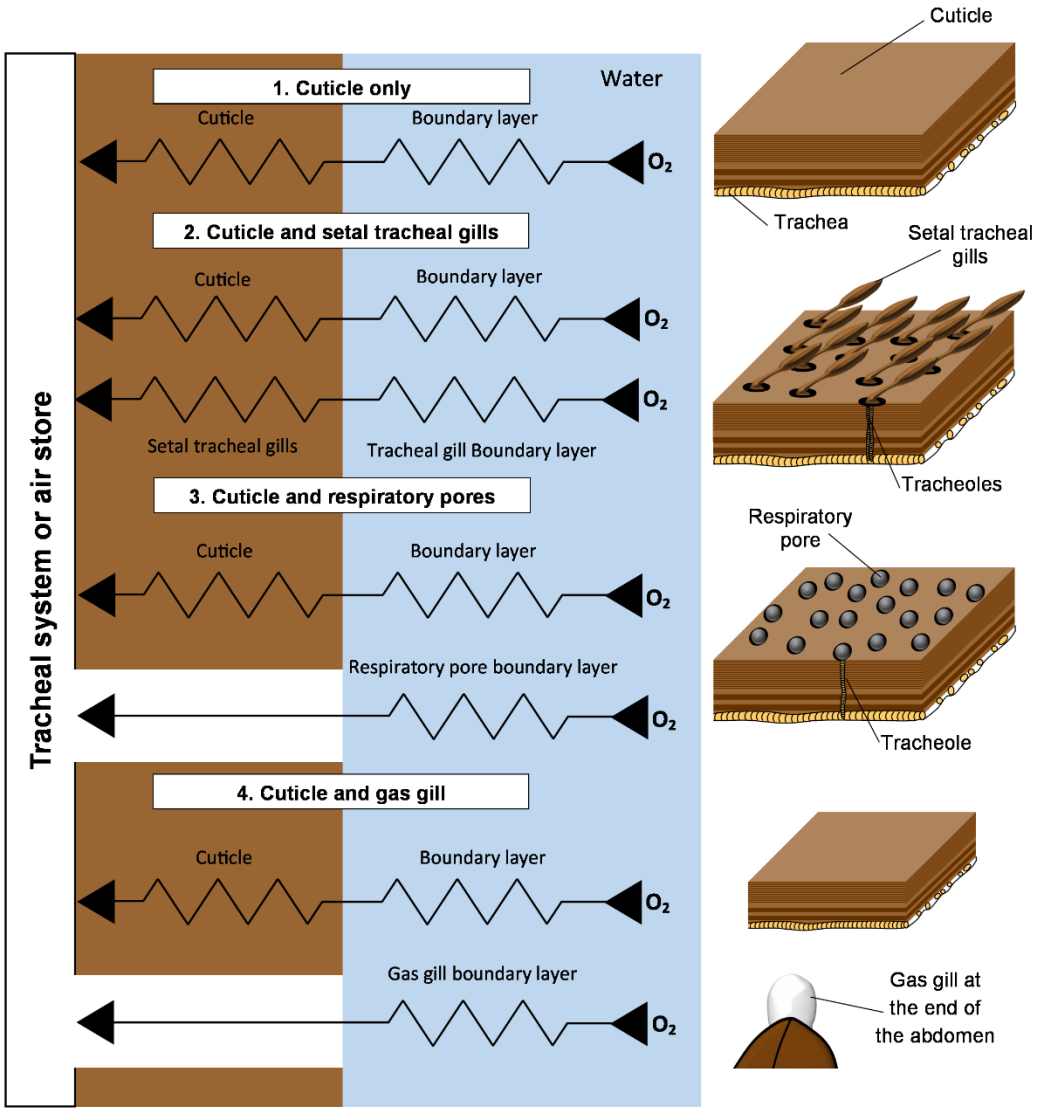

Figure 4. Diagrammatic representation of the diffusion model showing the four modes of respiration. (1) Cutaneous only, (2) diffusion through setal tracheal gills and cuticle, (3) diffusion through plastron like respiratory pores, and (4) diffusion through the cuticle and compressible gas gill held at the end of the abdomen. Lines represent O_2 diffusion from the water into the tracheal system or air store with arrows indicating the direction of diffusion, and conductances shown with zigzags. Placement of conductances indicates whether they are in series or parallel in a particular model. Once the O_2 has reached the gas within the air store, tracheal system or on the inside of the cuticle this is regarded as the end point of the model.

Setal tracheal gills, respiratory pores and cutaneous respiration

The most effective model for maintaining the ΔP_{O_2} below 19 kPa at the largest size is the setal tracheal gill model (Fig. 5). The 19 kPa ΔP_{O_2} represents the maximum theoretical P_{O_2} difference required before O_2-consumption rate becomes limited (Seymour et al., 2015). The setal tracheal gills have a higher total conductance relative to the pore model due to the larger setal gill surface area, despite the lower conductance provided by setae. In convected water at 10°C, a beetle of 1000 mg could remain submerged indefinitely with setal tracheal gills. However, beetles experiencing higher temperatures and stagnant water are more likely to be limited in size with this mode of respiration. The largest beetle that can remain submerged using setal tracheal gills in stagnant water at 10°C is only ~10 mg. This correlates well with the size of *Deronectes aubei* (calculated mass 10.7 mg) and the largest *Deronectes* species (6 mm, calculated mass 17.9 mg) (Fig. 5, masses calculated using the length regression in Table 5, (Miller and Bergsten, 2016; Ribera and Nilsson, 1995)).

The pore model represents the pores as small bubble interfaces (Fig. 4). However, pore structures vary considerably and some may be gas filled pores while others are in fact similar to setal tracheal gills where tracheaed structures are found within the pore (Madsen, 2012). In the latter case, the setal tracheal gill model would be a better representation of diffusion. At 10°C in stagnant water the largest beetle that can remain under water indefinitely is ~5 mg. As with *Deronectes*, species that have pores and are submergence-tolerant are small (<8 mm, the largest known species with pores is *Stictotarsus duodecimpustulatus* at 5.5 mm; Madsen, 2012; Miller and Bergsten, 2016).

The size and density of pores and setae vary between species and would, therefore, influence the O_2 diffusion rate. *D. aubei* has ~20 µm long spoon-shaped setae at 5,900 per mm^2 which covers 30% of the elytra (Kehl and Dettner, 2009). If other *Deronectes* have similar sized setae, coverage would vary between 27 – 45%. This assumes a setal + puncture area of 70 μm^2 (estimated from Fig. 2 in Verberk et al., 2018), where punctures are small openings in the cuticle surface from which structures emerge (Wolfe and Zimmerman, 1984). Surface area of individual respiratory pores are 7 – 43 μm^2 at 3,400 to 14,000 per mm^2 covering 2 – 15% of the elytral surface (Madsen, 2012). However, despite these differences the beetles with these modes of respiration are unlikely to become much larger.

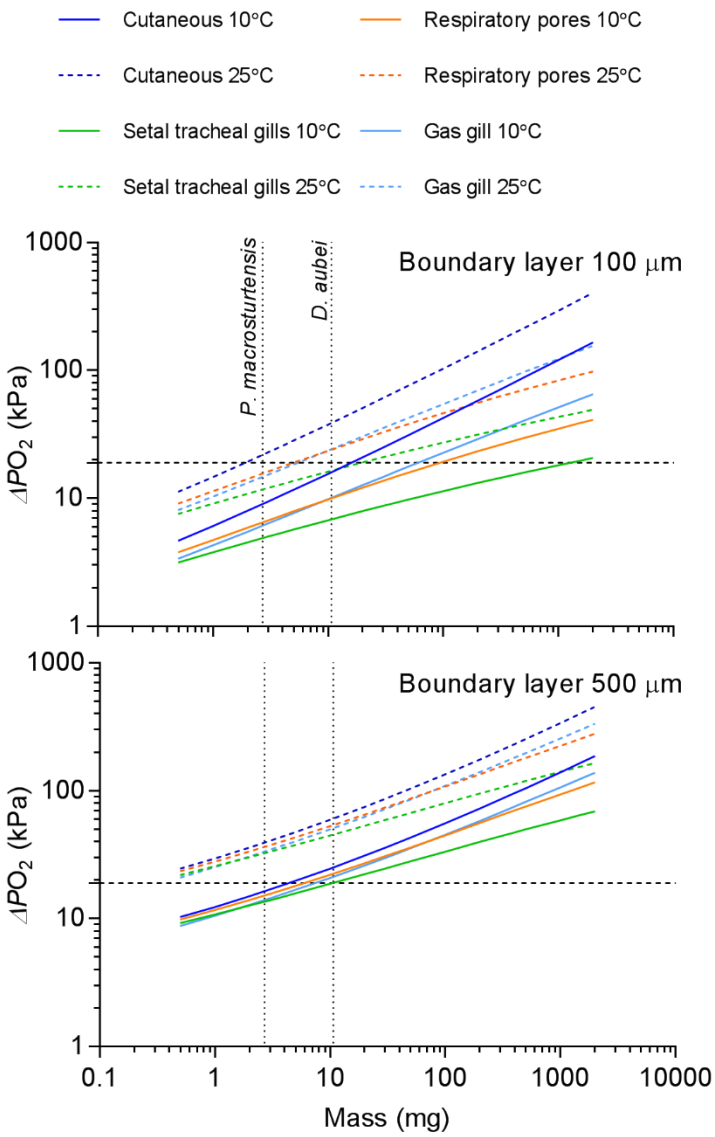

Figure 5. ΔP_{O_2} required to maintain the O_2-consumption rate of dytiscids using different modes of respiration. Respiration modes include (1) cutaneous only, (2) diffusion through setal tracheal gills and cuticle, (3) diffusion through plastron like respiratory pores, and (4) diffusion through the cuticle and compressible gas gill held at the end of the abdomen. Temperature is set to 10°C or 25°C, with convected (100 µm boundary layer) or stagnant water (500 µm boundary layer). Horizontal dashed line indicates the 19 kPa ΔP_{O_2} representing the maximum theoretical P_{O_2} difference without reducing O_2-consumption rate (Seymour et al., 2015). Vertical dotted lines show the mass of a cutaneously respiring subterranean dytiscid (*Paroster macrosturtensis* (Jones et al., 2018a)) and the surface species *D. aubei* which uses setal tracheal gills. Mass of *D. aubei* calculated from body length (Ribera and Nilsson, 1995) and allometric equation for length (Table 5).

Small dytiscids, using cutaneous respiration without cuticular elaboration, can survive underwater indefinitely (Fig. 5, (Jones et al., 2018a)). However, it is the most restrictive mode of respiration. The estimated maximum size for cutaneously respiring beetle at 10°C in stagnant water is ~4

mg, and in convected water at 10°C ~10 mg and at 25°C 1.5 mg (Fig. 5). These predicted body masses are similar to the values calculated in previous study of subterranean dytiscids (~5 mg (Jones et al., 2018a)) despite differences in regressions used for surface area and metabolic rate. Although small dytiscids can rely solely on cutaneous respiration, larger species have developed the respiratory setae and possibly pores that work in conjunction with the cuticle to increase O_2 conductance and enable a larger beetle to remain underwater.

The model in Figure 5 assumes O_2 diffusion into the beetle is linear and considers only the resistances mentioned. There is an added layer of complication in beetles with setal tracheal gills and respiratory pores because of the potential development of "diffusion shells" over these structures. These are in effect small boundary layers over individual setae or pores (See Stephan's diffusion law (Simkiss, 1986; Tøien et al., 1988)). More O_2 would diffuse into the setae and pores than the surrounding cuticle due to the cuticles' lower conductance, resulting in heterogeneous P_{O_2} in the water over the surface of the beetle. However, O_2 diffusion through these diffusion shells is likely to be determined by several factors, including shape and distance between pores and setae, internal resistances, water convection and O_2 demand. This problem is analogous to many of the questions relating to gas diffusion through stomata on leaves and diffusion through pores in egg shells (Lee and Gates, 1964; Simkiss, 1986; Tøien et al., 1988). Given the diversity of potential respiratory structures on the surfaces of dytiscids, in size, structure and density (Kehl and Dettner, 2009; Madsen, 2012; Verberk et al., 2018), the effectiveness of each seta or pore morphology would have to be considered individually to fully understand to what degree these structures benefit individual beetle species.

Gas gill function

Compressible gas gills can extend the dive duration of dytiscids, but must be replenished at the surface, unlike beetles using cutaneous, setal tracheal gill, or pore respiration. This is because hydrostatic pressure on the bubble increases total bubble pressure above atmospheric, and, therefore, the partial pressure of N_2 within the gill increases above the surrounding water causing it to diffuse out into the water (Rahn and Paganelli, 1968). However, by maintaining a high P_{O_2} within the gas gill, the P_{N_2} difference between the gill and water remains smaller, reducing the rate of N_2 loss (Rahn and Paganelli, 1968). This would occur at low temperatures when the beetles have low metabolic rates.

Small beetles benefit most from gas gills, where a relatively small ΔP_{O_2} enables sufficient O_2 diffusion to sustain metabolism (Fig. 5). When beetles are small (i.e. < 5 mg in convected water),

the gas gill model performs slightly better than the pore model. However, as the beetles become larger, the O_2 conductance decreases relative to the pore model because gas gill surface area scales with a lower exponent (0.59) than surface area of the pores (0.69), which is related to body surface area. Nevertheless, the gas gills do extend dive duration and enable species that do not benefit greatly from cutaneous respiration, either due to large size or lack of respiratory structures, to still gain O_2 from the water.

The gas gill size in this study was calculated from the width of the last abdominal tergite. When exchanging gas at the surface the last abdominal segment folds down to open the air store (Gilbert, 1986), and the bubble is held in place by hydrophobic hairs at the end of the abdomen (Kehl, 2014). Gas gill diameter is related to the width of the last abdominal tergite and is modelled as a sphere. In *P. decempunctatus*, this produces a gill volume of 1.45 µL, well within the range measured previously from images (<1.8 µL (Jones and Seymour, 2018)). The use and size of gas gill varies between dytiscid species (De Ruiter et al., 1951; Jones and Seymour, 2018), and the regression for gas gill size in this study would need to be validated by measurements in living beetles. Nevertheless, the contribution of the gas gill to the amount of O_2 consumed during a dive in dytiscids is very small.

Conclusion

Temperature and water convection play a significant role in determining the effectiveness of the different modes of respiration used by the dytiscids. Increased temperature increases O_2 demand and reduced water convection decrease O_2 conductance potentially leading to O_2 limitation. At 25°C in stagnant water none of the modes of respiration are sufficient to allow the beetles to remain submerged (Fig 5). However, the beetles can use the air store if necessary, and this behaviour has been observed in submergence-tolerant surface dytiscids that don't surface in well-convected water, but surface regularly in still or slowly moving water (Madsen, 2008). Despite this, O_2 diffusion still occurs and the beetles derive some benefit from all forms of respiration. However, the amount of O_2 diffusion from the water depends on the size of the beetle and its mode of respiration. This in turn affects dive duration and surfacing frequency, and ultimately the beetles' interactions with their surrounding environment.

6. Acknowledgements

We would like to thank Chris Watts from the South Australian Museum for assisting with identification of beetles and providing information regarding collection locations. Tom Nelson and Steve Cooper for helping collect beetles, and Qiaohui (Vivi) Hu for helping maintain them. Jo

Morton and Terry Walsh (Verdun), Kym and Iris Gladigau (Mt Torrens), and Carmel and Brendan Reynolds (Willow Springs Station) for allowing access to their properties for collecting beetles. This study was supported by the Australian Government Research Training Program Scholarship to KKJ.

7. Supplementary material

Table S1. Surface area of dytiscids. Surface area was determined by measuring the length and width of dytiscids from photographs taken next to a scale. Beetles were assumed to be a lozenge shape, the sum of an elliptical cylinder and an ellipsoid with semi-axes *a*, *b* and *c*, and an elliptical cylinder length of *L* which is equal to beetle length minus 2*a* (See (Jones et al., 2018a) for surface area and volume equations). Axes *a* and *b* are equal and are half the beetle width. Semi-axis *c* is half the depth of the beetle determined by producing a linear regression of mass for each species given the density of the beetle and the volume of the lozenge shape with an increasing value for c. This linear regression was then rearranged to calculate *c* for that particular species given its mass. Surface area was then determined for the lozenge given those axes. Beetle surface area (mm^2) = 5.95 $M_b^{0.69}$. Equations for ellipsoid volume, and elliptical cylinder volume and surface area are derived from Spiegel et al. (2013), and the approximate equation for the surface area of an ellipsoid (Knud-Thomsen approximation) from Michon (2015).

					Ellipsoid and Elliptical cylinder semi-axes and length (mm)					
Species	Mass (mg)	Length (mm)	Width (mm)	Density (g cm^3)	*a*	*b*	*c*	*L*	Surface area (mm^2)	*N*
O. scutellaris	1319.42	28.9	14.6	1.07710	7.293	7.293	2.293	14.283	884.183	6
C. tripunctatus	1009.29	26.2	13.6	1.08184	6.786	6.786	2.088	12.594	740.946	8
H. shuckardi	627.45	19.2	10.7	1.09457	5.342	5.342	2.267	8.560	453.946	8
P. decempunctatus	28.54	7.4	4.0	1.08710	1.979	1.979	0.722	3.426	62.592	8
H. elegans	12.75	5.1	3.0	1.08696	1.509	1.509	0.633	2.059	33.505	7
N. dispar	7.66	4.6	2.3	1.09058	1.160	1.160	0.525	2.253	23.987	6
C. nebulosus	4.29	3.5	2.1	1.09356	1.046	1.046	0.443	1.418	16.091	6
S. calvatus	3.89	3.7	1.9	1.11701	0.955	0.955	0.396	1.793	15.630	6

Table S2. The size of the hypothetical gas gill was calculated from the width of the last abdominal tergite, tergite VIII, where the width was equal to the diameter of a spherical gas gill. The width of the tergite was determined by removing the elytra and viewing ethanol preserved beetles under a dissecting microscope with a camera attached. The beetles were placed next to a scale in the same plane as the tergite and an image taken. The tergite width was then measured with ImageJ. Gas gill volume and gas gill surface area were calculated as the volume and surface area of a sphere (Spiegel et al., 2013). Gas gill surface area (mm^2) = 0.64 $M_b^{0.59}$.

Species	Mass (mg)	Tergite VIII width (mm)	Gas gill vol. (µl)	Gas gill surface area (mm^2)	*N*
O. scutellaris	1319.42	3.7	25.89	42.3	8
C. tripunctatus	1009.29	2.4	7.43	18.4	8
H. shuckardi	627.45	4.2	38.47	55.1	8
P. decempunctatus	28.54	1.4	1.45	6.2	6
H. elegans	12.75	1.1	0.63	3.5	6
N. dispar	7.66	0.8	0.23	1.8	6
C. nebulosus	4.29	0.6	0.10	1.1	6
S. calvatus	3.89	0.7	0.17	1.5	6

Chapter Six: Conclusion
Significance and contribution

Aquatic insects are integral parts of freshwater ecosystems. Understanding how they interact with their environment is important to understand changes within those ecosystems and interactions between organisms at varying scales. The relationships of aquatic insects with their environment are in part governed by their need to acquire O_2. These insects either have to invest time and energy in returning to the surface to replenish their bubbles, or are constrained to particular habitats, morphologies and sizes, due to factors that influence the efficacy of O_2 gain from the water. The research in this thesis set out to improve our understanding of how different modes of respiration in aquatic insects function and how the ability of these modes to supply O_2 changes in response to physiological and environmental variables under a range of physical constraints. This goal was achieved with a combination of experiments, measurements and mathematical modelling.

In chapter 2, I explored the conditions under which the plastron breathing bug *Aphelocheirus* is able to live without O_2-limitation. The study combines measurements of plastron PO_2 in response to temperature, convection and activity, with data from previous studies to develop a model based on Fick's diffusion equation. The model shows the temperature and convective conditions under which maximum and resting metabolic rate become O_2-limited. The results compared favourably with observations of *Aphelocheirus* at different PO_2 levels in a previous study, but indicated that factors beyond O_2-limitation may set the critical thermal temperatures for this species recorded in another study (Verberk and Bilton, 2015).

The focus of chapter 3 was to determine if subterranean dytiscids use cutaneous respiration to enable then to survive underwater and, if so, does this limit them to small size? Through a series of experiments and observations we found that the beetles do use cutaneous respiration. They lack structures on the surfaces of their bodies that could have respiratory function, consume O_2 from the water and, most convincingly, have O_2-boundary layers surrounding their bodies indicating O_2 diffusion across the surface of their cuticle. A model based on Fick's diffusion equation showed that as the beetles become larger, a combination of increasing cuticle thickness and O_2-consumption rate with declining relative surface area led to a decrease in metabolic scope. At sizes greater than 5 mg and approximately 5 mm long the metabolic scope of the beetles may not be wide enough to be functional, limiting the beetles to a small size. However, the ability of these species to utilise cutaneous respiration has enabled the development of the most diverse assemblage of subterranean dytiscids in the world (Balke et al., 2004).

Chapter 4 was a detailed study into respiration, gas exchange and dive behaviour in the medium sized dytiscid *P. decempunctatus* to develop a more comprehensive understanding of gas exchange in surface dwelling dytiscids that use air stores and compressible gas gills. A wide range of experiments and measurements were undertaken that showed O_2-consumption rate, dive characteristics, activity, respiratory gas volume, air store PO_2 and gas gill size. These data were incorporated into a model based on Fick's equation, which showed the contribution of the gas gill and cutaneous respiration to dive duration. Although the contribution of the gas gill to extending dive duration is small, especially when compared to other aquatic insects, it can still be significant in particular conditions. Interestingly, cutaneous respiration can contribute equally, if not more, to the dive than the gas gill, despite the relatively thick cuticle and lower surface area relative to O_2-consumption rate of this species due to its moderate size.

The final research chapter, chapter 5, combined the methodology and knowledge from previous chapters to understand how characteristics of respiration, gas exchange and dive behaviour changed with beetle size in dytiscids. Allometric regressions showed the relationships of O_2-consumption rate, dive duration, surfacing duration, surfacing frequency and respiratory gas volume with mass. This allowed comparisons of dive characteristics with other studies, to better understand the relationships between O_2-consumption rate, O_2-store volume and dive characteristics. The data from chapter 5 and previous studies were incorporated into a model based on Fick's equation to assess the four different modes of respiration dytiscids use to exchange gas with the water: cutaneous, setal tracheal gills, respiratory pores, and gas gills. Cutaneous respiration is the most restrictive form of respiration, and only very small beetles that use this mode of gas exchange are able to remain underwater indefinitely. Setal tracheal gills and respiratory pores potentially increase O_2 conductance into the beetles, however they permit only a small increase in the size of beetles compared to those that use cutaneous respiration exclusively. Small beetles using gas gills, although unable remain under water indefinitely, benefit the most from their use, increasing the relative amount of O_2 diffusion from the water due to the favourable surface area to mass ratio. For setal tracheal gills and respiratory pores this study provides the first quantitative test of their functionality. Chapter 5 illustrates why dytiscids that use setal tracheal gills, respiratory pores and cutaneous respiration, which enable them to remain underwater, must be small. This related to how metabolic rate, surface area for gas exchange and cuticle thickness change with size.

Challenges

Fick's general diffusion equation has been used throughout this thesis to better understand aquatic insect gas exchange. However, the assumption that diffusion is linear through the boundary layer to a respiratory surface may not hold true in particular circumstances. O_2 diffusion into respiratory pores or setal tracheal gills may result in the formation of what are effectively small boundary layers over the top of the pores or setae called "diffusion shells". Diffusion shells and their effects on gas exchange have been investigated in studies of avian egg shell pores and plant stomata (Lee and Gates, 1964; Simkiss, 1986; Tøien et al., 1988). If these shells form in dytiscids, there will be heterogeneous O_2 levels within the main boundary layer as a result of differences in O_2 conductance through the respiratory structures and the surrounding cuticle. Under these conditions diffusion could no longer be considered linear. Whether the O_2 levels do vary spatially like this likely depends on respiratory structure size, density and shape, which vary between species (Kehl and Dettner, 2009; Madsen, 2012; Verberk et al., 2018). The pores or setae may be sufficiently close and large enough in size that diffusion is effectively linear.

The second case where diffusion may not be linear is diffusion to the surface of the small cutaneously respiring subterranean diving beetle *P. mesosturtensis*. The O_2-consumption rate per unit surface area calculated for this species is similar to the larger species *L. palmulaoides*, and therefore the expected boundary layer thickness would be similar. The thinner boundary layer measured in *P. mesosturtensis* may indicate higher O_2 conductance to the surface of this species. Diffusion may therefore be radial rather than linear. Radial diffusion may also occur into the gas gill used by *P. decempunctatus* given the gill's size, which would lead to a higher contribution of O_2 from the gas gill to the dive. A combination of optode boundary layer measurements and finite-element analysis could help clarify these uncertainties regarding the nature of O_2 diffusion in these circumstances.

In chapters 4 and 5 we investigated the relationships between gas exchange and dive behaviour. In both studies there was considerable variation in dive behaviour both within and between species, and between experimental set ups. This variation makes it difficult to resolve relationships between variables like dive duration, surfacing frequency and surfacing duration with size and O_2-consumption rate. This variation is likely attributed to a number of factors, including time and location of beetle collection, inherent variation within the individual species, and the behaviour of the beetles being modified under experimental conditions when compared

to natural conditions. Control dive chambers were used to provide an environment where dive behaviour could be quantified, yet the beetles were in a more natural environment and hopefully exhibited behaviour similar to that under natural conditions. However, there was still considerable variation. Further investigations should actively try to minimise the introduction of additional factors that could lead to variation when measuring dive characteristics.

Future directions

Given the diversity of subterranean dytiscids in Australia, with many having evolved independently from surface species, there is the potential for variation in the form of cutaneous respiration used by these species. Although it has been suggested that the Australian subterranean dytiscids lack respiratory setae (Kehl, 2014), there is un-investigated variation, and some species may have pores or setal type structures that have a respiratory function. Additionally, it would be interesting and important to understand the transition from the surface to underground living, and from using primarily air stores and gas gills to only cutaneous respiration. It is thought that surface-dwelling dytiscids transitioned through water-filled gravels where surface waters interface ground waters, or where groundwater habitats were used as a refuge when surface waters dried up, before becoming fully subterranean (Kato et al., 2010; Leys et al., 2010; Leys and Watts, 2008). There are also more closely related surface-dwelling species to the subterranean species than were used in this study, including numerous *Paroster* and *Limbodessus* (Leys and Watts, 2008; Watts, 1978; Watts and Hamom, 2014; Watts and Humphreys, 2006), as well as species that live in water-filled gravels and springs, which would be valuable for investigating the transition between surface and underground living. Examples of species that live in the intermediate habitats include *Exocelina saltusholmesensis*, *Limbodessus rivulus*, and *Limbodessus gemellus* and *Exocelina australiae* (Larson, 1994; Leys et al., 2010; Watts et al., 2016).

In chapter 5, gas gill size was assumed to be related to the width of the last abdominal turgite. This is the area where the gill is held when pushed out of the air store (Gilbert, 1986; Kehl, 2014), and the width of the segment appears to be correlated to gas gill size. Although this correlation produced reasonable values in *P. decempunctatus*, and correlates reasonably well with estimates in other species (Fig. 1), this may not hold true for all species. Other dytiscids may not use gas gills, or there may be other morphological and physical factors that contribute to gill size, including the largest relative bubble volume able to be maintained at the tip of the abdomen. Environmental variables, including water convection, temperature and PO_2 may also influence

when a gas gill is used and its size. Diving bell spiders *Argyroneta aquatica* appear to adjust the size of their diving bell, a bubble held underwater with spider web which functions like a gas gill, in response to higher O_2 demand and lower aquatic PO_2 (Seymour and Hetz, 2011). Future investigations of dytiscids could be undertaken to better understand gas gill size, how it relates to morphology and if environmental variables affect their use and size.

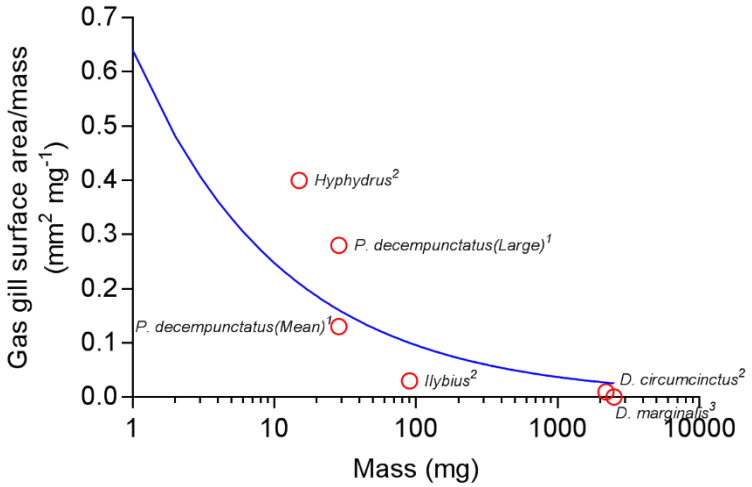

Figure 1. Gas gill surface area relative to mass with increasing body mass in dytiscids. Solid line shows the gas gill surface area calculated from the model used in chapter 5. Circles show measurements or estimates of gas gill surface area in different dytiscids from [1] Chapter 4 (large = largest gas gill size recorded, mean = average sized gas gill), [2] Ege (1915), and [3] De Ruiter et al. (1951).

The factors that affect surfacing duration in dytiscids are not fully understood. The allometric results in chapter 5 and a previous study (Calosi et al., 2012) show similar exponents for mean surfacing duration (0.24 and 0.26, respectively) which are not too different from what would be expected if surfacing duration were determined by linear diffusion through the tracheal system (0.33). However, many of the surfacing durations observed in this thesis and previous studies (Calosi et al., 2007; Calosi et al., 2012) seem to be on average longer than necessary to replenish the respiratory gas. This suggests, at least in experimental conditions, the time at the surface is not set by the balance between the rate of O_2 replenishment and minimisation of the time at the surface to avoid predators and parasites (Calosi et al., 2007; Calosi et al., 2012). However, dytiscids that are in an environment with a perceived threat or disturbance may exhibit more consistent surfacing durations. The use of exotic gases like sulphur hexafluoride and helium could be used to help understand the rate of diffusion into the dytiscid respiratory system and may influence surfacing durations, as observed in backswimmers (Jones et al., 2015).

As dytiscid dive behaviour seems to be altered under experimental conditions it would be valuable to observe the beetles' dive behaviour under more natural conditions. A known number of beetles could be placed in pond or tank that replicates a natural environment where surfacing events could be monitored for frequency and duration, and temperature could be manipulated. These data could be used to estimate dive duration and O_2 demand, and may show a stronger relationship with temperature than those recorded in the respirometry chambers and control dive chambers. Other behaviours like interactions between beetles and foraging may contribute to variation, but these behaviours may be quantifiable and separable from diving responses associated with temperature. These data may be useful for interpreting behaviour and estimating metabolic demand of diving beetles and other aquatic insects in their natural habitat, as well as, understanding how these factors change seasonally.

References

Aiken, R. B. (1985). Attachment sites, phenology, and growth of larvae of *Eylais* sp. (Acari) on *Dytiscus alaskanus* J. Balfour-Browne (Coleoptera: Dytiscidae). *Canadian Journal of Zoology* **63**, 267-271.

Aiken, R. B. (1986). Diel activity of a boreal water beetle (*Dytiscus alaskanus*: Coleoptera; Dytiscidae) in the laboratory and field. *Freshwater Biology* **16**, 155-159.

Balke, M., Watts, C. H. S., Cooper, S. J. B., Humphreys, W. F. and Vogler, A. P. (2004). A highly modified stygobiont diving beetle of the genus *Copelatus* (Coleoptera, Dytiscidae): taxonomy and cladistic analysis based on mitochondrial DNA sequences. *Systematic Entomology* **29**, 59-67.

Bartels, H. (1971). Diffusion coefficients and Krogh's diffusion constants. In *Respiration and Circulation*, (eds. P. L. Altman and D. S. Dittmer), pp. 21-22. Bethesda, Maryland, USA: Federation of American Societies for Experimental Biology.

Bartholomew, G. A. and Casey, T. M. (1977). Body temperature and oxygen consumption during rest and activity in relation to body size in some tropical beetles. *Journal of Thermal Biology* **2**, 173-176.

Bäumer, C., Pirow, R. and Paul, R. J. (2000). Respiratory adaptations to running-water microhabitats in mayfly larvae *Epeorus sylvicola* and *Ecdyonurus torrentis*, Ephemeroptera. *Physiological and Biochemical Zoology* **73**, 77-85.

Blomberg, S. P., Garland, T. and Ives, A. R. (2003). Testing for phylogenetic signal in comparative data: behavioral traits are more labile. *Evolution* **57**, 717-745.

Boardman, L. and Terblanche, J. S. (2015). Oxygen safety margins set thermal limits in an insect model system. *Journal of Experimental Biology* **218**, 1677-1685.

Bozinovic, F. and Pörtner, H. O. (2015). Physiological ecology meets climate change. *Ecology and Evolution* **5**, 1025-1030.

Calosi, P., Bilton, D. T. and Spicer, J. I. (2007). The diving response of a diving beetle: effects of temperature and acidification*. *Journal of Zoology* **273**, 289-297.

Calosi, P., Bilton, D. T., Spicer, J. I., Verberk, W. C. E. P., Atfield, A. and Garland, T. (2012). The comparative biology of diving in two genera of European Dytiscidae (Coleoptera). *Journal of Evolutionary Biology* **25**, 329-341.

Carlson, R. L. and Lauder, G. V. (2011). Escaping the flow: boundary layer use by the darter *Etheostoma tetrazonum* (Percidae) during benthic station holding. *Journal of Experimental Biology* **214**, 1181-1193.

Chaui-Berlinck, J. G. and Bicudo, J. E. P. W. (1994). Factors affecting oxygen gain in diving insects. *Journal of Insect Physiology* **40**, 617-622.

Chaui-Berlinck, J. G., Bicudo, J. E. P. W. and Monteiro, L. H. A. (2001). The oxygen gain of diving insects. *Respiration Physiology* **128**, 229-233.

Chen, J. and Wu, G. (2013). Beetle forewings: Epitome of the optimal design for lightweight composite materials. *Carbohydrate Polymers* **91**, 659-665.

Chown, S. L. and Gaston, K. J. (1999). Exploring links between physiology and ecology at macro-scales: the role of respiratory metabolism in insects. *Biological Reviews* **74**, 87-120.

Chown, S. L., Marais, E., Terblanche, J. S., Klok, C. J., Lighton, J. R. B. and Blackburn, T. M. (2007). Scaling of insect metabolic rate is inconsistent with the nutrient supply network model. *Functional Ecology* **21**, 282-290.

Clark, T. D., Sandblom, E. and Jutfelt, F. (2013). Aerobic scope measurements of fishes in an era of climate change: respirometry, relevance and recommendations. *Journal of Experimental Biology* **216**, 2771-2782.

Cooper, S. J. B., Bradbury, J. H., Saint, K. M., Leys, R., Austin, A. D. and Humphreys, W. F. (2007). Subterranean archipelago in the Australian arid zone: mitochondrial

DNA phylogeography of amphipods from central Western Australia. *Molecular Ecology* **16**, 1533-1544.

Cooper, S. J. B., Hinze, S., Leys, R., Watts, C. H. S. and Humphreys, W. F. (2002). Islands under the desert: molecular systematics and evolutionary origins of stygobitic water beetles (Coleoptera: Dytiscidae) from central Western Australia. *Invertebrate Systematics* **16**, 589-598.

De Ruiter, L., Wolvekamp, H. P., Van Tooren, A. J. and Vlasblom, A. (1951). Experiments on the efficiency of the "physical gill" (*Hydrous piceus* L., *Naucoris cimicoides* L., and *Notonecta glauca* L.). *Acta Physiologica et Pharmacologica Neerlandica* **2**, 180-213.

Dejours, P. (1981). Principles of comparative respiratory physiology. Amsterdam, Netherlands: Elsevier/North-Holland Biomedical Press.

Dettner, K. (1985). Ecological and phylogenetic significance of defensive compounds from pygidial glands of Hydradephaga (Coleoptera). *Proceedings of the Academy of Natural Sciences of Philadelphia* **137**, 156-171.

Di Giovanni, M. V., Pirisinu, Q., Giangiuliani, G., Goretti, E. and Pampanella, L. (1999). Oxygen consumption in two aquatic Coleoptera species: *Hydrous piceus* and *Dytiscus marginalis*. *Italian Journal of Zoology* **66**, 329-332.

Dolmen, D. and Solem, J. O. (2002). Locomotor activity patterns in *Ilybius fenestratus* (Fabricius)(Coleoptera, Dytiscidae) in a Central Norwegian lake, with evidence for breeding-induced arrhythmicity. *Aquatic Insects* **24**, 207-211.

Ege, R. (1915). On the respiratory function of the air stores carried by some aquatic insects (Corixidae, Dytiscidae and Notonecta). *Zeitschrift für Allgemeine Physiologie* **17**, 81-124.

Eriksen, C. H. (1986). Respiratory roles of caudal lamellae (gills) in a lestid damselfly (Odonata: Zygoptera). *Journal of the North American Benthological Society* **5**, 16-27.

Flynn, M. R. and Bush, J. W. M. (2008). Underwater breathing: the mechanics of plastron respiration. *Journal of Fluid Mechanics* **608**, 275-296.

Foottit, R. G. and Adler, P. H. (2009). Insect biodiversity: science and society. Oxford, UK: John Wiley & Sons.

Gibert, P., Huey, R. B. and Gilchrist, G. W. (2001). Locomotor performance of *Drosophila melanogaster*: interactions among developmental and adult temperatures, age, and geography. *Evolution* **55**, 205-209.

Gilbert, M. (1986). The respiratory system and respiratory technique of *Hydroporus palustris* (L.)(Coleoptera, Dytiscidae). *Entomologica Basiliensia* **11**, 43-65.

Gittelman, S. H. (1975). Physical gill efficiency and winter dormancy in the pigmy backswimmer, *Neoplea striola* (Hemiptera: Pleidae). *Annals of the Entomological Society of America* **68**, 1011-1017.

Gokan, N. (1966). On the tracheation and distribution of the air sacs in elytra of scarabaeid beetles. *Memoirs of the Tokyo University of Agriculture* **10**, 56-63.

Guzik, M. T., Cooper, S. J. B., Humphreys, W. F. and Austin, A. D. (2009). Fine-scale comparative phylogeography of a sympatric sister species triplet of subterranean diving beetles from a single calcrete aquifer in Western Australia. *Molecular Ecology* **18**, 3683-3698.

Guzik, M. T., Cooper, S. J. B., Humphreys, W. F., Ong, S., Kawakami, T. and Austin, A. D. (2011). Evidence for population fragmentation within a subterranean aquatic habitat in the Western Australian desert. *Heredity* **107**, 215-230.

Halsey, L. G., Butler, P. J. and Blackburn, T. M. (2006). A phylogenetic analysis of the allometry of diving. *The American Naturalist* **167**, 276-287.

Harrison, J., Frazier, M. R., Henry, J. R., Kaiser, A., Klok, C. J. and Rascón, B. (2006). Responses of terrestrial insects to hypoxia or hyperoxia. *Respiratory Physiology and Neurobiology* **154**, 4-17.

Harrison, J. F., Wong, C. J. H. and Phillips, J. E. (1990). Haemolymph buffering in the locust *Schistocerca gregaria*. *Journal of Experimental Biology* **154**, 573-579.

Hasler, C. T., Butman, D., Jeffrey, J. D. and Suski, C. D. (2016). Freshwater biota and rising pCO_2? *Ecology Letters* **19**, 98-108.

Hervant, F., Mathieu, J. and Messana, G. (1998). Oxygen consumption and ventilation in declining oxygen tension and posthypoxic recovery in epigean and hypogean crustaceans. *Journal of Crustacean Biology* **18**, 717-727.

Hilsenhoff, W. L. (1987). Effectiveness of bottle traps for collecting Dytiscidae (Coleoptera). *The Coleopterists Bulletin* **41**, 377-380.

Hinton, H. E. (1969). Plastron respiration in adult beetles of the suborder Myxophaga. *Journal of Zoology London* **159**, 131-137.

Hinton, H. E. (1976). Plastron respiration in bugs and beetles. *Journal of Insect Physiology* **22**, 1529-1550.

Hoerner, S. F. (1965). Fluid-Dynamic Drag: Practical Information on Aerodynamic Drag and Hydrodynamic Resistance. Midland Park, New Jersey, USA: Hoerner Fluid Dynamics

Humphreys, W. F., Watts, C. H. S., Cooper, S. J. B. and Leijs, R. (2009). Groundwater estuaries of salt lakes: buried pools of endemic biodiversity on the western plateau, Australia. *Hydrobiologia* **626**, 79-95.

Hüppop, K. (1985). The role of metabolism in the evolution of cave animals. *The NSS Bulletin* **47**, 136-146.

Hurlbert, A. H., Ballantyne IV, F. and Powell, S. (2008). Shaking a leg and hot to trot: the effects of body size and temperature on running speed in ants. *Ecological Entomology* **33**, 144-154.

Hutchinson, G. E. (1981). Thoughts on aquatic insects. *BioScience* **31**, 495-500.

Iwamoto, M., Chen, J., Kurashiki, K. and Ni, Q.-Q. (2002). Chitin fibre and its laminated structure of the fore-wing of beetle. *WIT Transactions on The Built Environment* **59**, 127-136.

Jennissen, H. P., Sanders, A., Schnittler, H. J. and Hlady, V. (1999). TIRF-Rheometer for measuring protein adsorption under high shear rates: constructional and fluid dynamic aspects. *Materialwissenschaft und Werkstofftechnik* **30**, 850-861.

Jones, K. K., Cooper, S. J. B. and Seymour, R. S. (2018a). Cutaneous respiration by diving beetles from underground aquafers of Western Australia (Coleoptera: Dytiscidae) Thesis chapter 3.

Jones, K. K., Hetz, S. K. and Seymour, R. S. (2018b). The effects of temperature, activity and convection on the plastron PO_2 of the aquatic bug *Aphelocheirus aestivalis* (Hemiptera; Aphelocheiridae). *Journal of Insect Physiology* **106**, 155-162.

Jones, K. K. and Seymour, R. S. (2018). Respiration, gas exchange and dive characteristics in the diving beetle *Platynectes decempunctatus* (Coleoptera: Dytiscidae). Thesis chapter 4.

Jones, K. K., Snelling, E. P., Watson, A. P. and Seymour, R. S. (2015). Gas exchange and dive characteristics of the free-swimming backswimmer *Anisops deanei*. *Journal of Experimental Biology* **218**, 3478-3486.

Kaiser, A., Klok, C. J., Socha, J. J., Lee, W.-K., Quinlan, M. C. and Harrison, J. F. (2007). Increase in tracheal investment with beetle size supports hypothesis of oxygen limitation on insect gigantism. *Proceedings of the National Academy of Sciences* **104**, 13198-13203.

Kato, M., Kawakita, A. and Kato, T. (2010). Colonization to aquifers and adaptations to subterranean interstitial life by a water beetle clade (Noteridae) with description of a new *Phreatodytes* species. *Zoological Science* **27**, 717-722.

Kehl, S. (2014). Respiration and Tracheal System. In *Ecology, Systematics, and the Natural History of Predaceous Diving Beetles (Coleoptera: Dytiscidae)*, (ed. D. A. Yee), pp. 189 - 198. Dordrecht, Netherlands: Springer.

Kehl, S. and Dettner, K. (2009). Surviving submerged—Setal tracheal gills for gas exchange in adult rheophilic diving beetles. *Journal of Morphology* **270**, 1348-1355.

Krogh, A. (1919). The rate of diffusion of gases through animal tissues, with some remarks on the coefficient of invasion. *The Journal of Physiology* **52**, 391-408.

Lane, S. J., Shishido, C. M., Moran, A. L., Tobalske, B. W., Arango, C. P. and Woods, H. A. (2017). Upper limits to body size imposed by respiratory–structural trade-offs in Antarctic pycnogonids. *Proceedings of the Royal Society of London B* **284**, 20171779.

Larson, D. J. (1994). *Boongurrus rivulus*, a new genus and species of water beetle (Coleoptera: Dytiscidae: Bidessini) from Northern Queensland, Australia. *Australian Journal of Entomology* **33**, 217-221.

Lee, D. J., Gutbrod, M., Ferreras, F. M. and Matthews, P. G. D. (2018). Changes in hemolymph total CO_2 content during the water-to-air respiratory transition of amphibiotic dragonflies. *Journal of Experimental Biology* **221**, jeb181438.

Lee, R. and Gates, D. M. (1964). Diffusion resistance in leaves as related to their stomatal anatomy and micro-structure. *American Journal of Botany* **51**, 963-975.

Leijs, R., Van Nes, E. H., Watts, C. H. S., Cooper, S. J. B., Humphreys, W. F. and Hogendoorn, K. (2012). Evolution of blind beetles in isolated aquifers: a test of alternative modes of speciation. *PLoS One* **7**, e34260.

Lemb, M. and Maier, G. (1996). Prey selection by the water bug *Aphelocheirus aestivalis* Fabr. (Heteroptera: Aphelocheiridae). *Internationale Revue der Gesamten Hydrobiologie und Hydrographie* **81**, 481-490.

Levich, V. G. (1962). Physicochemical Hydrodynamics. Englewood Cliffs, New Jersey, USA: Prentice-Hall

Leys, R., Roudnew, B. and Watts, C. H. S. (2010). *Paroster extraordinarius* sp. nov., a new groundwater diving beetle from the Flinders Ranges, with notes on other diving beetles from gravels in South Australia (Coleoptera: Dytiscidae). *Australian Journal of Entomology* **49**, 66-72.

Leys, R. and Watts, C. H. S. (2008). Systematics and evolution of the Australian subterranean hydroporine diving beetles (Dytiscidae), with notes on *Carabhydrus*. *Invertebrate Systematics* **22**, 217-225.

Leys, R., Watts, C. H. S., Cooper, S. J. B. and Humphreys, W. F. (2003). Evolution of subterranean diving beetles (Coleoptera: Dytiscidae: Hydroporini, Bidessini) in the arid zone of Australia. *Evolution* **57**, 2819-2834.

Madsen, B. L. (2008). A new respiratory adaptation in some stream waterbeetles. *Verhandlungen der Internationalen Vereinigung für Theoretische und Angewandte Limnologie* **30**, 133-135.

Madsen, B. L. (2012). Submersion respiration in small diving beetles (Dytiscidae). *Aquatic Insects* **34**, 57-76.

Malard, F. and Hervant, F. (1999). Oxygen supply and the adaptations of animals in groundwater. *Freshwater Biology* **41**, 1-30.

Marden, J. H. and Kramer, M. G. (1994). Surface-skimming stoneflies: a possible intermediate stage in insect flight evolution. *Science* **266**, 427-430.

Marx, M. T. and Messner, B. (2012). A general definition of the term "plastron" in terrestrial and aquatic arthropods. *Organisms Diversity and Evolution* **12**, 403-408.

Matthews, P. G. D. and Seymour, R. S. (2006). Diving insects boost their buoyancy bubbles. *Nature* **441**, 171.

Matthews, P. G. D. and Seymour, R. S. (2008). Haemoglobin as a buoyancy regulator and oxygen supply in the backswimmer (Notonectidae, *Anisops*). *Journal of Experimental Biology* **211**, 3790-3799.

Matthews, P. G. D. and Seymour, R. S. (2010). Compressible gas gills of diving insects: measurements and models. *Journal of Insect Physiology* **56**, 470-479.

Meijering, E., Dzyubachyk, O. and Smal, I. (2012). Methods for cell and particle tracking. *Methods in Enzymology* **504**, 183-200.

Michon, G. P. (2015). http://www.numericana.com/answer/ellipsoid.htm#thomsen.

Miller, K. B. and Bergsten, J. (2016). Diving beetles of the world: Systematics and biology of the dytiscidae. Baltimore, Maryland, USA: JHU Press.

Miller, P. L. (1994). The responses of rectal pumping in some zygopteran larvae (Odonata) to oxygen and ion availability. *Journal of Insect Physiology* **40**, 333-339.

Morgan, A. H. and O'Neil, H. D. (1931). The function of the tracheal gills in larvae of the caddis fly, *Macronema zebratum* Hagen. *Physiological Zoology* **4**, 361-379.

Morgan, K. H. (1993). Development, sedimentation and economic potential of palaeoriver systems of the Yilgarn Craton of Western Australia. *Sedimentary Geology* **85**, 637-656.

Mueller, C. A. and Seymour, R. S. (2011). The importance of perivitelline fluid convection to oxygen uptake of *Pseudophryne bibronii* eggs. *Physiological and Biochemical Zoology: Ecological and Evolutionary Approaches* **84**, 299-305.

Ni, Q.-Q., Chen, J., Iwamoto, M., Kurashiki, K. and Saito, K. (2001). Interlaminar reinforcement mechanism in a beetle fore-wing. *JSME International Journal Series C Mechanical Systems, Machine Elements and Manufacturing* **44**, 1111-1116.

Noh, M. Y., Muthukrishnan, S., Kramer, K. J. and Arakane, Y. (2016). Cuticle formation and pigmentation in beetles. *Current Opinion in Insect Science* **17**, 1-9.

Ordish, R. G. (1976). Two new genera and species of subterranean water beetle from New Zealand (Coleoptera: Dytiscidae). *New Zealand Journal of Zoology* **3**, 1-10.

Pinder, A. W. and Feder, M. E. (1990). Effect of boundary layers on cutaneous gas exchange. *Journal of Experimental Biology* **143**, 67-80.

Polhemus, D. A. and Polhemus, J. T. (1988). The Aphelocheirinae of tropical Asia (Heteroptera: Naucoridae). *Raffles Bulletin of Zoology* **36**, 167-300.

Pörtner, H. O. (2001). Climate change and temperature-dependent biogeography: oxygen limitation of thermal tolerance in animals. *Naturwissenschaften* **88**, 137-146.

Pörtner, H. O. (2010). Oxygen-and capacity-limitation of thermal tolerance: a matrix for integrating climate-related stressor effects in marine ecosystems. *Journal of Experimental Biology* **213**, 881-893.

Pritchard, G., McKee, M. H., Pike, E. M., Scrimgeour, G. J. and Zloty, J. (1993). Did the first insects live in water or in air? *Biological Journal of the Linnean Society* **49**, 31-44.

Rahn, H. and Paganelli, C. V. (1968). Gas exchange in gas gills of diving insects. *Respiration Physiology* **5**, 145-164.

Rasmussen, A. (1996). Least oxygen dependent. In *University of Florida Book of Insect Records*, (ed. T. J. Walker), pp. 46-48. Florida, USA: University of Florida Gainesville.

Reinhold, K. (1999). Energetically costly behaviour and the evolution of resting metabolic rate in insects. *Functional Ecology* **13**, 217-224.

Ribera, I., Foster, G. N. and Holt, W. V. (1997). Functional types of diving beetle (Coleoptera: Hygrobiidae and Dytiscidae), as identified by comparative swimming behaviour. *Biological Journal of the Linnean Society* **61**, 537-558.

Ribera, I. and Nilsson, A. N. (1995). Morphometric patterns among diving beetles (Coleoptera: Noteridae, Hygrobiidae, and Dytiscidae). *Canadian Journal of Zoology* **73**, 2343-2360.

Rogowitz, G. L. and Chappell, M. A. (2000). Energy metabolism of eucalyptus-boring beetles at rest and during locomotion: gender makes a difference. *Journal of Experimental Biology* **203**, 1131-1139.

Sand-Jensen, K. and Mebus, J. R. (1996). Fine-scale patterns of water velocity within macrophyte patches in streams. *Oikos* **76**, 169-180.

Schmidt-Nielsen, K. (1997). Animal Physiology: Adaption and environment. Cambridge, UK: Cambridge University Press.

Schmitz, A. (2015). Functional morphology of the respiratory organs in the cellar spider *Pholcus phalangioides* (Arachnida, Araneae, Pholcidae). *Journal of Comparative Physiology B* **185**, 637-646.

Schmitz, A. and Perry, S. F. (2001). Bimodal breathing in jumping spiders: morphometric partitioning of the lungs and tracheae in *Salticus scenicus* (Arachnida, Araneae, Salticidae). *Journal of Experimental Biology* **204**, 4321-4334.

Schmitz, A. and Perry, S. F. (2002). Morphometric analysis of the tracheal walls of the harvestmen *Nemastoma lugubre* (Arachnida, Opiliones, Nemastomatidae). *Arthropod Structure & Development* **30**, 229-241.

Seymour, R. S. (1994). Oxygen diffusion through the jelly capsules of amphibian eggs. *Israel Journal of Zoology* **40**, 493-506.

Seymour, R. S. and Hetz, S. K. (2011). The diving bell and the spider: the physical gill of *Argyroneta aquatica*. *The Journal of Experimental Biology* **214**, 2175-2181.

Seymour, R. S., Jones, K. K. and Hetz, S. K. (2015). Respiratory function of the plastron in the aquatic bug *Aphelocheirus aestivalis* (Hemiptera, Aphelocheiridae). *Journal of Experimental Biology* **218**, 2840-2846.

Seymour, R. S. and Matthews, P. G. D. (2013). Physical gills in diving insects and spiders: theory and experiment. *Journal of Experimental Biology* **216**, 164-170.

Seymour, R. S. and Roberts, J. D. (1995). Oxygen uptake by the aquatic eggs of the Australian frog *Crinia georgiana*. *Physiological Zoology* **68**, 206-222.

Simkiss, K. (1986). Eggshell conductance — Fick's or Stefan's law? *Respiration Physiology* **65**, 213-222.

Simmons, J. A., Sprittles, J. E. and Shikhmurzaev, Y. D. (2015). The formation of a bubble from a submerged orifice. *European Journal of Mechanics-B/Fluids* **53**, 24-36.

Smrž, J. (1981). Respiration – a new function of some hydroporine elytra (Coleoptera, Dytiscidae, Hydroporinae). *Acta Entomologica Bohemoslovaca* **78**, 209-215.

Snelling, E. P., Duncker, R., Jones, K. K., Fagan-Jeffries, E. P. and Seymour, R. S. (2017). Flight metabolic rate of *Locusta migratoria* in relation to oxygen partial pressure in atmospheres of varying diffusivity and density. *Journal of Experimental Biology* **220**, 4432-4439.

Spiegel, M. R., Lipschutz, S. and Liu, J. (2013). Mathematical handbook of formulas and tables. USA: The McGraw-Hill Companies, Inc.

Statzner, B. (1988). Growth and reynolds number of lotic macroinvertebrates: a problem for adaptation of shape to drag. *Oikos* **51**, 84-87.

Terblanche, J. S., Sinclair, B. J., Klok, C. J., McFarlane, M. L. and Chown, S. L. (2005). The effects of acclimation on thermal tolerance, desiccation resistance and metabolic rate in *Chirodica chalcoptera* (Coleoptera: Chrysomelidae). *Journal of Insect Physiology* **51**, 1013-1023.

Thorpe, W. H. (1950). Plastron respiration in aquatic insects. *Biological Reviews* **25**, 344-390.

Thorpe, W. H. and Crisp, D. J. (1947a). Studies on plastron respiration I. The biology of *Aphelocheirus* [Hemiptera, Aphelocheiridae (Naucoridae)] and the mechanism of plastron retention. *Journal of Experimental Biology* **24**, 227-269.

Thorpe, W. H. and Crisp, D. J. (1947b). Studies on plastron respiration II. The respiratory efficiency of the plastron in *Aphelocheirus*. *Journal of Experimental Biology* **24**, 270-303.

Tøien, Ø., Paganelli, C. V., Rahn, H. and Johnson, R. R. (1988). Diffusive resistance of avian eggshell pores. *Respiration Physiology* **74**, 345-354.

Tsuge, H. and Hibino, S. I. (1978). Bubble formation from a submerged single orifice accompanied by pressure fluctuations in gas chamber. *Journal of Chemical Engineering of Japan* **11**, 173-178.

Ubhi, R. and Matthews, P. G. (2018). The transition from water to air in aeshnid dragonflies is associated with a change in ventilatory responses to hypoxia and hypercapnia. *Journal of Insect Physiology* **106**, 172-178.

Ueno, S. I. (1957). Blind aquatic beetles of Japan, with some accounts of the fauna of Japanese subterranean waters. *Archiv für Hydrobiologie* **53**, 250-296.

Van de Kamp, T. and Greven, H. (2010). On the architecture of beetle elytra. *Entomologie Heute* **22**, 191-204.

Verberk, W. C. E. P. and Bilton, D. T. (2015). Oxygen-limited thermal tolerance is seen in a plastron-breathing insect and can be induced in a bimodal gas exchanger. *Journal of Experimental Biology* **218**, 2083-2088.

Verberk, W. C. E. P., Calosi, P., Spicer, J. I., Kehl, S. and Bilton, D. T. (2018). Does plasticity in thermal tolerance trade off with inherent tolerance? The influence of setal tracheal gills on thermal tolerance and its plasticity in a group of European diving beetles. *Journal of Insect Physiology* **106**, 163-171.

Verberk, W. C. E. P., Overgaard, J., Ern, R., Bayley, M., Wang, T., Boardman, L. and Terblanche, J. S. (2016). Does oxygen limit thermal tolerance in arthropods? A critical review of current evidence. *Comparative Biochemistry and Physiology Part A: Molecular and Integrative Physiology* **192**, 64-78.

Vlasblom, A. G. (1970). The respiratory significance of the physical gill in some adult insects. *Comparative Biochemistry and Physiology* **36**, 377-385.

Vogel, S. (1994). Life in Moving Fluids: The Physical Biology of Flow. New Jersey, USA: Princeton University Press.

Wallace, J. B. and Anderson, N. H. (1996). Habitat, life history, and behavioral adaptations of aquatic insects. In *An introduction to the aquatic insects of North America*, eds. R. W. Merritt and C. K.W.), pp. 41-73. Dubuque, Iowa, USA: Kendall/Hunt Publishing Company.

Watts, C. H. S. (1978). A revision of the Australian Dytiscidae (Coleoptera). *Australian Journal of Zoology Supplementary Series* **26**, 1-166.

Watts, C. H. S. and Hamom, H. (2014). Pictorial Guide to the Diving Bettles (Dytiscidae) of South Australia. Adelaide, South Australia, Australia: Entomology Department South Australian Museum.

Watts, C. H. S., Hendrich, L. and Balke, M. (2016). A new interstitial species of diving beetle from tropical northern Australia provides a scenario for the transition of epigean to stygobitic life (Coleoptera, Dytiscidae, Copelatinae). *Subterranean Biology* **19**, 23.

Watts, C. H. S. and Humphreys, W. F. (2006). Twenty-six new Dytiscidae (Coleoptera) of the genera *Limbodessus* Guignot and *Nirripirti* Watts & Humphreys, from underground waters in Australia. *Transactions of the Royal Society of South Australia* **130**, 123-185.

Watts, C. H. S. and Humphreys, W. F. (2009). Fourteen new Dytiscidae (Coleoptera) of the genera *Limbodessus* Guignot, *Paroster* Sharp, and *Exocelina* Broun from underground waters in Australia. *Transactions of the Royal Society of South Australia* **133**, 62-107.

White, C. R. (2003). Allometric analysis beyond heterogeneous regression slopes: use of the Johnson-Neyman technique in comparative biology. *Physiological and Biochemical Zoology* **76**, 135-140.

Wichard, W. and Komnick, H. (1974). Structure and function of the respiratory epithelium in the tracheal gills of stonefly larvae. *Journal of Insect Physiology* **20**, 2397-2406.

Wigglesworth, V. B. (1953). The Principles of Insect Physiology. England: Methuen.

Wigglesworth, V. B. and Lee, W. M. (1982). The supply of oxygen to the flight muscles of insects: a theory of tracheole physiology. *Tissue and Cell* **14**, 501-518.

Wolfe, G. W. and Zimmerman, J. R. (1984). Sensilla, punctation, reticulation, and body shape in the Hydroporinae (Coleoptera: Dytiscidae). *International Journal of Insect Morphology and Embryology* **13**, 373-387.

Yee, D. A. and Kehl, S. (2015). Chapter 39 - Order Coleoptera. In *Thorp and Covich's Freshwater Invertebrates*, (eds. J. H. Thorp and D. C. Rogers), pp. 1003-1042. Boston: Academic Press.

Zar, J. H. (1998). Biostatistical analysis. Englewood Cliffs, New Jersey, USA: Prentice-Hall.